UNIVERSITY OF CAPE TOWN
IYUNIVESITHI YASEKAPA • UNIVERSITEIT VAN KAAPSTAD

South African Research Chair in Cancer Biotechnology
Department of Integrative Biomedical Sciences
Institute for Infectious Disease & Molecular Medicine
Faculty of Health Sciences
University of Cape Town

Development of SNAP-tag-based fusion proteins targeting HIV-1 viral reservoirs

Siphelele Sanele Cingo

Supervisor:

Prof. Dr. Dr. Stefan Barth

SUBMITTED TO THE UNIVERSITY OF CAPE TOWN

In fulfilment of the requirements for the degree of

Master of Science (Med) in Chemical Biology

MAY 2020

DECLARATION

I, ***Siphelele Sanele Cingo***, hereby declare that the work on which this dissertation/thesis is based is my original work (except where acknowledgements indicate otherwise) and that neither the whole work nor any part of it has been, is being, or is to be submitted for another degree in this or any other university.

I empower the university to reproduce for the purpose of research either the whole or any portion of the contents in any manner whatsoever.

Signature: Signed by candidate

Date: 26/09/2020

In loving memory of my dearest mother

uMaMcobothi, uGogela, Sgwampa esimanywampunuwampu.

Your life was a blessing, your memory a treasure
You are loved beyond words and missed beyond measure

Acknowledgements

I would like to acknowledge the following people for their contributions to this project:

To Prof. Dr. Dr. Stefan Barth for his bottomless well of knowledge from which I hope to drink for many years to come, and for instilling confidence in me and getting the best out of me.

To Dr. Shivan Chetty, Dr. Krupa Naran for coaching me through my research pointing me in the right direction.

To Dr. Zenda Woodman and Bianca Abrahams for providing the HIV Env isoforms which were so instrumental in this study, and for training me in their laboratory.

To Mrs Susan Cooper for championing the confocal microscopy analyses.

To the MB&I team who have all helped me in many ways throughout this journey. Your contributions are incalculable. To Maryam Karaan and Sandra Jordaan for coaching my writing of this dissertation.

To my dear friends, “Stocko”, for the nights I can’t remember, with the people I will never forget. To Siyabulela Freddy Jr Magugu, the best friend a man can ever hope for. To Dini and Ogone for keeping me sane.

To Ms Onele Soqashe, the love of my life, for her endless support that cannot be quantified.

And most importantly, to my dad Mr B.S. Cingo,

uNyawuze ka Dakhile, uFaku ofakayo, uZiqelekazi, uTahla, uHlamba ngobubende amanzi ekhona.

Thank you for your endless support and encouraging me to follow my dreams. To my loving siblings Nolwando, Athi, Asanda, Kele, Eso, and Esinako for the unconditional love and support.

List of abbreviations

HIV	Human immunodeficiency virus
AIDS	Acquired immunodeficiency syndrome
cART	Combination antiretroviral therapy
ETA	*Pseudomonas aeruginosa* exotoxin A
HER2	Human epidermal growth factor-2
BG	Benzylguanine
ORF	Open reading frame
scFv	Single-chain variable fragment
dsFv	Disulphide-stabilised variable fragment
HEK	Human embryonic kidney cells
ELISA	Enzyme-linked immunosorbent assay
CCR5	C-C chemokine receptor type 5
CXCR4	C-X-C chemokine receptor type 4
NF-κB	Nuclear factor kappa B
P-TEFb	Positive transcription elongation factor B
NK	Natural killer cell
DC	Dendritic cell
OPC	Oropharyngeal candidiasis
PCP	*Pneumocystis carinii* pneumonia
MTB	*Mycobacterium tuberculosis*
CNS	Central nervous system
NRTi	Nucleoside reverse transcriptase inhibitor
NNRTi	Non-nucleoside reverse transcriptase inhibitor
ARV	Antiretroviral
PI	Protease inhibitor
CTL	Cytotoxic T-lymphocyte
bNAb	Broadly neutralising antibody
nNAb	Non-neutralising antibody
MPER	Membrane proximal external region
Gp	Glycoprotein
ADCC	Antibody-dependent cell cytotoxicity

PKC	Protein kinase C
HDACi	Histone deacetylase inhibitors
HMTi	Histone methylation inhibitors
DNMTi	DNA methyltransferase inhibitors
LRA	Latency reversing agents
IT	Immunotoxins
CL	Constant light chain
VL	Variable light chain
VH	Variable heavy chain
Fc	Fragment crystalline
Ig	Immunoglobulin
FR	Framework region
CDR	Complementarity-determining region
DT	Diphtheria toxin
IL	Interleukin
HR	Heptad-repeat
AGT	O^6-Alkylguanine DNA alkyltransferase
ADC	Antibody-drug conjugate
CMV	Cytomegalovirus
PVDF	polyvinylidene difluoride
PCR	Polymerase chain reaction
SDS-PAGE	Sodium-dodecyl sulphate polyacrylamide gel electrophoresis
FPLC	Fast protein liquid chromatography
SEC	Size-exclusion chromatography
RIPA	Radio Immuno-Precipitation Assay
LB	Luria-Bertani
TB	Terrific Broth
CFU	Colony-forming units
OE-PCR	Overlap-extension polymerase chain reaction
IMAC	Immobilised-metal affinity chromatography
IPTG	Isopropyl β- d-1-thiogalactopyranoside
DTT	Dithiothreitol

PEI	Polyethylenimine

List of Figure and Tables

Table of Contents

Abstract

Background

Globally, the HIV/AIDS epidemic has cost over 35 million lives and approximately a further 37 million people are currently infected with HIV. In South Africa alone, more than 7 million people are HIV positive. Since the initiation of combination antiretroviral therapy (cART), viral replication can be supressed below the limit of detection by conventional testing. There is, however, no approved therapy for the cure of HIV. This is because HIV establishes viral reservoirs in memory CD4+ T-cells, where replication is low or arrested, allowing prolonged survival. Since there is little or no replication, a therapeutic strategy which targets the viral production and replication becomes ineffective and upon cessation of antiretroviral therapy a dramatic viral relapse occurs. The eradication of HIV, therefore, requires the targeted killing of the reservoir cells, or latency reversal followed by the prevention of further infection using cART.

Targeting of cell-surface antigens for therapeutic purposes is the basis of immunotherapy. FDA-approved monoclonal antibodies such as Trastuzumab have been used to treat breast cancer via the human epidermal growth factor 2 (HER2) receptor. Immunotoxins (ITs) composed of an antibody fragment fused to apoptosis-inducing protein toxins targeting cell-surface antigens have been used for therapy of refractory leukaemia. The anti-CD22 recombinant IT Moxetumomab pasudotox based on *Pseudomonas aeruginosa* exotoxin A (ETA) has been FDA approved to treat hairy cell leukaemia. Moxetumomab pasudotox targets the antigen CD22 found on the surface of tumour cells. The HIV neutralizing VHH-nanobody J3, isolated from an immunised Llama has demonstrated anti-HIV properties against more than 95 % of HIV strains *in vitro*. As part of an ongoing project to develop a J3-ETA IT, this work sought to produce a J3-SNAP fusion protein by osmotic stress expression in the presence of compatible solutes in the periplasmic space of *E. coli*. SNAP-tag is a self-labelling protein that covalently binds benzylguanine (BG)-modified substrates in a 1:1 stoichiometric ratio. When recombinantly fused to any protein of interest, SNAP-tag allows the stable labelling of the protein of interest of *in vitro* and *in vivo* imaging. The periplasmic space of bacteria has been reported as a dedicated compartment to express functional proteins of interest. Furthermore, osmotic stress expression in the presence of compatible solutes has been reported to result in up to a thousand-fold increase in protein yield for difficult to express proteins. This study ultimately aimed to understand whether a functional J3-SNAP or J3-ETA can be expressed under osmotic stress in the presence of compatible solutes, in the periplasmic space of *E. coli*.

Experimental work

In this study, a SNAP-tag-based fusion protein and an ETA-based IT were designed using J3, an anti-HIV-1 Env VHH-nanobody isolated from an immunised llama. Using the SnapGene® software (v.5.0.8, GSL Biotech LLC, USA), *in silico* design and cloning of an ETA-based IT J3-ETA and SNAP-tag-based fusion protein J3-SNAP was performed. Molecular cloning of designed open reading frames (ORFs) was performed into appropriate bacterial expression plasmid vectors. Plasmid vectors confirmed to contain the required ORFs by Sanger sequencing were transformed into *E. coli* BL21-DE3. Histidine-tagged J3-SNAP was expressed by osmotic stress in the presence of compatible solutes. J3-SNAP was purified by IMAC and assessed by SDS-PAGE and Western blot analysis. To ascertain the binding of J3-SNAP to cells expressing HIV-1 Env *in vitro*, recombinant Env protein was transiently transfected into HEK293T-cells to generate an Env expressing cell line. Cell-surface binding of SNAP-Surface® Alexa Fluor® 488 -conjugated J3-SNAP on Env expressing HEK293T-cells was assessed by confocal microscopy analysis.

Results

Successful expression of J3-SNAP in *E. coli* BL21-DE3 was confirmed by SDS-PAGE and Western blot analysis. The J3-SNAP fusion protein was subsequently purified by IMAC. Purified J3-SNAP was conjugated to the benzyl guanine-modified fluorophore SNAP-Surface® Alexa Fluor® 488 and full-length conjugated protein was confirmed by combinations of SDS-PAGE and Western blot analysis. Cell-surface binding of J3-SNAP to HIV-1 Env-expressing HEK293T-cells was demonstrated *in vitro* by confocal microscopy analysis. These results prompted the generation of the IT, J3-ETA, by replacing SNAP-tag with ETA.

Conclusion

Successful binding studies suggest using J3 to target HIV-1 Env. Accessing patient probes would allow for the confirmation of these results for future human applications. Future *in vitro* studies would need to confirm the selective elimination of Env expressing T-cells by J3-ETA and thereafter confirmed on Env-positive patient probes.

Chapter 1. Introduction

1.1 HIV and AIDS

1.1.1 Origin and Epidemiology

In 1981, three hospitals in the state of California (USA) were reported to have treated five homosexual men for *Pneumocystis carinii* pneumonia [1]. The U.S. Centers for Disease Control and Prevention then received numerous cases of opportunistic infections such as *Pneumocystis carinii* and Kaposi's Sarcoma affecting men who engage in sexual intercourse with men. By 1982, more than 250 cases of severe immunodeficiency among homosexual men had been reported in America, France, and Spain. This rare disease, now named Acquired Immune Deficiency Syndrome (AIDS), was later reported to have affected haemophiliacs, people who injected drugs and patients that had received contaminated blood transfusions [2]. In 1984, the retrovirus Human Immunodeficiency Virus (HIV-1), isolated from an infected patient, was acknowledged as having caused AIDS [2], [3]. By 1990, the enzyme-linked immunosorbent assay (ELISA) blood test for HIV-1 had been approved by the U.S. Food and Drug Administration (FDA) and approximately 10 million people had been diagnosed with HIV-1 worldwide. This number would grow to approximately 37 million by 2017 [2]–[4]; [5]. The year 1997 saw a peak of new cases of HIV-1 with approximately 3.16 million people being reported worldwide. HIV-1-related deaths would later peak at almost 2 million in the year 2004 [6]. By the year 2018 however, new infections had been reduced by 40 % since the year 1997. AIDS-related deaths had also declined by 56 % since the year 2004 and by 33 % since the year 2010. The reduction in new infections and death is attributed to the development of antiretroviral therapy. It is estimated that only half of the people living with HIV are virally suppressed, despite almost two-thirds of people living with HIV being on antiretroviral therapy and 4 out of 5 people living with HIV-1 being aware of their status[4], [7], [8].

Certain population groups are disproportionally affected by HIV/AIDS when compared to entire populations. The risk of contracting HIV-1 is more than ten times higher in transgender people and more than twenty times higher in sex workers, homosexual men and recreational intravenous drug users [4], [8], [9]. The occurrence of HIV-1 in the incarcerated population is projected to be five times that of the general population in North America, and up to fifteen times higher in North Africa and the Middle East. This is thought to be the result of key populations, such as recreational drug users, being concentrated in prisons, as well as the prevalence of unprotected consensual sex and sexual assault in jails and prisons [10]–[14]. The incidence has been shown to differ across continents and countries. High-income nations, such

as those in North America and Western Europe, report a sub 0.5 % prevalence of HIV-1, with 9 in 10 infected individuals accessing antiretroviral therapy [8], [15]–[17]. Other regions that report low prevalence of HIV-1 include Latin America, where less than two million people were estimated to be HIV-1 positive, and only Bahamas, Belize, Guyana, Haiti, Jamaica, and Suriname report HIV incidence above 1% [8], [15], [16]. In 2012, North Africa and the Middle Eastern countries were reported to have approximately 260 000 people living with HIV-1. At 0.1 %, the prevalence in this region is among the lowest globally [8], [15], [16]. Asia is the second most burdened region concerning the HIV-1 epidemic, with approximately five million people living with HIV-1 as of 2017 [8], [15], [16]. Despite a decrease in the global incidence of HIV-1 to less than two million new cases in 2017, sub-Saharan Africa has the highest incidence of HIV-1. HIV/AIDS remains one of the leading causes of death in this region. In 2017, sub-Saharan Africa was reported to have accounted for two-thirds of all new HIV-1 infections. Almost three-quarters of all people living with HIV-1 reside within sub-Saharan Africa. Three-quarters of all HIV-1-related deaths were also reported to be in sub-Saharan Africa [5], [7], [16], [18]. These variations are thought to be related to the following; (1) The prevalence rate of contraceptives. Regions where contraceptive rate is high report lower HIV-1 incidence rates. The opposite is true for regions such as sub-Saharan Africa where the rate of contraceptive use is lower. (2) Availability of physicians. A positive correlation has been identified between the density of physicians and the incidence of HIV-1. (3) Religious and cultural practices. Regions such as the Middle East, where drug use, homosexuality, and extramarital sex are prohibited, report lower HIV-1 incidence rates. (4) Age of sexual initiation. Countries where girls initiate sex at a young age also report higher HIV-1 incidence rates. Lastly, (5) Education. Regions of the world that have a more educated population report lower HIV-1 incidence rates as populations are said to make smarter and safer decisions regarding their health [19]. As depicted in Figure 1.1 below, sub-Saharan Africa reported the highest number of deaths per 100 000 people in 2017. Contrary to the global estimates where 50% of HIV infected people are women, in sub-Saharan Africa, this figure rises to 59% [8]. Among other reasons, the disparity can be explained by the biological differences between men and women, where women have a larger mucus area that is susceptible to infection [20]. Furthermore, young women in particular, a more susceptible to contracting HIV. Both social and biological factors contribute to this disparity. A poorly developed cervix and low mucus production increase the risk contracting HIV. This risk is increased by gender inequality, a lack of autonomy for women in general and young women in particular, and poverty that drives women into situations where sexual intercourse is traded for money or goods [20]. Within sub-

Saharan countries, the prevalence of HIV-1 varies between the countries as well as the states/provinces and district municipalities within each country [18], [21]. In South Africa, for example, provinces where most males (aged 15 – 49) are circumcised report lower HIV-1 prevalence than provinces where most males are not circumcised. Furthermore, provinces, where males are circumcised in early adolescence, report lower HIV-1 prevalence than provinces where males are circumcised later in their adolescence or early adulthood [22].

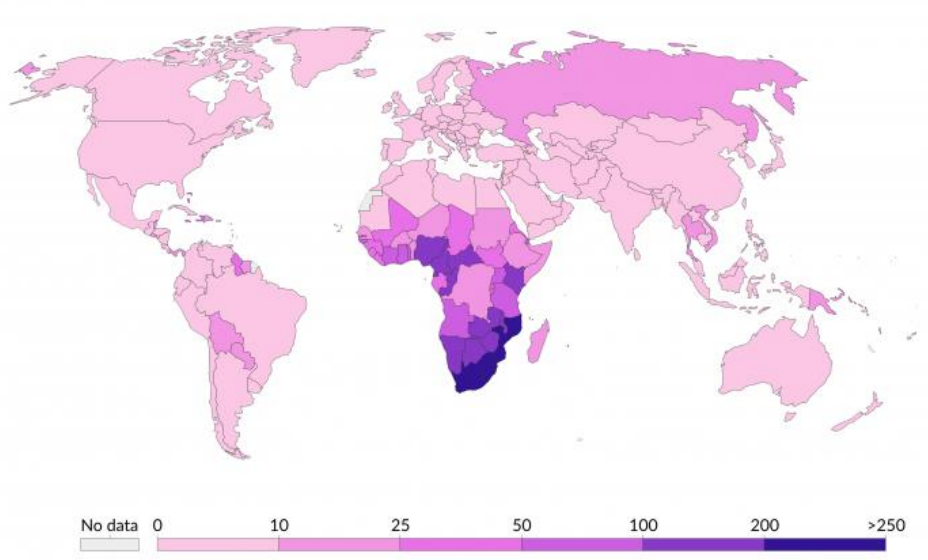

Max Roser and Hannah Ritchie (2020) - "HIV / AIDS". Published online at OurWorldInData.org. Retrieved from: 'https://ourworldindata.org/hiv-aids' [Online Resource]

Figure 1.1: Distribution of the annual number of HIV-related deaths per 100 000 people in 2017. Estimates of global HIV-related deaths. Sub-Saharan Africa reported the highest burden of HIV/AIDS in 2017. Many countries reported incidences of less than 10 deaths per 100 000. With more than 200 deaths per 100 000, South Africa and Mozambique reported the highest death rate in 2017.

1.1.2 Pathogenesis and disease progression

HIV is a retrovirus belonging to the family *Lentiviridae*. There are currently two recognised species of HIV, namely HIV-1, and HIV-2. F. Barrй-Sinoussi and L. Montagnier received the Nobel Prize in Physiology or Medicine in 2008 for having discovered HIV-1 in 1984 and identifying it as the causative agent of AIDS [23]–[25]. HIV-2 was discovered in 1986 by F. Clavel and colleagues [26], [27]. The most common of the two HIV strains is HIV-1, which is further divided into several genetic subtypes (M, N, O, and P), of which the genetic group M (main) is most common. HIV-1 will be the focus if this study will therefore be referred to as "HIV". HIV-2 has nine genetic groups (A-I). Within each genetic group, there are more than 10 subtypes, such as with HIV-1 genetic group M (as reviewed [28]–[32]).

HIV is spherical with a cylindrical core and a lipid envelope (Figure 1.2). The single-stranded positive-sense RNA strand is covered by a protein shell. Three of the proteins encoded by the HIV genome include the group-specific antigen (*gag*), DNA polymerase (*pol*), and envelope protein (*env*). *Env* codes for the gp120 glycoprotein and gp41, both of which form the gp160 complex (Env protein). The *pol* gene codes for the viral reverse transcriptase, protease, and integrase enzymes. The *gag* gene codes for the protein shell that encapsulates the viral genome. Additionally, the viral genome encodes regulatory genes that code for proteins which modulate the following: (1) The activation of reverse transcription (*tat* – trans-activator of transcription), (2) Regulation of viral structural protein transcription (*rev* – regulator of expression of virion proteins), (3) Prevention of antigen presentation on the surface of HIV infected cells, and (4) Elicitation of chemokine production that activates resting T-cells (*Nef* – negative regulator factor). Other genes encode proteins that suppress the synthesis of antiviral proteins (*Vif* – virion infectivity factor), stimulate transcription of viral RNA and translation of viral proteins (*Vpr* – viral protein R) and promote virion release (*Vpu* – viral protein U) in ref [33]–[36].

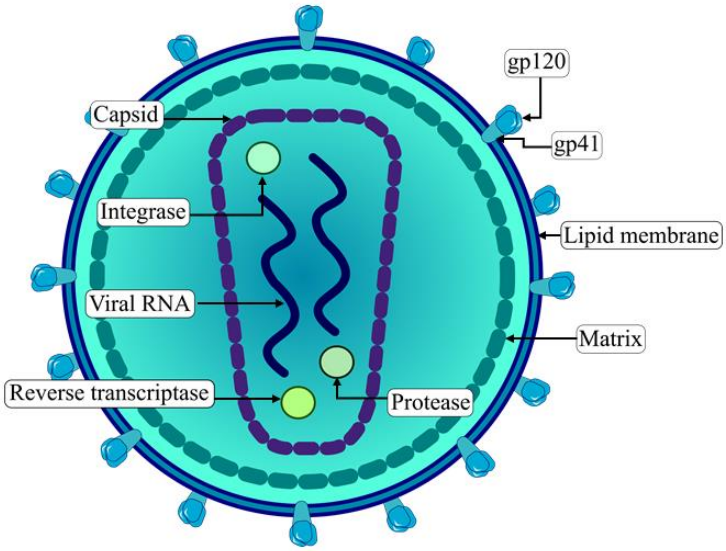

Figure 1.2: Schematic diagram of the HIV particle. HIV is a spherical lentivirus composed of a lipid bilayer membrane. Gp120 and gp41 are found on the surface and facilitate integration into host cells. Matrix protein covers the inner capsid. Capsid protein covers viral proteins and ribonucleic acids (RNA). The capsid of the virus encloses the viral genome (two RNA strands) as well as the reverse transcriptase, integrase, and protease enzymes. (adapted from [37])

HIV infection commences when the the viral membrane protein, cyclophilin-A, attaches to the human protein heparan [38], [39]. This weak association precedes the binding of HIV glycoprotein gp120 to CD4 (cluster of differentiation 4) molecules predominantly found on

CD4+ T-cells and, less commonly, on macrophages, dendritic cells, monocytes, glial cells and astrocytes. When gp120 attaches to CD4 molecules, a conformational change in the CD4 molecule results, allowing gp120 to also bind to the chemokine co-receptors CCR5 (C-C chemokine receptor type 5) or CXCR4 (C-X-C chemokine receptor type 4) (Figure 1.3 – step 1). The fusion peptide is exposed, which then penetrates the membrane of the host cell, followed by the formation of a fusion pore. Membrane fusion is facilitated by the six-helix bundle of gp41 which draws the two membranes closer to one another. The core of HIV enters the target cells while the envelope and its proteins remain on the surface of the host cell [40]–[47] (Figure 1.3 – step 2). In the cytoplasm of the host cell, uncoating of HIV occurs, followed by synthesis of proviral DNA from HIV genomic RNA, mediated by the reverse transcriptase enzyme [47]–[50] (Figure 1.3 – step 3). Viral DNA is then transported to the nucleus by the pre-initiation complex, where the viral integrase enzyme incorporates proviral DNA into transcriptionally active regions of the host genome [47], [51]–[54] (Figure 1.3 – step 4). Transcription of viral RNA in the host cells occurs when T-cells are activated, followed by the activation of pro-transcription factors including nuclear factor kappa-β (NF-κβ), Tat, and positive transcription elongation factor (P-TEFb) [55]–[60] (Figure 1.3 – step 5). The HIV protease then processes viral polyproteins before viral morphogenesis in the cytoplasm, followed by virions leaving the cell in exosomes by budding [61]–[67] (Figure 1.3 – steps 6-7).

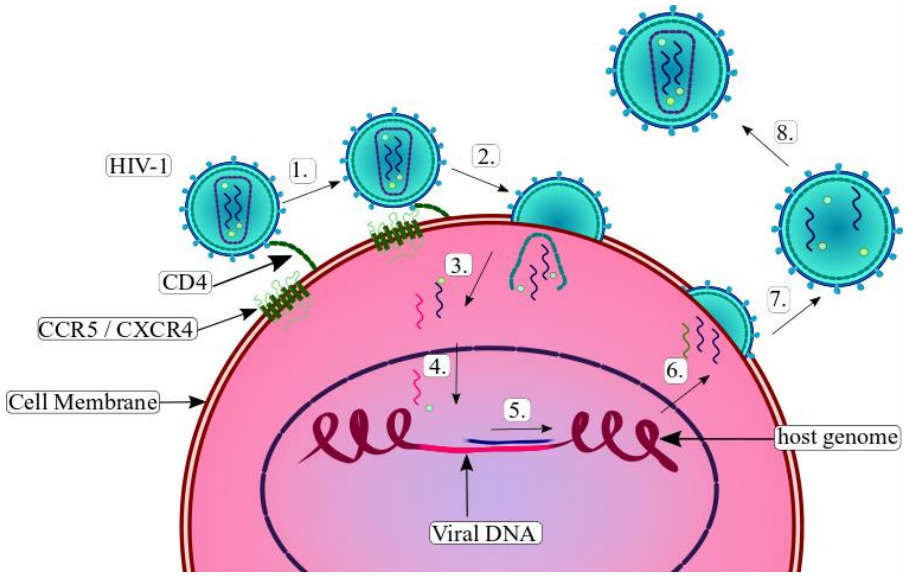

Figure 1.3: HIV replication cycle in host cells. HIV binds the CD4 receptor on host cells. 1. **Binding**: The CD4 receptor undergoes a conformational change and draws the virus close to the cell. 2. **Membrane fusion**: Coreceptors CCR5 or CXCR4 interact with the virus and the virus enters host cells by membrane fusion. 3: **Reverse transcription**: Following the uncoating of HIV within the host cell, the synthesis of viral

DNA from viral RNA is then catalysed by reverse transcriptase. 4. **Integration**: Integrase catalyses the incorporation of viral DNA into the host genome. 5. **Transcription**: HIV then uses host mechanisms to transcribe proviral DNA to make viral RNA and essential viral proteins. 6. **Assembly**: Viral RNA and proteins assemble at the surface of the host cell. 7. **Budding**: Immature virions bud off from the host cell. 8. **Maturation**: Protease cleaves viral proteins into their active forms and virions can now infect new cells. (adapted from [68]).

HIV uses a variety of mechanisms to establish infection and progress from acute to chronic infection while avoiding the host's immune system. Innate immune evasion by HIV is aided, in part, by the error-prone nature and poor proofreading ability of HIV RNA polymerase which results in genetic variability [69], [70]. HIV typically enters the body through mucosal barriers. It penetrates through intercellular spaces before reaching its target cells within the mucosal barrier where the infection of HIV is typically established [69]. Upon infection, the infected T-cells migrate to secondary lymphoid tissue where they interact with B-cells and T-helper cells. Secondary lymphoid tissue has a high concentration of HIV susceptible follicular T-helper cells. It is in secondary lymphoid tissue where HIV replicates and infects susceptible cells, resulting in a substantial increase in viremia during acute infection [69]. The functions of macrophages, natural killer (NK) cells, and dendritic cells (DC) are altered during HIV infection due to dysregulation of pro- and anti-inflammatory cytokines [69], [71]. The inhibition of interferon production during HIV infection results in reduced NK-cell function. Heightened NK-cell activity has been linked with increased resistance to HIV infection, and an increase in plasma NK-cell frequency has been shown to reduce HIV viremia, thus the dysregulation of NK-cell function is crucial for disease progression [69], [71], [72]. In the gut mucosa, NK-cells function to promote the survival of the epithelial cell lining. The integrity of gut mucosa is critical for the prevention of the translocation of gut microbes which increases immune activation and subsequent immune exhaustion during HIV infection. Together with NK-cells, T-helper 17 (Th17) cells help preserve the integrity of gut mucosa. Th17 cells are, however, susceptible to HIV infection due to the expression of the CD4 receptor on their surface. During HIV infection, these cells are depleted and must be regenerated. The high turnover number of CD4+ T-cell production results in the production of short-lived T-cells and is not conducive to Th17 cell production. This results in a compromised intestinal lining and subsequent intestinal microbe translocation, immune activation [73]–[78].

Chronic HIV is characterised by immune activation as a result of gut microbe translocation, evidenced by reduced circulating lipopolysaccharides during cART. Disease progression is better depicted by immune activation rather than viral load [74], [79]. Immune dysregulation,

T-cell exhaustion, and subsequent immune exhaustion in chronic HIV infection can leave victims of HIV susceptible to a myriad of opportunistic infections. The patient is said to have acquired immunodeficiency syndrome (AIDS) at this stage. The opportunistic infections include bacterial, fungal, protozoal and viral infections. Neoplasms such as lymphoma, squamous cell carcinoma and Kaposi sarcoma have been frequently reported [80]–[83]. Oropharyngeal candidiasis (OPC), cryptococcal meningitis, *Pneumocystis carinii* pneumonia (PCP), cerebral toxoplasmosis and tuberculosis are among the most frequently reported AIDS-associated illnesses. Approximately 90 % of HIV-infected individuals are thought to suffer from mouth sores at some stage of the disease, mainly due to OPC. *Candida albicans* is typically the cause of OPC, affecting the soft buccal mucosa [84]–[86]. *C. Albicans* is, however, the less severe of the AIDS-defining fungal infections. *Cryptococcus neoformans* is a yeast infection that rarely causes infection in healthy individuals, but in immunocompromised individuals results in *cryptococcal* meningitis and meningoencephalitis. Mortality caused by *cryptococcal* meningitis in poorer countries remains higher than that of developed regions (43 % and 25 % respectively) [87]–[90]. *Mycobacterium tuberculosis* (MTB) dominates the list of bacterial infections of which HIV infected individuals are at high risk. Annually, more than one million HIV-positive people contract active MTB, with sub-Saharan Africa contributing to three-quarters of all new MTB cases [91], [92]. Much like the previously mentioned opportunistic infections, exposure of healthy individuals to the infectious agent is common and results in latent asymptomatic infection due to a cell-mediated immune response that prevents disease manifestation [93]. Though antiretroviral therapy has significantly resulted in reduced incidence and mortality due to pulmonary TB, it remains the leading cause of death among HIV infected people in sub-Saharan Africa [94]. After being responsible for more than 20 000 new cases at the beginning of the epidemic, the first AIDS-defining disease to be identified was PCP. It was the diagnosis of several homosexual men with PCP that led to the discovery of AIDS [95]. Since the initiation of combination antiretroviral therapy (cART), the number of reported cases worldwide has since been reduced significantly [95]. PCP infection only progresses to a diseased state following severe immunosuppression. [95]–[98]. The most common central nervous system (CNS)-affecting opportunistic disease after cryptococcal meningitis is the protozoal infection cerebral toxoplasmosis [99]–[101]. Causing multifocal lesions, encephalitis and the formation of cysts in many organs, cerebral toxoplasmosis has been found in some studies to be an AIDS-defining illness in approximately 75 % of the cases [99]–[102]. Cerebral toxoplasmosis is typically due to *toxoplasma gondii* and is generally ingested through the consumption of oocysts-contaminated foods or water [100], [102]. Cell-

mediated immunity involving T-cells, macrophages, (interleukin) IL-2, and interferon γ all function in tandem to prevent the progression to a diseased state in healthy individuals following exposure to pathogens. In immunocompromised HIV positive individuals, the components of the immune system responsible for controlling the infection are impaired or dysfunctional [100]–[102]. Furthermore, in healthy individuals, *toxoplasma gondii* is controlled but not eliminated, allowing disease progression should the immune system ever be compromised [102]. Though early cART has been shown to improve survival and reduce the relapse of toxoplasmosis, the disease remains among the most common cerebral opportunistic pathogens in both developing and developed nations [99], [101]. Antiretroviral therapy has therefore played a vital role in mitigating or, in some cases, preventing AIDS-associated illnesses.

1.1.3 Antiretroviral Therapy

In 1987, the British pharmaceutical company GlaxoSmithKline was awarded FDA approval for the first therapy against HIV, Zidovudine. A nucleoside analogue initially trialled as an anticancer agent, Zidovudine was found to impede the viral enzyme reverse transcriptase, preventing the synthesis of proviral DNA and subsequent synthesis of new virions [103]–[105] In 1996, another class of antiretrovirals would receive FDA approval: Protease inhibitors (PIs) that inhibited HIV maturation were being used together with nucleoside reverse transcriptase inhibitors (NRTIs) such as zidovudine [103], [106]. A year later, in 1997, non-nucleoside reverse transcriptase inhibitors (NNRTIs) would receive FDA approval [107]–[110].

Antiretrovirals are strategically used in cART to inhibit HIV pathogenesis at the following stages; (1) entry, (2) reverse transcription, (3) integration, and (4) maturation. One of the newest classes of ARVs is viral entry inhibitors. The FDA approved drug, Maraviroc, is a CCR5 antagonist that binds to a hydrophobic transmembrane pocket on the CCR5 receptor, resulting in conformational changes that prevent interaction with gp120 [103], [111], [112]. The first class of antiretrovirals to be approved, NRTIs, is a class of nucleoside substrates that cause termination of reverse transcription. They may be guanosine, thymidine, or cytidine analogues, but all lack a 3’ hydroxyl group required for the formation of a 3’-5’ phosphodiester linkage which links nucleotides together during DNA synthesis. The pre-integration complex which integrates the viral genome into the host cell, requires the complete genome. Termination therefore attenuates progression of HIV [103], [113], [114]. NNRTIs are non-competitive inhibitors of reverse transcriptase with the same effect as NRTIs. NNRTIs bind to a hydrophobic pocket near the enzyme active site, inducing a conformational change that reduces

enzyme activity. FDA-approved examples include Etravirine, Delavirdine, Efavirenz and Nevirapine [103], [110], [115]. Integrase inhibitors such as Raltegravir prevent the irreversible step of viral genome integration into the host genome which is responsible for making HIV infection a lifelong illness. Integrase is responsible for 3'- end processing of viral DNA and subsequent strand transfer via the pre-integration complex. Integrase inhibitors prevent viral genome integration by binding to the pre-integration complex [103], [116], [117]. Introduced in 1995, protease inhibitors such as ritonavir, saquinavir, and indinavir inhibit HIV maturation by binding to the enzyme active site and inhibiting the HIV aspartyl protease enzyme responsible for cleaving the HIV gag and gag-pol polyprotein into the shorter functional proteins such as protease, reverse transcriptase, RNase H, and integrase [118], [119]. This multi-pronged approach was the basis of cART, utilizing a combination of three forms of therapy, NRTIs, NNRTIs, and PIs, to combat HIV. This combination would later be shown to reduce viremia to below detectable levels [103]. Owing to the side-effect profile of PIs, this class has since been used less frequently with integrase inhibitors taking preference [119]–[121].

1.1.4 Barriers to a cure

Despite the improvements in antiretroviral therapy, HIV remains a burden on society. While antiretroviral therapy can reduce viremia to below detectable levels, it is not curative. cART must be maintained for life in to prevent a relapse of viremia. This is because, during the acute stage of infection, HIV establishes reservoirs in multiple CD4+ T cell subtypes and can, therefore, persist in a latent or transcriptionally active state. Long-lived memory CD4+ T-cells typically house a majority of latent integrated HIV provirus [122]–[126]. Mechanisms undertaken by HIV to regulate the transcription of the viral genome include DNA methylation, as well as histone deacetylation and methylation [127]–[132]. These repressive epigenetic modifications make DNA less accessible to the transcription factors, NF-κβ and pTEFb, which are also downregulated or absent during latency. Reduced access of transcription factors to proviral DNA means viral mRNA cannot be transcribed and subsequent viral protein translation is prevented. Antiretroviral therapy is therefore rendered inactive against latent infection, as it targets different stages of an actively replicating virus [130], [132]. CD4+ T-cells harbouring latent HIV provirus are thought to be the main barrier to attaining a functional cure. Targeting T-cells harbouring latent HIV provirus requires a deeper understanding and an accurate estimation of the proportions of T-cells harbouring latent provirus. However, not all CD4+ T cells contain integrated and replication-competent provirus. It is estimated that latently

infected cells represent not more than 0.1 % of all CD4+ T cells [133]. Strategies to a cure require an accurate means of estimating the true size of the viral reservoir. Several strategies have been undertaken to estimate the size of the reservoir and each has its advantages and disadvantages. For example, an assay that quantified total HIV DNA within a host cell would include both integrated and non-integrated viral DNA, with the latter being up to 100-fold higher in concentration compared to the former. As a result, this technique would most probably underestimate the size of the reservoir. Quantitative viral outgrowth assays, which quantify active viruses, are thought to underestimate the size of the reservoir considering the estimation that at any given time since only 1 % of the replication-competent reservoir is actively replicating. The sequencing of an integrated provirus may be the best approximation of the size of the reservoir. However, this technique, much like the viral outgrowth assays, is financially unfeasible, time-consuming, and labour-intensive (as reviewed [134]).

The early initiation of cART has been shown to greatly reduce the size and the complexity of the reservoir [135], [136]. Conversely, Goonetilleke *et al.* (2019) postulated that cART can contribute to the formation of a stable reservoir. Following the depletion of CD4+ T-cells during the acute phase of the HIV infection, the introduction of cART replenishes the CD4+ T-cell population which subsequently transitions to memory CD4+ T-cells vulnerable to infection by HIV [137]. Other authors have postulated that stable reservoirs are established from cell proliferation rather than from new infections [137]–[143]. The composition of the reservoir is thought to be largely influenced by a phenomenon known as clonal expansion. Viremia circulating the blood of a chronically infected HIV patient shows genetic variations that result over time. Only a sample of these clones will be found in the genital tract, and the selection pressure only increases concerning viremia presence in the transmission fluid of the donor [144], [145]. There is typically no genetic variation in the blood of a newly infected individual due to the tough selection pressure that usually allows only one clone to overcome the barriers presented by the recipient's mucosa during infection [144], [145]. Heterogeneity of HIV is then restored upon disease progression. Studies have found that when persons with a heterogeneous population of viremia are treated with cART for a prolonged period the heterogeneity of the viremia is reduced, and the population can be dominated by a single clone or two. This is known as clonal expansion. The infection of multiple cells by a single dominant viral species may lead to genetic similarities. However, identical sequences arise from a clonal expansion during cART and contribute to the maintenance of a stable reservoir [138]–[140], [142], [143]. Upon analysis of the site of the viral genome in clones that persist during cART,

it was observed that clonal expansion was common when integration of the viral genome occurred in active transcription units [146]. The maintenance of a stable reservoir is the largest barrier to an HIV cure [122]–[126].

1.1.5 Emerging therapeutic strategies

Given the barriers to a functional cure for HIV, several strategies have been undertaken, aiming to undo the mechanisms by which HIV achieves and maintains latency. Strategies involve early initiation of cART, gene therapy, immune therapy, and the "Shock and Kill" strategy [147]–[150]. Minimizing the size of the viral reservoir is an essential step in the pursuit of eliminating HIV. Early initiation of cART has been shown to reduce the size of the reservoir and preserve the immune system. Early initiation of cART has also been shown to increase the rate at which the viral reservoir decays [135], [150]–[152]. The extent to which the CD8+ T-cell population and function can be restored depends partially on how early cART is initiated [153]. CD8+ T-cells are thought to play an important role in the eradication of viral reservoirs, owing to their ability to kill viruses, particularly during acute infection. CD8+ T-cells become dysfunctional in the chronic state, evidenced by reduced T-cell differentiation and proliferation, reduced cytolytic activity, and reduced signalling through interferon-γ, tumour necrosis factor-α, interleukin-2, and macrophage inflammatory protein-1β [153]–[156]. The ineffective T-cell response in patients with or without cART as well as insufficient T-cell restoration results in HIV viral rebound. Reservoir clearance, therefore, requires the restoration of CD8+ T-cell function [156]. As early as 1998, canarypox HIV vaccines were shown to induce a cytotoxic T-lymphocyte (CTL) response [157]. The CTL response was further improved by immunisation with both the live canarypox vaccine expressing gp120 and gp41 when co-immunised with recombinant gp120 [158], [159]. Furthermore, vaccines are yet to be curative. Though early vaccines demonstrated immunogenicity, elucidating an antibody and CTL response, they ultimately fell short, owing to their inability to prevent infection [156] [160].

In response to HIV infection, some patients have developed broadly neutralizing antibodies (bNAbs) that can neutralise HIV by target mainly five regions on the HIV Env protein; (1) the CD4 binding site on gp120, (2) second and third variable loops (V2 and V3), (3) proteoglycan moieties, (4) membrane-proximal external region (MPER) of the transmembrane domain of Env, and (5) the gp120-gp41 interface [161], [162]. Several antibodies binding to different regions of the same epitope have been isolated for all the above-mentioned epitopes, each depicting varying specificity for HIV isolates from patient samples [163] [164]. In addition to their ability to neutralise a variety of HIV strains, bNAbs have also been shown to prevent

infection across different animal models and routes of infection. When used in combination, bNAbs targeting various epitopes of Env have demonstrated and maintained efficient suppression of viremia in animal models and humans [164] [165]. In addition, the half-life plays a critical role in HIV neutralization. Studies have shown that when bNAbs have been modified to have increased affinity for neonatal Fc receptors, the half-life of the bNAbs was prolonged with subsequent sustained protection against HIV [164]. While non-neutralizing antibodies (nNAbs) have also been studied for their anti-HIV effects, they have fared poorly. nNAbs show poor antigen-binding activity, viral suppression, and an inability to prevent further infection in animal models [166], [167]. Their inability to induce antibody-dependent cell cytotoxicity (ADCC) and their narrow specificity make nNAbs less favourable compared to bNAbs [168].

To date, the only means of therapy to have successfully cured HIV is hematopoietic stem cell transplantation. An HIV-positive patient diagnosed with leukaemia received hematopoietic stem cells from a donor with a rare CCR5Δ32 mutation that results in shortened CCR5 that is not translocated to the cell surface. HIV, therefore, has no co-receptor with which to react and cannot infect the cell in question [169] [170]. Two patients from Boston also received hematopoietic stem cells. The donors, however, did not have the CCR5Δ32 mutation. Despite the reduction of the size of the viral reservoir, viral rebound was observed within a year [171]. More recently, an HIV positive patient in London received allogeneic stem-cell transplantation with cells containing the CCR5Δ32 mutation and has been able to live free of cART with no detectable viremia [172]. This has sparked interest in gene therapy studies aimed at removing the CCR5 gene in the hopes of preventing HIV infection. Genome editing using zinc-finger nucleases, transcription activator-like effectors, and clustered regularly interspaced short palindromic repeats (CRISPR)-Cas9 technology have been identified as possible means of elimination of CCR5 in CD4+ T-cells, and possibly stem cells, to make CD4+ T-cells and other susceptible cells resistant to HIV infection [164], [173]–[175]. The most prominent strategy for combatting HIV is the "Shock and Kill" strategy. This strategy involves the reversal "shock" of latent infection in long-lived memory CD4+ T-cells using latency-reversing agents. Latency reversal is mediated by agents such as protein kinase C (PKC) agonists, histone deacetylase inhibitors (HDACi), histone methylation inhibitors (HMTi), DNA methyltransferase inhibitors (DNMTi), among others. PKC modulates the levels of the transcription factor NF-κB, which subsequently contributes to the transcription of HIV proviral DNA. Epigenetic modifications are one of the most prominent means of latency achieved by

HIV. HDACis, DNMTis, and HMTis act by reducing the methylation of histone proteins and DNA, allowing access of transcription factors to the target loci housing HIV proviral DNA. The effectiveness of latency reversing agents (LRAs) can be improved by using multiple LRAs in combination with cART. Latency reversal must then be coupled with other means of therapy such as cART to prevent more infections, as well as bNAbs capable of eliminating viremia and eliciting an ADCC response (as reviewed [176]–[178]).

1.2 Immunotoxins

1.2.1 Design of Immunotoxins (ITs)

In the fight against HIV, there may be some lessons that can be learned from the fight against cancer. Antibodies and antibody technology have taken a lead role in the fight against cancer with more than one hundred antibody-based being approved for clinical use. The list of approved therapies includes monoclonal antibodies and ITs [179]–[181]. An IT is a fusion protein comprised of an antigen-binding domain fused either chemically or recombinantly to an effector domain in the form of a protein toxin. The binding domain is typically a growth factor or an antibody [182]–[185]. The first generation of ITs composed of whole monoclonal antibodies fused to full-length plant or bacterial protein toxins as effector domain. This format suffered major drawbacks including lack of specificity, off-target effects, and the combination was unstable [183]–[186]. Second generation ITs sought to combat some of these drawbacks by removing the binding domain in the toxins as they served no function since the targeting domain was already the antibody. Furthermore, this reduced bystander effects as toxins could only enter cells when there was an epitope-paratope interaction between the antibody fragment and the cell-surface antigen of the target cell [183]–[186]. Due to the size of the full-length antibody and that of the toxin, tumour penetration remained an issue, and conditions like vascular leak syndrome and pleuritis resulted. In attempts to mitigate some of these issues, T-cell and B-cell epitopes were mutated on the toxin. More importantly, antibody the variable regions (Fab) of antibodies were used rather than whole antibodies. As advanced as ITs have become, they still employ bacterial toxins. First, second and third generation ITs are depicted in Figure 1.5. The latest generation of ITs employs the effector domains of human cytolytic and pro-apoptotic enzymes such as granzymes and angiogenin [183]–[186].

Immunoglobulins or antibodies are heterodimeric protein structures containing two identical heavy chains (50 kDa) and two identical light chains (25 kDa) in the form of β-barrels, linked together by disulphide bridges [187]–[189]. IgG is the most abundant of the immunoglobulin

classes that naturally occur in human serum, accounting for up to 20 % of serum proteins [187], [189]. The light chain of IgG comprises the constant light chain (CL) and a variable light chain (VL). The heavy chain comprises a variable heavy chain (VH), and three constant heavy regions (CH1. CH2, and CH3). VH, CH1, VL, and CL make up the Fab region of the antibody which is linked by a hinge region to the fragment crystalline (Fc) region [189]. The hinge region confers flexibility to the immunoglobulins and is a function of the length of the amino acid sequence in this region. Within a class of antibodies such as IgG, hinge regions may vary between 62 amino acids (IgG3) and 12 amino acids (IgG2 and IgG4) [189]. The variable domain (Fv) of the immunoglobulin, composed of VH and VL, confers antigen recognition and binding capabilities [187]–[189]. Each variable domain (VH or VL) is composed of four relatively constant framework regions (FR) and three highly variable complementarity-determining regions (CDR) [187]–[189]. Three CDR regions from VH and three CDR regions from VL make up the antigen-binding site [188]. The constant regions of IgG antibodies confer the ability to elicit an immune response through complement activation and interaction with Fc receptors on Fc receptor-expressing cells. Upon opsonization of an antigen, the interaction of IgG with Fc receptors results in phagocytosis or some form of antibody-dependent cell-mediated cytotoxicity [187]–[189]. Figure 1.4 depicts common antibody fragments. Fab antibody fragments are composed of just the Fab region of the antibody, stabilised by linkers and disulphide bridges. Fv antibody formats are either stabilised by disulphide bridges (dsFv) or by a linker (scFv). Llama IgG has a unique, single-domain antibody format with an Fc domain linked to a heavy chain (VHH) [187].

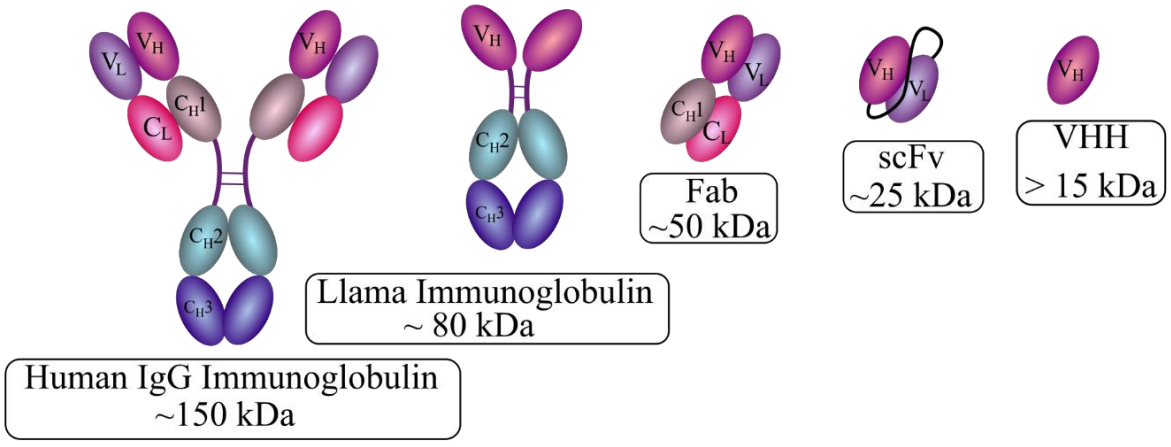

Figure 1.4: IgG antibody fragments. Human IgG is 150 kDa in size. IgG is composed of an Fc region (CH2 and CH3) and a Fab region (VH, VL, CH1, CL) stabilised by disulphide bridges. Llama immunoglobulin

is an 80 kDa heterodimer composed of an Fc region and a heavy chain. Single-chain variable fragments (scFv) comprise of VH and VL joined by a linker. VHH comprises of only the heavy chain of a camelid IgG.

Two of the most well-studied IT effector domains are diphtheria toxin (DT) and *Pseudomonas aeruginosa* exotoxin A (ETA). DT is composed of an enzymatic domain and a binding domain. The binding domain of DT-based fusion proteins includes cytokines (IL-2, and IL-3) or antibodies (CD3 scFv, CD22 scFv, CD19 scFv) [190]. The low pH of endosomes allows for the infolding of DT. The enzymatic domain is then translocated into the cytosol through a channel formed by a TH8 and TH9 hairpin. Apoptosis is induced when the elongation factor 2 undergoes ADP ribosylated by nicotinamide adenine dinucleotide, causing cessation of protein translation (as reviewed [183], [185]). DT-based ITs have been clinically successful, leading to FDA approval of IL-2Receptor-targeting DT toxin Danileukin diftitox for treatment of cutaneous T-cell lymphoma [183]. Moxetumomab pasudotox is an IT that has also received FDA approval for the treatment of hairy cell leukaemia. Moxetumomab pasudotox is a BL-21-targeting IT that employs ETA as its protein toxin. Moxetumomab pasudotox comprises of a truncated ETA that is recombinantly fused to the anti-CD22 (Fv) antibody [191]. ETA is composed of a binding, translocation, and catalytic domain (Figure 1.5). ETA enters a cell by interaction with the macrotubulin receptor and is internalised into endosomes, where the protease furin, cleaves domain 2. ETA is then translocated to the cytosol where it facilitates the ADP ribosylation of EF-2. ED-2 is then irreversibly inactivated, leading to the cessation of protein translation and subsequent apoptosis [183], [192], [191]. DT and ETA have been used to develop other ITs. Cytokines IL-2, IL-3, and IL-4 have been used as the targeting domains of both DT-based and ETA-based ITs in immunotherapy. Antibodies targeting CD3, CD7, CD19, CD20, CD22, and epidermal growth factor receptor (EGFR) fused to both ETA and DT have been developed as ITs for potential cancer therapy [190].

A

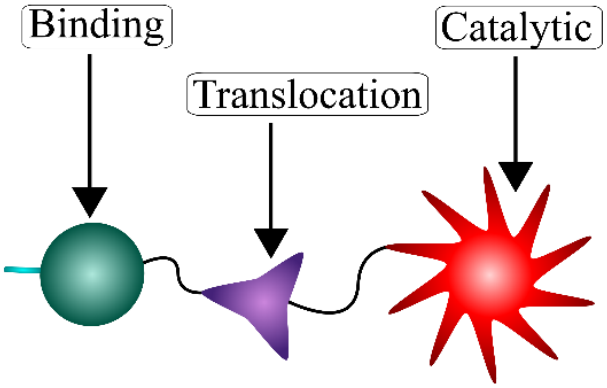

B

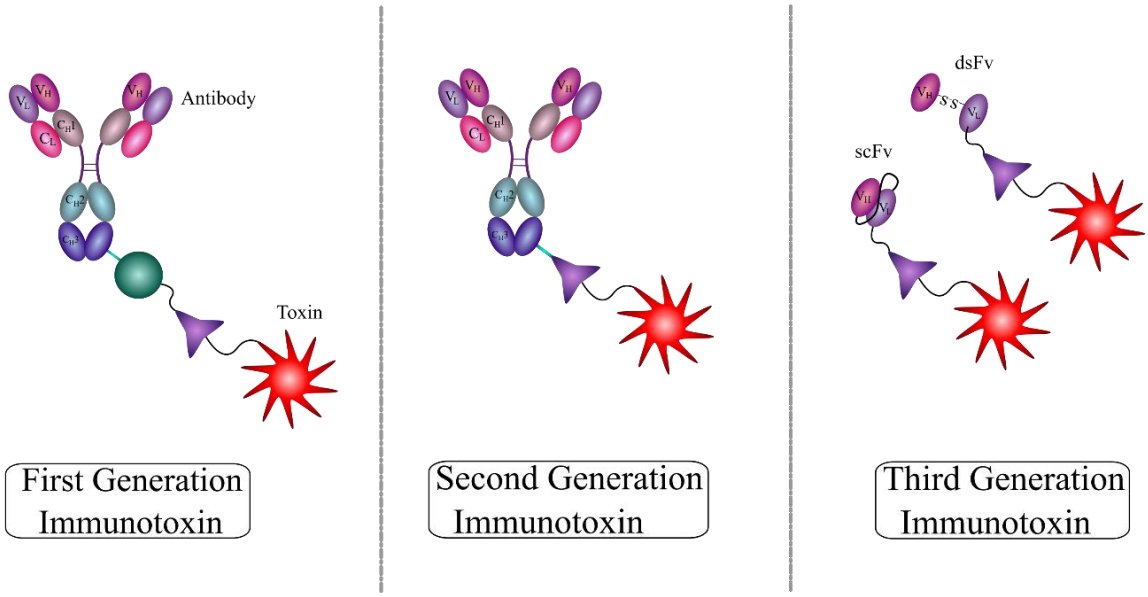

Figure 1.5: Evolution of Immunotoxins. (A) Diphtheria toxin and *Pseudomonas aeruginosa* Exotoxin A are composed of 3 domains; Binding, Translocation, and catalytic domains. (B) First-generation immunotoxins (IT) were composed of full-length monoclonal antibodies conjugated to toxins. Second generation ITs were composed of full-length antibodies with toxins missing the binding domain. Third generation ITs were composed of antibody fragments such as Fab, disulphide-stabilised single-chain variable fragments (dsFv), or single-chain variable fragments (scFv). (Adapted from [184])

1.3 Gp120

Since the late 1980s, researchers have attempted to use ITs to combat HIV. Initially, researchers used truncated ETA fused to the CD4 molecule to specifically target gp120 which is found on

the surface of HIV infected CD4+ T-cells. Though CD4-ETA ITs showed the specific killing of target cells in culture, the efficacy did not translate to phase 1 clinical trials [193]. Instead, the researchers found that CD4-ETA resulted in hepatotoxicity, or resistance to the IT developed rapidly [194]–[197]. ETA-based ITs composed of murine anti-gp120 monoclonal antibodies and anti-gp120 antibodies isolated by phage display technology have demonstrated specificity for HIV infected cells [198], [199]. Taken together, this shows the potential of gp120 as a molecular target for HIV infected cells.

The HIV envelope glycoprotein (Env) is synthesised as monomers in the rough endoplasmic reticulum (RER). The monomers then oligomerise in the ER before being trafficked to the Golgi apparatus. Furin cleaves gp160 into the cell-surface gp120 and transmembrane gp41. Glycoproteins gp120 and gp41 remain in complex owing to non-covalent interactions. The gp120/gp41 complex is then transported to the cell membrane to be added to budding virions (Figure 1.3). At the plasma membrane, other than incorporation into budding virions, gp120 may be shed or the whole complex may be endocytosed into early endosomes. The complex can be recycled back to the cell membrane or may move into late endosomes and then lysosomes for degradation [200]–[202]. The rapid recycling process is thought to help evade the host immune system [200].

Gp120 (Figure 1.6) comprises conserved sites including the CD4 binding site, a less constant co-receptor binding site, a variable loop (V3), and hypervariable loops 1 and 2 (V1 and V2) [200], [202]. The variable domains are not involved in binding interaction with CD4 but are primarily targeted by antibodies [202]. Upon interaction with CD4, gp120 changes conformational and exposes the co-receptor binding site. Gp41 is responsible for anchoring Env into the host cell membrane and owes this to its fusion peptide which is typically hidden within the complex and is exposed when the conformation of gp120 is altered. The fusion peptide penetrates the host cell membrane, causes destabilization and forms a fusion pore. A six-helix bundle, formed by hydrophobic regions of gp41 known as heptad-repeat regions 1 and 2 (HR1 and HR2), fuses the viral membrane by drawing the viral and host membranes together [200]–[202].

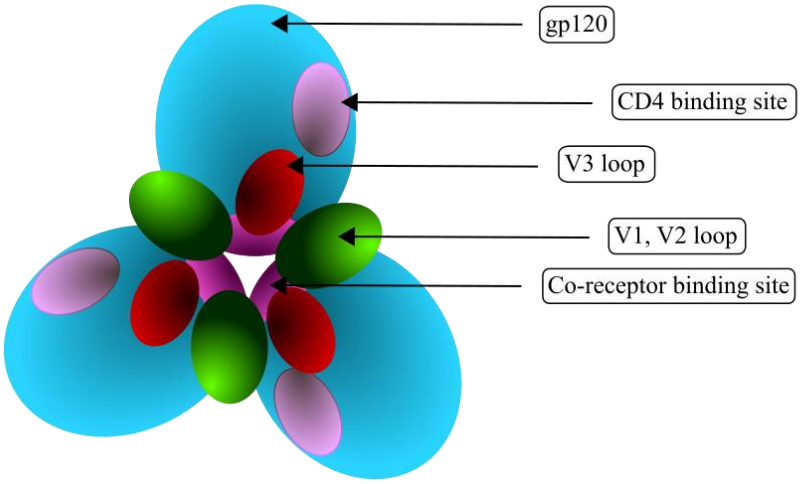

Figure 1.6: Gp120 schematic diagram showing three gp120 subunits. HIV glycoprotein gp120 schematic diagram depicting CD4 binding site, variable loops 1, 2, and 3 (V1, V2, V3), and coreceptor binding sites. (adapted from [203])

1.4 Nanobody targeting of the CD4 binding region on gp120 of the Env protein

Naturally occurring antibody formats unique to camelids are composed of an Fc region and a variable heavy chain only [187]. Their sequence similarity to humans is predicted to result in low immunogenicity and is expected to be relatively easy to humanise. Similar to other heavy chain domains, the VHH fragment of the Fab domain is composed of three CDR regions but with a few seemingly significant differences. VHH nanobodies have a longer CDR3 region and lack a hydrophobic region as there is no accompanying VL. The extended CDR3 region is thought to allow VHH nanobodies to reach into antigen cavities that other antibody formats may be unable to achieve. Some rare human bNAbs such as PG19, found to bind conserved epitopes of the HIV Env protein have also been found to have long CDR3 regions [204]. pH stability and improved tissue penetration further add to the advantages of VHH nanobodies, despite the size also being a disadvantage concerning its contribution to a shorter serum half-life [205]. VHH nanobodies have been mainly used in the development of cancer diagnostics and therapeutics. VHH-based ETA ITs have demonstrated promising anti-cancer effects against T-cell lymphoblastic leukaemia in mice [206], [207].In recent years, VHH nanobodies have been raised, capable of neutralizing various strains of HIV. Of interest, J3, a VHH that was reported to neutralise more than 95 % of one hundred HIV strains tested, and six simian-HIV pseudoviruses. J3, a novel VHH generated by the immunisation of camelids with gp140

trimers was selected based on its ability to neutralise pseudoviruses from several HIV subtypes and strains, by targeting the conserved CD4 binding region on gp120. [208].

1.5 SNAP-tag technology

In 2003, scientists from the Swiss Federal Institute of Technology Lausanne described the repurposing of a DNA-repair enzyme for covalent labelling of recombinant fusion proteins *in vivo*. In DNA repair, the DNA repair enzyme O^6-Alkylguanine DNA alkyltransferase (AGT) catalyses the transfer of an alkyl group from its substrate to a cysteine residue on AGT. According to Keppler *et al.* (2003), AGT reacted to its substrate O^6-Alkylguanine-DNA, but also to O^6-benzylguanine with a substituted benzyl group. As a result, SNAP-tag was developed. SNAP-tag is a self-labelling protein capable of reacting covalently in a 1:1 stoichiometric ratio with any benzylguanine (BG)-modified substrate. This may include fluorophore or small molecule toxin to which a benzyl group has been attached to its cysteine 145 residue (Figure 1.7) [209]–[211]. In therapeutics, the use of antibodies to deliver small molecule toxins to tumours by mere conjugation to cysteine or lysine residues, as is done in several antibody-drug-conjugates (ADCs), has several drawbacks. ADCs exhibit heterogeneity concerning drug-to-antibody ratios such that reaching required cytotoxic payloads may be difficult due to the uneven number of drug molecules to antibodies. ADCs have also been reported to be unstable as heterogeneity can be further aggravated by toxin conjugation at different sites [212]–[214]. SNAP-tag, therefore, provides a more stable alternative to the delivery of quantifiable cytotoxic payloads to target cells. The small molecule toxin can, as previously mentioned, be substituted for a fluorophore, arming the technology with far-reaching diagnostic capabilities [215].

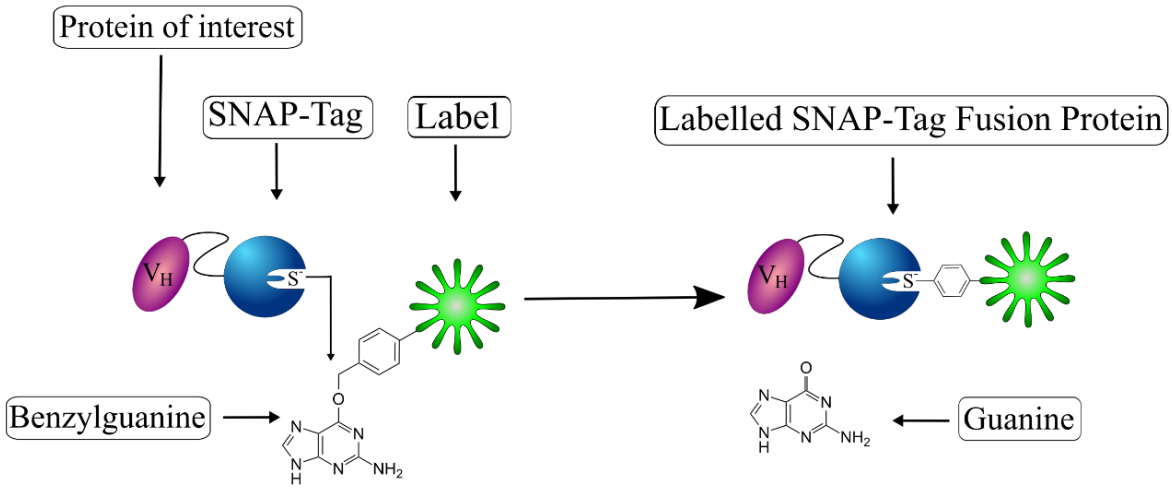

Figure 1.7: Schematic diagram of VHH antibody fragment recombinantly fused to SNAP-tag. The reaction of the SNAP-tag-based fusion protein with a benzylguanine-modified substrate (green) (small molecule toxin or fluorophore). SNAP-tag (blue) is recombinantly fused to VHH nanobody (purple). (Adapted from [212])

1.6 Expression of recombinant proteins

Several expression systems can be used to produce recombinant proteins based on the advantages and disadvantages of each system. Mammalian and bacterial host cells are most commonly used [216]. The expression of recombinant proteins in bacteria presents advantages such as the rapid growth of bacterial cells, with a doubling time of approximately 20 minutes under optimal conditions [217]. Bacterial cell culture is relatively inexpensive. *E. coli* genetics are well-studied and are hence easily manipulated to achieve desired outcomes. Strains of bacteria are genetically engineered to achieve high yields of protein. However, bacterial protein expression has its drawbacks. Bacteria cannot produce large and complex proteins as they are unable to post-translationally modify proteins. In addition, full-length antibodies, for example, cannot be produced in bacteria. Codon bias is another hurdle that must be overcome when aiming to produce recombinant proteins in bacteria. Proteins produced in bacteria can be locked in inclusion bodies, making the extraction complicated (reviewed in [216], [218]–[223].)

Some of the challenges faced when producing recombinant proteins in bacteria have been addressed. Enzymes such as glutathione reductase have been added to the genome of the bacteria to increase disulphide bond formation. Bacteriophage T7 promoter and RNA polymerase have been added to increase the rate of mRNA production and thus the rate of protein production. A signal leader peptide can be added to the open reading frame of the protein of interest which results in translocation of the protein to the periplasmic space where chaperones can assist in folding, avoiding the challenges of inclusion bodies and proteases. Protein solubility can also be increased by the reduction of temperature after inducing expression. Codon optimisation can be used to select for codons commonly found in bacteria (as reviewed [216], [218]–[223]). Barth *et al.* (2000) have proposed a method for the production of difficult-to-express proteins in bacteria [224]. To increase the yield of soluble recombinant protein, this protocol proposed the use of osmotic stress, which has been reported to drive growth rate maximization [224], [225]. Specialised osmotolerant bacteria typically combat osmotic environments using organic osmolytes (compatible solutes), which are thought to stabilise proteins and organisms under these challenging environmental conditions. This

protocol, therefore, made use of osmotic stress in the presence of compatible solutes to produce recombinant ITs in *E. coli* [224], [226].

HEK293T-cells have been used to produce pseudovirus in vaccine studies, or to express HIV epitopes in order to act as HIV infected cells when transfected with recombinant HIV plasmid DNA [227], [228]. Plasmids vectors pcDNA-TOPO and pRK have been used for membrane surface expression of the HIV Envelope protein on HEK293T-cells to generate pseudoviruses for vaccine studies [227], [228]. The complexity of the gp120-gp41 complex is such that other expression systems cannot be used. The complex protein folding mechanisms and post-translational modifications for membrane proteins exclude bacteria and yeast expression systems [229], [230]. Other factors that must be taken into consideration when expressing membrane proteins include the promoter strength; the transfection reagent, its efficiency, and its possible toxicity; as well as the antibiotic resistance genes for positive selection in *E. coli*. The CMV promoter is typically used for mammalian expression as it is a strong constitutive promoter [227]–[230].

1.7 Aims of this dissertation

Having claimed more approximately 37 million lives to date, HIV remains one of the worst epidemics in recorded history [4]. The development and initiation of cART have, however, resulted in a dramatic decrease in the number of new infections. cART can reduce viremia in the blood beyond the limit of detection. A cure has, however, remained elusive due to the establishment of viral reservoirs in long-lived memory CD4+ T-cells by HIV. Viral reservoirs allow HIV latency in the presence of cART but a swift rebound occurs following the cessation of therapy [99], [101]. Strategies to reverse latency have made great strides but are likely to fail without cART to prevent new infections, and targeted therapy to eliminate both transcriptionally active and latently infected CD4+ T-cells [147]–[150]. Various antibody-based cancer therapeutics have received approval for human application. ETA-based ITs have been used to treat hairy-cell leukaemia [191]. Lessons from cancer therapeutics have therefore informed this study. An ETA-based IT targeting HIV-infected Env-expressing CD4+ T-cells is a potential therapeutic in the fight against HIV/AIDS. The development of this therapeutic, however, must be preceded by the validation of antibody specificity to the antigen. This study, therefore, aimed to understand whether (1) a SNAP-tag-based fusion protein, J3-SNAP), can be expressed in the periplasmic space of *E. coli* by osmotic stress in the presence of compatible

solutes; and (2) can demonstrate functionality by reacting with readily SNAP-Surface® Alexa Fluor® 488 and possibly bind to the cell-surface gp120 of the Env protein. These aims were achieved by the following objectives (Figure 1.8 below): (1) *in silico* design of J3-SNAP, (2) molecular cloning to generate the pMT-J3-SNAP recombinant plasmid, (3) osmotic stress expression in *E. coli* BL21 DE3, (4) protein purification by immobilised metal affinity chromatography, and (5) confocal microscopy to validate cell surface binding to Env expressing cells *in vitro*. Upon confirmation of preliminary binding of J3 to Env, *in silico* design and molecular cloning of J3-ETA were commenced.

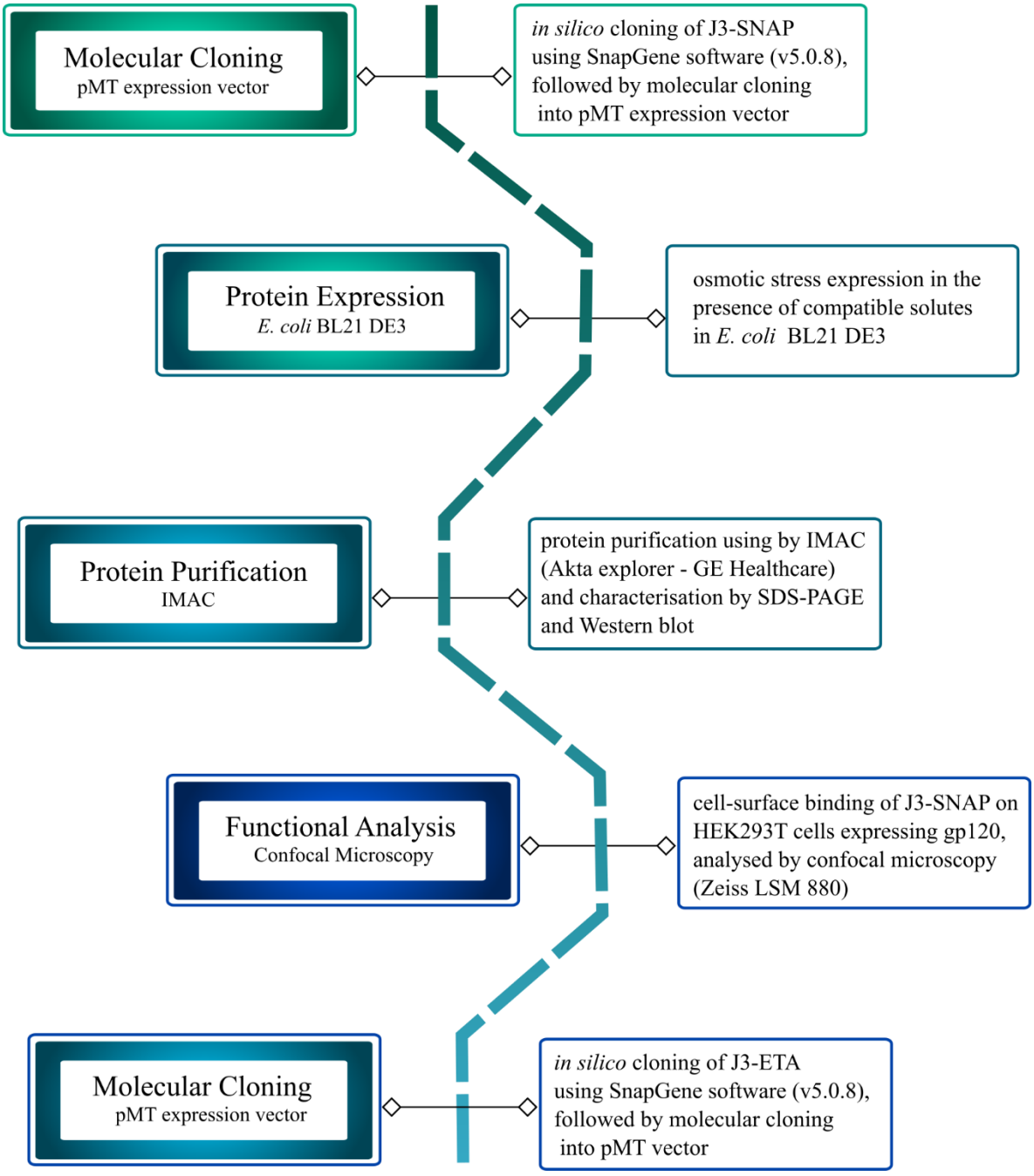

Figure 1.8: Flow chart of the research plan. J3-SNAP was cloned into pMT vector and transformed into E. coli BL21 DE3. Protein was expressed under osmotic stress in the presence of compatible solutes. Protein was then purified by immobilised metal affinity chromatography (IMAC) and size exclusion chromatography (SEC). Purified protein was analysed by SDS-PAGE and Western blot. Protein was then conjugated to SNAP-Surface® Alexa Fluor® 488 and cell surface binding to HIV Env expressing cells was detected by confocal microscopy.

Chapter 2: Materials and Methods

2.1 Materials

2.1.1 Chemicals and consumables

Unless otherwise stated, chemical reagents were acquired from Sigma-Aldrich (Germany). Luria Broth medium and Luria-Bertani agar medium were obtained from Anatech (South Africa). Plastic consumables were obtained from Bio-Smart Scientific (South Africa) and Lasec (South Africa).

2.1.2 Buffers and medium

Buffer solutions and media were prepared according to laboratory protocols using deionised or MilliQ water, as appropriate. Aqueous NaOH or HCl was used to adjust the pH of buffer solutions. Where necessary, sterile filtration (0.45 µm filter) or autoclaving for 20 minutes at 121 °C was used to sterilise the solutions. Buffers for IMAC protein purification were filtered and de-gassed using a 0.45 µm polyvinylidene difluoride (PVDF) membrane. In cases where the medium was supplemented with antibiotics, the following final concentrations were used: kanamycin 50 µg/mL, ampicillin 100 µg/mL, penicillin 100 U/mL, streptomycin 100 µg/mL, zeocin 100 µg/mL.

2.1.2.1 Buffers

Buffer	Composition	Concentration
10x Tris-acetate-EDTA (TAE) buffer	Tris base Glacial acetic acid EDTA	400 mM 200 mM 10 mM
10x Phosphate-buffered saline (PBS)	NaCl Na_2HPO_4 KCl KH_2PO_4	1.4 M 88 mM 27 mM 17.5 mM
10x Tris-buffered saline (TBS) pH 7.6	Tris base NaCl	200 mM 1.5 m
1x TBS-Tween	10x TBS dH_2O Tween 20	10 % (v/v) 90 % (v/v) 0.1 % (v/v)
10x Transfer buffer for Western blot	Tris Glycine	250 mM 2 M
1x Transfer buffer	10x Transfer Buffer Methanol dH_2O	10 % (v/v) 20 % (v/v) 70 % (v/v)
4x Incubation buffer for IMAC pH 8	NaH_2PO_4 NaCl Imidazole	200 mM 1.2 M 40 mM
Equilibration buffer for IMAC	NaH_2PO_4NaCl	50 mM

pH 8		300 mM
Elution buffer for IMAC **pH 8**	NaH_2PO_4 NaCl Imidazole	50 mM 300 mM 250 mM
Lysis solution 1	Tris-HCl pH 8.0 Glucose EDTA	50 mM 50 mM 10 mM
Lysis solution 2	NaOH SDS	0.2 M 1 % (w/v)
Lysis solution 3	Potassium acetate pH 6	3 M
RIPA (Radio Immuno-Precipitation Assay) buffer	Tris HCL pH 7.4 NaCl EDTA SDS Protease inhibitor cocktail	50mM 50mM 2mM 0.1% (w/v) 1 tab./50 mL
Lysis buffer	Tris-HCl pH 8.0 NaCl DTT Protease inhibitor cocktail Glycerol (Sigma-Aldrich)	75 mM 300 mM 5 mM 1 tab./50 mL 10 % (v/v)

2.1.2.2 Medium

Medium	Composition	Concentration
RPMI complex medium	RPMI 1640 plus GlutaMax Foetal bovine serum Penicillin Streptomycin	 10 % (v/v) 100 U/mL 100 µg/mL
Terrific Broth with compatible solutes	Glucose Sorbitol NaCl ZnCl Glycine-betain	3,5% (w/v) 5 M 4% (w/v) 0.5 mM 40 mM

2.1.3 Antibodies

Target	Antibody	Characteristic
HIV Envelope (primary)	Primary: Sheep anti-gp120 (ARP # 288)	Monoclonal
HIV Envelope (secondary)	Horseradish peroxidase-Goat anti-sheep IgG (Santa Cruz 2473)	conjugated to HRP
6x Histidine tag (primary)	Rabbit anti-his tag antibody (Cell Signalling Technologies, USA)	Monoclonal
6x Histidine tag (secondary)	Goat anti-rabbit horseradish peroxidase-conjugate antibody (Cat: 170-6515, Bio-rad Laboratories, USA)	Conjugated to HRP
β-actin (primary)	Mouse anti-actin (Sigma A2228)	Monoclonal
β-actin (secondary)	Horseradish peroxidase-goat-anti-mouse IgG (R&D HAF007)	conjugated to HRP

2.1.4 Enzymes and reaction kits

Kit	Purpose	Company
QIAqucik Gel Extraction Kit	DNA extraction from agarose gels	Qiagen (USA)
Zippy Plasmid Miniprep Kit	Plasmid DNA isolation	Zymo Research (USA)

2.1.5 Synthetic oligonucleotides

Name	Sequence	Tm [°C]
J3-F1	5' – TGAAGCTTATGGCCCAGCCGGCC – 3'	60
J3-R1	5' – AGCGAGCTCTGCGGCCGCAGAGGAAAC – 3'	60
J3-F2 Forward	5' – ATGGCCCAGCCGGCCGAAGTT – 3'	60
J3-R2 Reverse	5' – GAGTGCGGCCGCAGAGGAAAC – 3'	60
SNAP-F1	5' – GCCGCACTCGAGTCCAGAATGGAC – 3'	60
SNAP-R1	5' – TTATTGCTCAGCGCCAAGACC – 3'	60

2.1.6 Bacterial strains and human cell lines

Organism/strain/cell line	Genotype/origin	Reference
***E. coli* DH5α**	*fhuA2 Δ(argF-lacZ)U169 phoA glnV44 Φ80Δ (lacZ)M15 gyrA96 recA1 relA1 endA1 thi-1 hsdR17*	New England Biolabs
***E. coli* BL21 (DE3)**	*fhuA2 [lon] ompT gal (λ DE3) [dcm] ΔhsdS λ DE3 = λ sBamHIo ΔEcoRI-B int::(lacI::PlacUV5::T7 gene1) i21 Δnin5*	New England Biolabs
HEK293T	CRL-11268	ATCC

2.1.7 Plasmid vectors

Vector system	Purpose
pMT-J3-SNAP	Bacterial expression
pMT-J3-ETA	Bacterial expression
pcDNA-TOPO-gp120	Mammalian expression

2.2 Methods

2.2.1 Production and Preparation on DNA

2.2.1.1 *In silico* design of recombinant fusion proteins

The gene sequence of J3 (VHH) was obtained from patent no. WO 2013/036130 A1 and was thereafter, aligned to the germline sequence using the IMGT V-QUEST tool (www.imgt.org/imgt_vquest) to analyse the FR and CDR regions, and validated by IgBLAST (https://www.ncbi.nlm.nih.gov/igblast/). Following this, restriction endonuclease sites for *Sfi*I and *Not*I were added to either side of the J3 (VHH). *In silico* cloning was performed using SnapGene® software (v.5.0.8, GSL Biotech LLC, USA), where the sequence for J3 was inserted into appropriate expression plasmid vectors. J3 (VHH) and the plasmid vectors pMT-H22-ETA and pMT-H22-SNAP were digested using *Sfi*I and *Not*I. J3 (VHH) substituted H22 in the pMT-H22-ETA and pMT-H22-SNAP plasmids, to create pMT-J3-ETA and pMT-J3-SNAP. The ExPASy Translate tool (https://web.expasy.org/translate/) and the ExPASy compute pI/MW tool (https://web.expasy.org/cgi-bin/compute_pi/pi_tool) were used to determine the theoretical molecular weight (MW) and isoelectric point (pI) of J3-SNAP and J3-ETA.

2.2.1.2 Extraction of plasmid DNA from *E. coli*

pMT-H22-ETA and pMT-H22-SNAP plasmid DNA to be used for molecular cloning was isolated from *E. coli DH*5-α donated by Alex Akinrinmade (University of Cape Town, Faculty of Health Sciences). Glycerol stocks of *E. coli DH*5-α were inoculated into 50 mL Luria Broth supplemented with kanamycin (200 ng/µL) before being incubated overnight at 37 °C in a shaking incubator. Plasmid isolation was performed by alkaline lysis as described by Feliciello *et al.* (1993) [231] with a few modifications. Bacterial cells were then pelleted by centrifugation at 3000 rcf (relative centrifugal force) for 10 minutes at 4 °C. The supernatant was discarded, and the pellet was then resuspended using lysis solution 1. Cells were lysed and the DNA was denatured with lysis solution 2. The mixture was placed on ice for 5 minutes, then, circular DNA was renatured with lysis solution 3. Cell debris, denatured DNA, and SDS were then removed from the mixture by centrifugation at 13 000 rcf for 10 minutes. To the plasmid DNA-containing supernatant, RNase-A was added, and the mixture was incubated at 37 °C for one hour. Circular plasmid DNA was then precipitated by the addition of 30 % (v/v) isopropanol and then incubated at room temperature for 10 minutes. Plasmid DNA was then pelleted by centrifugation at 13 000 rcf for 20 minutes, then rinsed with cold 70 % ethanol and dried by vacuum centrifugation before being resuspended in nuclease-free water.

2.2.1.3 Polymerase chain reaction (PCR)

The gene fragment for J3, following commercial synthesis by Integrated DNA Technologies (USA), was amplified using the oligonucleotides in Table 2.1.5 (J3-F1 and J3-R1) and Phusion DNA polymerase (NEB) according to the manufacturer's instructions. The polymerase chain reaction was set up according to Table 2.2.1 below. The components were mixed gently, and the reaction was carried out in a thermocycler according to reaction conditions in Table 2.2.2. Amplified DNA was visualised by agarose gel electrophoresis. Following electrophoresis, J3 DNA was excised from the gel using the QIAquick Gel Extraction Kit (Qiagen) according to the manufacturer's instructions. The same protocol was used for mutation by overlap extension PCR (OE-PCR). For OE-PCR, the primers J3-F2 and J3-R2 were used to amplify J3. Thereafter, SNAP-tag was amplified with the primers SNAP-F1 and SNAP-R1 according to Table 2.2.1. J3 and SNAP-tag amplicons were electrophoresed as described in Chapter 2.2.1.5. The two amplicons were subsequently sewed together using the primers J3-F2 and SNAP-R1 according to table 2.2.1 before being electrophoresed as described in Chapter 2.2.1.5.

Table 2.2.1 Polymerase chain reaction composition using Phusion DNA polymerase.

Component	**Concentration**
5x Phusion HF Buffer	1x
10 mM dNTPs	0.2 mM
10 µM Forward Primer	0.5 µM
10 µM Forward Primer	0.5 µM
J3 gene fragment	0.1 µg
Phusion DNA polymerase	1000 U/mL
Nuclease-free H_20	13.3 µL
Total volume	20 µL

Table 2.2.2 PCR amplification thermocycler conditions.

Step	**Cycles**	**Temperature (°C)**	**Time**
Initial Denaturation	1	98	30 seconds
Denaturation	35	98	10 seconds
Annealing		60	30 seconds
Extension		72	30 seconds
Final Extension	1	72	5 minutes
Hold	1	4	∞

2.2.1.4 Restriction endonuclease digestion of DNA

All restriction enzymes were supplied by NEB and the restriction endonuclease digests were carried out according to NEB's specifications. Here, plasmid DNA (pMT-H22-SNAP and pMT-H22-ETA) and J3 or J3-SNAP were digested using restriction endonucleases *Sfi*I (3 hours at 50 °C) and *Not*I-HF (3 hours at 37 °C). Reactions were set up as according to Table 2.2.3 below.

Table 2.2.3 Restriction endonuclease digest reaction components

Component	**Concentration**
*Sfi*I	1000 U/mL
*Not*I	1000 U/mL
10x NEB Cutsmart Buffer	1x
DNA	2 µg
Nuclease-free H_2O	Adjusted to final volume
Final volume	20 µL

2.2.1.5 Agarose gel electrophoresis

DNA fragments were separated by agarose gel electrophoresis using a 1.2 % (w/v) agarose gel in 1x TAE buffer supplemented with SYBR safe (1:10 000 dilution) nucleic acid stain (Thermo-Fisher Scientific, catalogue number: S33102). As a molecular weight marker, the NEB 1 kb and 100 bp marker were used. The gel was electrophoresed at 120 V for 1 hour before being visualised under blue light excitation (470 nm). The desired DNA fragments were excised from the agarose gel and purified using the QIAquick gel extraction kit according to the manufacturer's instructions.

2.2.1.6 Ligation of DNA fragments

Digested, gel-separated, and purified DNA fragments (J3, J3-SNAP, pMT-ETA vector, and pMT-SNAP vector) were ligated (J3 + pMT-ETA, J3 + pMT-SNAP, J3-SNAP + pMT) using T4 DNA ligase (1000 U/mL) according to Table 2.2.3 below. Ligation reactions were performed with plasmid-to-vector ratios 1:3. And 1:5 at 16 °C overnight. The T4 DNA ligase was then inactivated at 65 °C for 10 minutes and allowed to cool.

Table 2.2.4 T4 DNA ligase reaction conditions

Component	Concentration (1:3)	Concentration (1:5)
10x T4 DNA Ligase buffer	1x	1x
Vector DNA (7090 bp)	50 ng	50 ng
Insert DNA (384 bp) [J3]	9 ng	14 ng
T4 DNA ligase	1000 U/mL	1000 U/mL
Nuclease-free water	Top up to 20 µL	Top up to 20 µL

2.2.1.7 Heat shock transformation of competent *E. coli*

J3 or J3-SNAP DNA ligated to the plasmid vectors pMT-ETA, pMT-SNAP or pMT (for J3-SNAP) was transformed into chemically competent *E. coli* DH5α cells as follows. First, 5 µL of the recombinant plasmid (pMT-J3-ETA, pMT-J3-SNAP) was added to 50 µL of competent *E. coli* DH5α cells. The competent cells were incubated on ice for 30 minutes before being subjected to heat shock at 42 °C for 1 minute and subsequently incubated on ice for 5 minutes. Thereafter, 450 µL of super optimum outgrowth (SOC) medium was added to the mixture before being incubated at 37 °C for 60 minutes. The mixture was subsequently centrifuged at 13 000 rcf for 1 minute. Following this, 300 µL of the supernatant was discarded and the pellet was then resuspended in the remaining 200 µL. 100 µL of the remaining mixture was inoculated on LB-agar plates supplemented with 50 µg/mL of kanamycin before being incubated at 37 °C overnight.

2.2.1.8 Confirmation of final constructs

Confirmation if molecular cloning had generated the desired recombinant plasmids (pMT-J3-ETA and pMT-J3-SNAP) was achieved as follows: several bacterial colonies were selected from each plate and grown on LB-agar plates were inoculated into 5 mL Luria broth cultures supplemented with 50 µg/mL of kanamycin before incubated at 37 °C overnight. The recombinant plasmid was then isolated from 4 mL of the culture using the Zippy plasmid mini kit (Zymo Research) as instructed by the manufacturer. SnapGene® software (v.5.0.8, GSL Biotech LLC, USA) was used to simulate a restriction endonuclease digest using *Pvu*II to generate DNA fragments different from that of the parental plasmid. The recombinant plasmids pMT-J3-ETA and pMT-J3-SNAP isolated from *E. coli* DH5α were thereupon digested using *Pvu*II (as with restriction endonuclease digest) at 37 °C overnight. Thereafter, digested DNA was analysed by electrophoresis using a 1.2 % agarose gel for 1 hour and before being visualised by blue light excitation (470 nm). Once positive clones were identified, the remaining 1 mL of the culture was inoculated into 50 mL of Luria broth supplemented with

kanamycin and incubated in a shaking incubator at 37 °C overnight. Thereafter, plasmid DNA was isolated using the alkaline lysis method (2.2.1.2) and analysed by Sanger sequencing at Inqaba Biotech (South Africa). The Sanger sequences were subsequently aligned to the consensus sequences to confirm homology and successful molecular cloning of pMT-J3-ETA and pMT-J3-SNAP.

2.2.2 Production of recombinant protein in *E. coli*

2.2.2.1 Transformation of competent *E. coli*

Confirmed DNA sequences were transformed into the chemically competent expression bacterial cell line *E. coli* BL21 (DE3) according to the previously outlined protocol (2.2.1.7).

2.2.2.2 Protein stress expression

Protein expression was carried out using the osmotic stress expression protocol as described by Barth *et al*. (2000) [226]. Briefly, a single *E. coli* BL21 (DE3) colony containing either pMT-J3-ETA or pMT-J3-SNAP was inoculated into 50 mL Terrific Broth (TB) medium supplemented with kanamycin and subsequently grown overnight at 28 °C in a shaking incubator at 225 rpm. Thereafter, 5 mL of this "Starter culture" was added to 250 mL fresh TB media ("main culture") and incubated at 26 °C at 200 rpm until OD_{600} = 1.6 is reached. Stress was induced by the addition of 4 % NaCl together with 0.5 M sorbitol, 10 mM Glycin-Betain, 0.5 mM $ZnCl_2$. The mixture was incubated for 30 minutes at 28 °C, after which, IPTG was added to a final concentration of 1 mM to induce recombinant protein expression. The culture was thereafter incubated at 26 °C for 16 hours. Thereafter, cells were centrifuged at 4000 rcf for 10 minutes at 4 °C. 3 supernatant was discarded, and the recombinant protein was harvested from the pellet. To harvest the recombinant protein from the bacterial cells, the pellet was resuspended in cold lysis buffer before being sonicated to release protein from the periplasmic space. The lysate was thereafter centrifuged at 24 000 rcf for 30 minutes. The supernatant was clarified using a 0.45 µm syringe filter before being enriched by IMAC.

2.2.3 Protein purification and analysis

2.2.3.1 Protein purification by IMAC

The recombinant fusion protein was enriched by fast protein liquid chromatography (FPLC) on an ÄKTA Explorer™ (GE Healthcare) using a HisTrap™ High Performance column (GE Healthcare, 17-5247-01). Using a flow rate of 5 mL/min (maintained throughout the purification process), the column was equilibrated with 10 column volumes of equilibration buffer. Cell lysate containing recombinant fusion protein was subsequently applied to the

column. The column was again washed with 10 column volumes of incubation buffer. Bound protein was then eluted with elution buffer using increasing concentrations of imidazole-containing elution buffer. Initially, 6 % imidazole in elution buffer was used to elute weakly-bound protein. The protein of interest was then eluted using 40 % imidazole, then 100 % imidazole. The eluted protein was concentrated using Amicon® Ultra-15 centrifugal filter units (Ref: UFC901008, Sigma) with 10 kDa cut off membranes. Protein fractions were pooled and concentrated using a 50 kDa Amicon® Ultra-15 centrifugal filter unit which traps proteins greater than 50 kDa. The centrifugation was carried out for 25 minutes at 4 °C at 4000 rcf. The flow-through was then applied to a 10 kDa Amicon® Ultra-15 centrifugal filter unit which further excluded all proteins below 10 kDa. The sample trapped by the 50 kDa Amicon® Ultra-15 centrifugal filter unit was kept for analysis. The protein of interest was expected to be below 50 kDa and above 10 kDa (J3-SNAP – 37.5 kDa). The flow-through that was not trapped by the 10 kDa Amicon® Ultra-15 centrifugal filter unit was kept for analysis by SDS-PAGE (Chapter 2.2.3.2) and Western blot (Chapter 2.2.3.3).

2.2.3.2 SDS-polyacrylamide gel electrophoresis

Enriched protein was separated by discontinuous SDS-PAGE using 10 % (w/v) SDS gels. As a protein standard, pre-stained protein marker was used. 15 µL of the fraction was mixed with 5 µL of 4x Laemmli Sample Buffer (Bio-rad, USA #1610747) before being boiled to denature and analysed by SDS-PAGE at 80 V for 30 minutes and then at 120 V for 1 hour. Protein bands were subsequently visualised by incubation of the gel in AcquaStain® solution (Bulldog Bio, USA) for at least 30 minutes.

2.2.3.3 Western blot

Where necessary, following protein separation by SDS-PAGE, the protein was transferred onto a nitrocellulose membrane as follows. The membrane was equilibrated for 5 min in methanol, followed by incubation for 5 min in water and, lastly, for 5min in transfer buffer. The transfer was subsequently carried out at 90 V for 90 minutes using The Mini Trans-Blot® cell (Bio-rad, USA). The membrane was then blocked with 10 % milk in 1x PBS for 1 hour at room temperature. Thereafter, the membrane was washed with 1x PBS-Tween three times for 10 minutes. The recombinant protein was detected using rabbit monoclonal anti-His-tag (1:1000, Qiagen Germany) and Goat anti-rabbit horseradish peroxidase-conjugate antibody (1: 5000) (Bio-rad, USA). For detection of β-actin, the membrane was then incubated with Mouse anti-actin antibody (Sigma A2228) for an hour at room temperature, and then Horseradish peroxidase-goat-anti-mouse IgG (R&D HAF007) for one hour at room temperature before

being viewed by Gel Doc Protein was then quantified using the Denovix DS-11 spectrophotometer (Alliance Global, USA).

2.2.4 Evaluation of protein functionality

2.2.4.1 Cell culture of HIV Env-expressing HEK293T-cell line

Human embryonic kidney 293T (HEK293T) cells were used for the generation of a cell line expressing cell-surface recombinant Env glycoprotein. To generate the Env-expressing cells, glycerol stocks of *E. coli* containing the plasmid pcDNA-TOPO-gp120, which encodes recombinant full-length Env protein (gp120 and gp41) were kindly donated by Dr. Zenda Woodman (University of Cape Town, South Africa). Plasmid DNA was isolated by the alkaline lysis method (as described in Chapter 2.2.1.2) before being transiently transfected into the HEK293T-cells. For transient transfection, 3 x 10^5 HEK293T-cells in supplemented RPMI-1640 cell culture medium, were seeded per well in a 6-well plate before being incubated at 37 °C overnight with 5 % CO_2. Thereafter, 3 µg of pcDNA-TOPO-gp120 plasmid was mixed with 9 µL polyethyleneimine (PEI) (1 mg/mL) in 400 µL of the supplement-free medium. The mixture was vortexed for 15 seconds before being incubated at room temperature for 20 minutes. Before the addition of the DNA-PEI complex, 1.5 mL fresh medium was added to each well and the complex was added gently in a dropwise manner. The HEK293T-cells were incubated at 37 °C with 5 % CO_2 for 6 hours. The medium was changed thereafter, and the cells were incubated for a further 48 hours. The cells were subsequently washed gently with 1x PBS twice before being incubated with 500 µL cold RIPA (Table 2.1.2) buffer on ice for 5 minutes. The cells were then resuspended, and the lysate was transferred to a microcentrifuge tube before being centrifuged at 13 000 rcf for 5 minutes. The protein was separated by SDS-PAGE and transferred onto nitrocellulose membrane where gp120 was detected using sheep anti-gp120 (ARP #288) and horseradish peroxidase goat-anti-sheep IgG (Santa Cruz 2473). As a positive control, HIV-1 IIIB gp120 Recombinant Protein (Cat # 11784) was used, having been obtained from the NIH AIDS reagent program (https://www.aidsreagent.org/).

2.2.4.2 Cell-surface binding study by confocal microscopy

To assess cell-surface binding of the enriched SNAP fusion protein on Env protein-expressing HEK293T-cells, the protein J3-SNAP (5 µM) was conjugated to the SNAP-Surface® Alexa Fluor® 488 (10 µM) to achieve a protein to fluorophore molar ratio of 1:2, in the presence of 1 mM DTT, and incubated for 30 minutes 37 °C in the dark. Thereafter, 3 x 10^5 Env protein-expressing HEK293T-cells were seeded in supplemented RPMI-1640 medium in a 4-chambered 30 mm dish and allowed to settle overnight. The cells were washed with 1x PBS

twice before being incubated with 2 µg of protein in 100 µL of 1x PBS for 30 minutes on ice. Unbound protein was washed off. The cells were then stained with Hoechst 33342 (1 µg/mL) in supplemented-free media for 10 minutes. The cells were washed with 1x PBS before being viewed using a Zeiss LSM 880 confocal microscope operated using ZEN software (Zeiss, South Africa).

2.2.5 Development of J3-ETA

Following the expression of J3-SNAP in bacteria and the conformation of functional activity by successful binding to Env protein-expressing HEK293T-cells, J3-ETA was developed as described in Chapter 2.2.1.

Chapter 3: Results

3.1 Development of J3-SNAP

Advances in medicine in general and antiretroviral therapy, in particular, have resulted in the development of cART capable of reducing viremia to undetectable levels (< 40 copies/mL) [103]. The initiation of cART has been shown to allow the restoration of immune competence [232], [233]. To prevent a relapse of viremia, however, lifelong cART must be maintained. This brings about increased likelihood of off-target toxicity and drug-drug interactions related to antiretroviral therapy [234]–[236]. Curative strategies are being investigated to combat the HIV/AIDS epidemic, which has claimed more than 38 million lives, but no cure has been found to date. Cardinal strides in the quest for an HIV vaccine have been made through the discovery of neutralizing antibodies capable of specific binding to the HIV Env protein expressed in various HIV subtypes [208]. One study tested isolated VHH nanobodies from immunised llamas for binding against one hundred HIV strains and found that one antibody (J3) was able to neutralise more than 95 % of the tested strains. Therefore, the major aim of this study was to determine whether functional J3-SNAP fusion protein could be expressed in *E. coli* BL21 DE3. Upon confirmation of functionality by cell-surface binding to Env protein-expressing cells, *in silico* design and molecular cloning of J3-ETA was commenced.

3.1.1 pMT-J3-SNAP *in silico* cloning

The *in silico* cloning began with the analysis of the plasmid vector pMT-H22-SNAP and pMT-H22-ETA. This was carried out to identify the appropriate restriction endonuclease sites for the introduction of the gene of interest. To realise the cloning of J3-SNAP and J3-ETA (as described in Chapter 2.2.1), a single-domain heavy-chain nanobody (VHH) sequence (J3) targeting HIV was obtained from patent no. WO 2013/036130 AI. To analyse the sequence of J3, validate the V gene, and identify the FR and CDR regions, the sequence was aligned to the human germline sequence IgHV3 using the IMGT V-QUEST tool (www.imgt.org/imgt_vquest) and validated by IgBLAST (https://www.ncbi.nlm.nih.gov/igblast/). J3 was validated to be a VH chain and shared a 64.87 % sequence identity to the human germline sequence. J3 exhibited a shorter CDR2 region when compared to the germline sequence and the variation from the germline sequence are represented in bold text (Figure 3.1A). J3 gene was modified to introduce restriction endonuclease cleavage sites to allow for incorporation into a suitable protein expression vector. SnapGene® software (v.5.0.8, GSL Biotech LLC, USA) was used for the *in silico* cloning of J3, where a simulation of J3 restriction endonuclease digest of J3 and subsequent ligation to a

suitable bacterial expression vector was performed. J3 was ligated to the pMT bacterial expression plasmid *in silico* as described in Figure 3.1 B. The resulting plasmids were designated pMT-J3-SNAP and pMT-J3-ETA (Figure 3.1 C-D). The MW and pI of J3-SNAP was estimated using the ExPASy translate tool (https://web.expasy.org/translate/) and the ExPASy compute pI/MW tool (https://web.expasy.org/cgi-bin/compute_pi/pi_tooland theorised to be approximately 37.55 kDa and 6.59 respectively. J3 was thereafter commercially synthesised as a gene fragment.

A

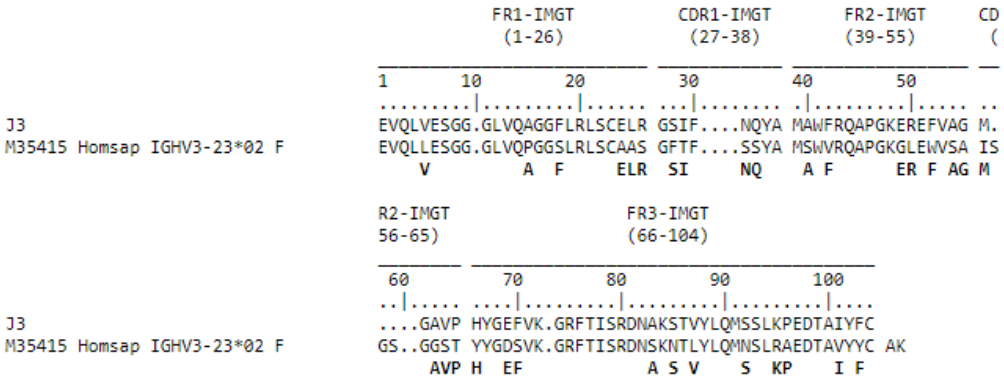

B

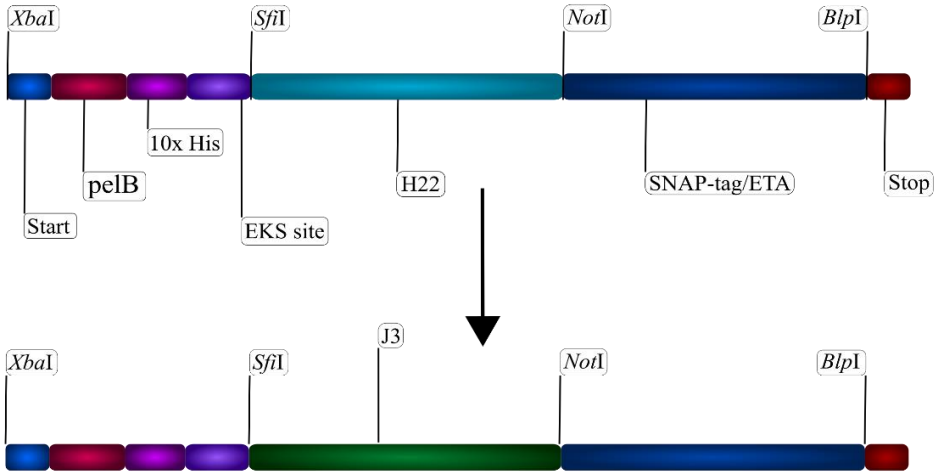

C

D

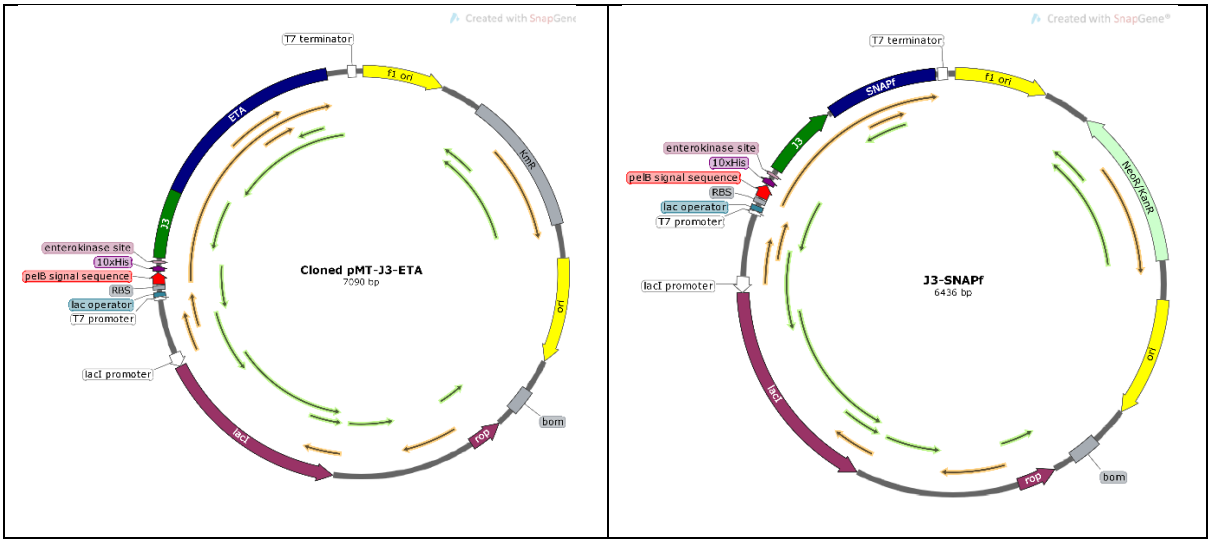

Figure 3.1: *In silico* design of the expression plasmids for pMT-J3-SNAP and pMT-J3-ETA. A) The amino acid sequence of J3 obtained from patent no. WO 2013/036130 AI, analysed by IMGT V-QUEST tool (www.imgt.org/imgt_vquest), aligned with a human germline sequence. FR and CDR regions identified. B) Open reading frame (ORF) of J3 (VHH) digested using restriction endonucleases *Sfi*I and *Not*I replacing H22 digested with the same restriction endonucleases to create J3-ETA and J3-SNAP. C) Plasmid vector map of pMT-J3-ETA containing the J3 (VHH) gene and pseudomonas exotoxin A (ETA). D) Plasmid vector map of pMT-J3-SNAP containing the J3 (VHH) gene and SNAP-tag. Both C and D plasmid vectors also contain the following genes; F1 bacteriophage origin of replication; kanamycin/neomycin resistance gene; the origin of replication; the basis of mobility region pBR322, which confers plasmid conjugation; Rop gene, which maintains plasmid at high copy number; LacI, the lac repressor gene bind to the lac operator and inhibits transcription in *E. coli* until the addition of isopropyl β- d-1-thiogalactopyranoside (IPTG); lacI promoter region; T7 promoter region for T7 bacteriophage RNA polymerase; RBS, ribosome binding site for RNA polymerase; **pelB signal sequence, signals that protein should be translocated to the periplasmic space of bacteria; 10x histidine affinity tag; EKS, enterokinase recognition and cleavage site; J3 (VHH) gene; ETA or SNAP-tag gene; T7 terminator, transcription termination site for T7 bacteriophage RNA polymerase.** (open reading frame in bold text) [as described in Chapter 2.2.1.1]

3.1.2 Development of pMT-J3-SNAP

The synthesised gene fragment of J3 was amplified by PCR using Phusion DNA polymerase (1000 U/mL) [Table 2.2.1]. The PCR amplicon was analysed by agarose gel electrophoresis. The PCR amplicon of J3 (Figure 3.2 A) was visualised at the expected size of approximately 380 bp. J3 was thereafter excised from the agarose gel and purified before being digested by *Sfi*I and *Not*I restriction endonucleases. The restriction endonuclease digested J3 was further analysed by agarose gel electrophoresis and visualised at approximately 380 bp before being again excised from the agarose gel and purified (as detailed Chapter 2.2.1.5).

To generate pMT-J3-SNAP, 3 µg of sequence-validated pMT-H22-SNAP plasmid was digested with *Sfi*I + *Not*I restriction endonucleases to replace H22 (scFv) by J3 [Table 2.2.3]. 50 µL of restriction endonuclease-digested pMT-H22-SNAP was subsequently mixed with 1:6 dilution of Gel Loading Dye, Purple (6X) [NEB - #B7024S] and analysed by agarose gel (1.2 % v/v) electrophoresis at 120 V for 1 hour (as described in Chapter 2.2.1.5). Successful restriction endonuclease digestion was confirmed by the presence of two distinct bands at approximately 800 bp (H22) (Figure 3.2 B) and 6 kb (pMT-SNAP) for the *Sfi*I + *Not*I digests. Restriction endonuclease digests were run in triplicate. Undigested pMT-H22-SNAP was used as a negative control. Single-enzyme digests with either *Sfi*I or *Not*I were included as positive controls.

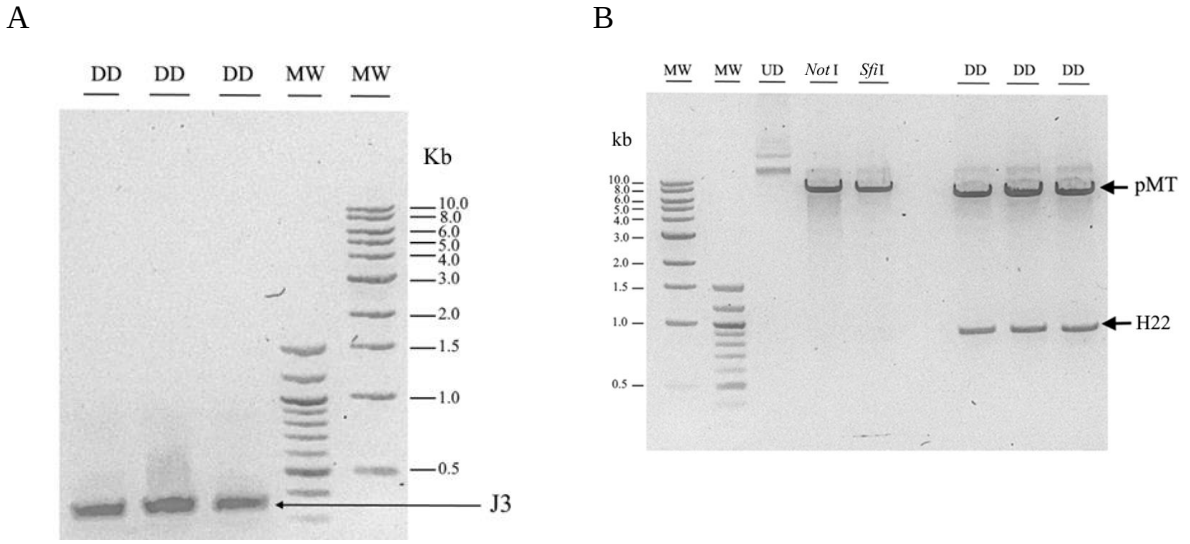

Figure 3.2: Construction of pMT-J3-SNAP by polymerase chain reaction amplification of J3 and endonuclease digest of J3 and pMT-H22-SNAP. A) 1 ng of J3 was amplified by PCR. 20 µL of PCR product was mixed with Gel Loading Dye, Purple (6X) [NEB - #B7024S] (1:6 dilution) and analysed by agarose gel electrophoresis. J3 was then excised and purified from agarose gel. J3 (A) and 3 µg of pMT-H22-SNAP (B) were digested using 1000 U/mL *Sfi*I and *Not*I restriction endonucleases for 3 hours at 50 °C and overnight at 37 °C respectively. 50 µL of digest product was mixed with 1:6 dilution of Gel Loading Dye, Purple (6X) [NEB - #B7024S] immediately before being loaded onto an agarose gel. Gels A and B were 1.2 % agarose gels run at 120 V for 1 hour before being viewed under blue light excitation (470 nm). UD – undigested control. NotI/SfiI - single-enzyme digest control. DD, double enzyme digest. MW – molecular weight marker (as detailed in Chapter 2.2.1).

The insert, J3, and the plasmid vector, pMT-SNAP, were ligated using their 5'-phosphorylated and 3'-hydroxylated compatible ends generated through *Sfi*I + *Not*I restriction endonuclease digestion. For this reaction, 9 ng and 14 ng of J3 was ligated to using T4 DNA ligase 50 ng of pMT-SNAP in a 3:1 and 5:1 insert-to-vector molar ratio, respectively (Table 2.2.4). The ligation reaction product, pMT-J3-SNAP, was transformed into chemically competent DH5α

E. coli cells before being grown on LB-agar plates supplemented with kanamycin (50 µg/mL) overnight at 37 °C. A vector + ligase control was included as a negative control that lacks the insert J3 and hence has linearized plasmid. Nevertheless, we observed a colony-forming units (CFU) value of 0.61 x 10^4 in the negative control (Figure 3.3 A). The CFU for the 3:1 (Figure 3.3 B) and 5:1 (Figure 3.3 C) test samples were approximately 5.52 x 10^4 and 4.72 x 10^4 respectively.

A

pMT-SNAP

vector-only control

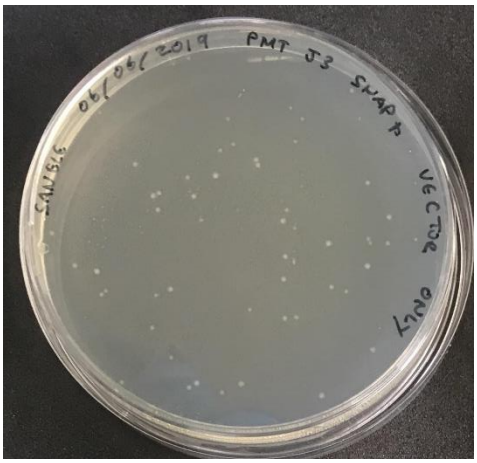

B

pMT-J3-SNAP

(3:1)

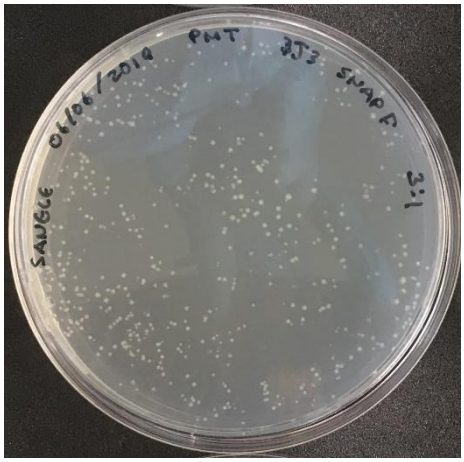

C

pMT-J3-SNAP

5:1

Figure 3.3: DH5α *E. coli* cells transformed with pMT-J3-SNAP grown on LB-Agar plates supplemented with kanamycin. Recombinant pMT-J3-SNAP plasmids generated through ligation of J3 to pMT-SNAP with an insert to vector ratio of 3:1 and 5:1 for each were transformed in DH5α *E. coli* cells as described and were subsequently grown on kanamycin-supplemented (50 µg/mL) LB-Agar plates for 16 hours at 37 °C. Kanamycin was used as selection pressure, allowing only cells that have taken up ligated circular recombinant plasmid to grow (as detailed in Chapter 2.2.1.7).

To verify the identity of the plasmids contained within the bacterial clones in Figure 3.3 B and C, four colonies were selected at random from each plate and inoculated into 5 mL LB-broth media supplemented with 50 µg/mL of kanamycin. The inoculated 5 mL cultures were incubated to grow overnight at 37 °C, after which, 4 mL of the 5 mL was used for miniprep plasmid isolation. The isolated plasmid (pMT-J3-SNAP) was subsequently used for restriction endonuclease mapping using *Pvu*II. pMT-H22-SNAP was used as a control. 100 µg of the plasmid (pMT-J3-SNAP and pMT-H22-SNAP) was digested using 1000 U/mL of *Pvu*II at 37 °C for 2 hours before being analysed by agarose gel electrophoresis (Table 2.2.3). SnapGene® software (v.5.0.8, GSL Biotech LLC, USA) was used to simulate an agarose gel depicting the DNA fragments resulting from the *Pvu*II restriction endonuclease digest of either pMT-H22-SNAP or pMT-J3-SNAP (Figure 3.4 A). The simulation predicted that pMT-H22-SNAP digested using *Pvu*II resulted in three fragments of sizes 3724 bp, 1599 bp, and 999 bp. The simulation predicted that pMT-J3-SNAP digested using *Pvu*II resulted in two fragments of sizes 5344 bp and 999 bp. Consistently, the agarose gel (Figure 3.4 B) depicted that pMT-H22-SNAP digested using *Pvu*II resulted in three bands at the approximate size of the simulated gel. Although all four of the 3:1 and three of the 5:1 insert-to-vector ratio colonies corresponded to the SnapGene® simulation, one of the 5:1 ratio colonies (Figure 3.3 C) appeared similar to the pMT-H22-SNAP control instead of pMT-J3-SNAP (Figure 3.4 B – lane 8). Furthermore, rather than a 999 bp band in the 3:1 and 5:1 colonies, a 1599 bp band was observed. Nevertheless, the clones that appeared as expected were inoculated into 50 mL LB-broth cultures supplemented with 50 µg/mL of kanamycin overnight at 37 °C. Thereafter, the recombinant pMT-J3-SNAP plasmid was isolated by alkaline lysis method (as detailed in Chapter 2.2.1.2) and analysed by Sanger sequencing (Figure 3.4 D). Subsequent sequence alignment of Sanger sequences to the consensus sequence confirmed that the selected clones did indeed contain pMT-J3-SNAP. The Sanger sequencing also highlighted a mutation in the form of a deletion of a base pair. A nucleotide was missing between J3 and SNAP, resulting in a frameshift mutation and the introduction of premature stop codons in the open reading frame.

A

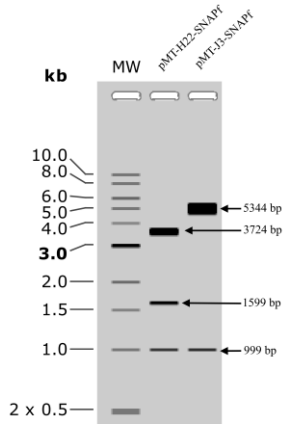

B

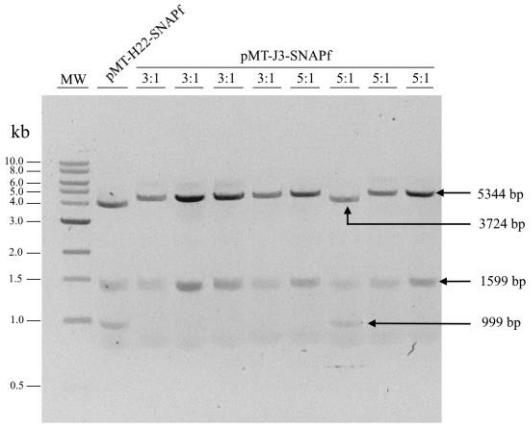

C

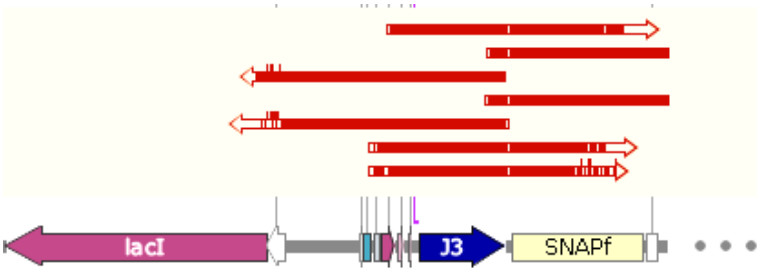

D

Figure 3.4: pMT-J3-SNAP Sequence confirmation by restriction endonuclease mapping of the recombinant plasmid. A) SnapGene® software (v.5.0.8, GSL Biotech LLC, USA) was used to simulate an agarose gel of pMT-H22-SNAP and pMT-J3-SNAP digested using *Pvu*II. B) 3 µg pMT-H22-SNAP, pMT-J3-SNAP was digested using 1000 U/mL of restriction endonuclease *Pvu*II at 37 °C overnight. 50 µL of restriction endonuclease digest product was mixed with a 1:6 dilution of Gel Loading Dye, Purple (6X) [NEB - #B7024S] and run on 1.2 % agarose gel at 120 V for 1 hour before being visualised under blue light excitation (470 nm). C-D) Alignment of J3-SNAP Sanger sequences to the consensus sequence (as detailed in Chapter 2.2.1.8).

3.1.3 Nucleotide base insertion by overlap-extension PCR

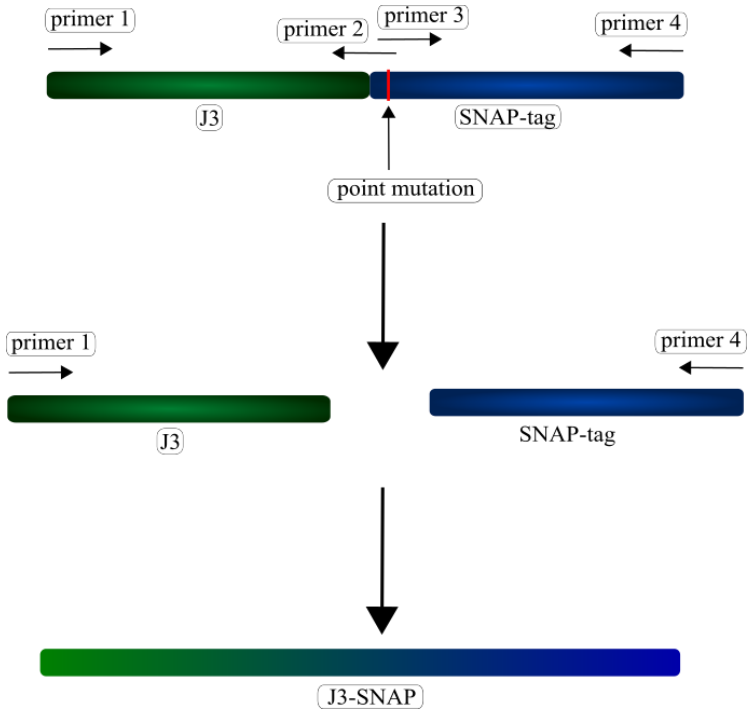

Figure 3.5: Illustration of point mutation by overlap-extension PCR. Primers J3-F2 and J3-R2 are used to amplify J3 in one reaction tube. Primers SNAP-F1 and SNAP-R1 and used to amplify SNAP-tag in a separate reaction tube. Primers J3-F2 and SNAP-R1 and used to join the J3 amplicon and the SNAP-tag amplicon. Primers J3-R2 and SNAP-F1 overlap over the site of the point mutation, binding to separate strands (Table 2.2.1).

To insert the missing nucleotide, overlap-extension PCR was used as illustrated in Figure 3.5. Four primers (Table 2.1.5) were designed to amplify J3 and SNAP individually from the mutated pMT-J3-SNAP plasmid vector. Two external primers were designed to bind to the different strands of DNA: a J3 forward primer (J3-F2) and a reverse primer for SNAP (SNAP-R1). Two internal primers were designed, which overlap with one another overlapping at the mutated region and binding to different strands: a reverse primer for J3 (J3-R2) and a forward primer for SNAP (SNAP-F1). J3 and SNAP were amplified separately by PCR (Table 2.2.1). PCR product was thereafter analysed by agarose gel electrophoresis (as described in Chapter 2.2.1.5). The individually amplified J3 and SNAP were excised from the agarose gel and purified before being joined together using the J3 forward primer and SNAP reverse primer in a second PCR step. PCR-amplified DNA was separated by agarose gel electrophoresis and the band corresponding to J3-SNAP was excised from the agarose gel and purified. Subsequently, the purified J3-SNAP DNA was digested using *Sfi*I and *Blp*I restriction endonucleases (Table 2.2.3), and the digest products were separated by agarose gel electrophoresis (Figure 3.6 D). Thereafter, J3-SNAP (*Sfi*I-*Blp*I) was excised from the agarose gel and purified. Concurrently,

the mutated pMT-J3-SNAP plasmid was digested using *Sfi*I + *Blp*I to remove the mutated J3-SNAP from the plasmid vector. Mutated pMT-J3-SNAP digested by *Sfi*I + *Blp*I was subsequently analysed by agarose gel electrophoresis. SnapGene® software (v.5.0.8, GSL Biotech LLC, USA) was used to simulate PCR amplicons of J3, SNAP, and J3-SNAP, as well as a restriction endonuclease digest of mutated pMT-J3-SNAP plasmid vector (Figure 3.6 A). The SnapGene® simulation predicted that J3 amplified would result in a 390 bp fragment (Figure 3.6 A – lane 2). This correlated with the agarose gel. A band was seen at approximately 400 bp (Figure 3.6 B – lanes 2-5). Accordingly, the SnapGene® simulation predicted that the amplified SNAP would be at 576 bp (Figure 3.6 A – lane 3), and on the agarose gel, a band was seen at approximately 600 bp (Figure 3.6 B – lanes 6-10). PCR-amplified J3-SNAP was visualised at approximately 900 bp (Figure 3.6 C), which corresponded to the simulated amplicon of 957 bp (Figure 3.6 A -lane 3). Mutated pMT-J3-SNAP digested with *Sfi*I and *Blp*I was expected to have two fragments, at 5499 bp, and at 930 bp, which corresponded with the experimental result (Figure 3.6 E). The PCR-generated J3-SNAP and the pMT plasmid vector without the defective J3-SNAP were extracted from the agarose gel and purified for the ligation reaction.

A

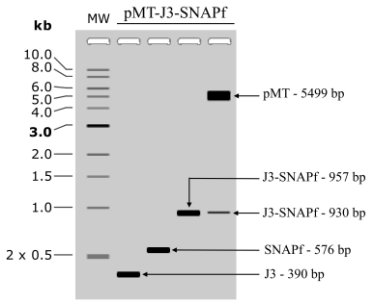

B

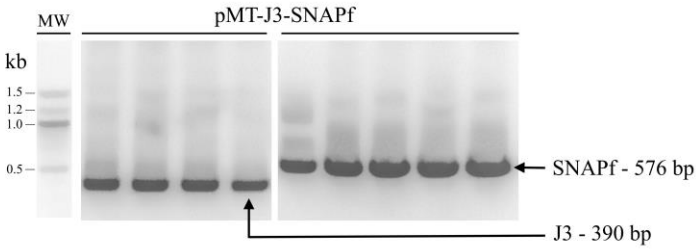

C

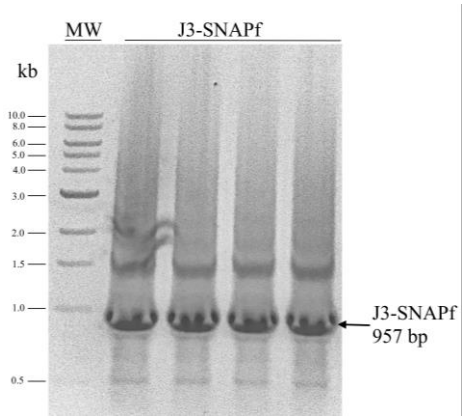

D

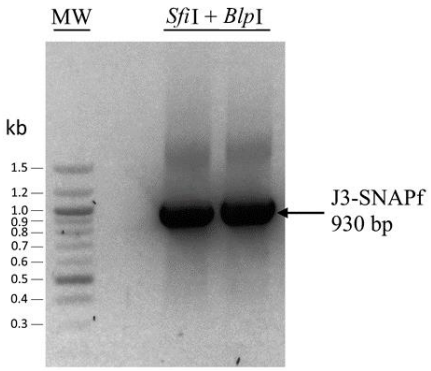

E

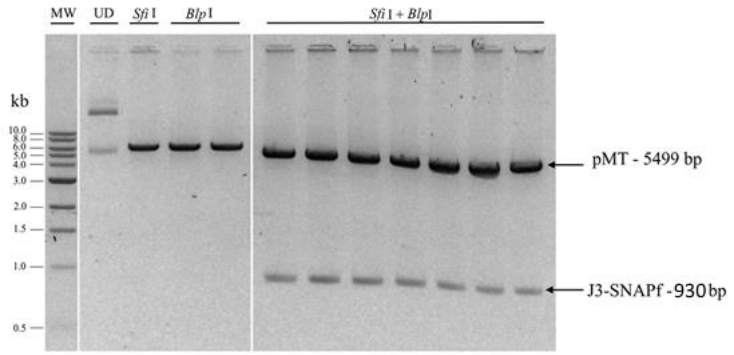

F

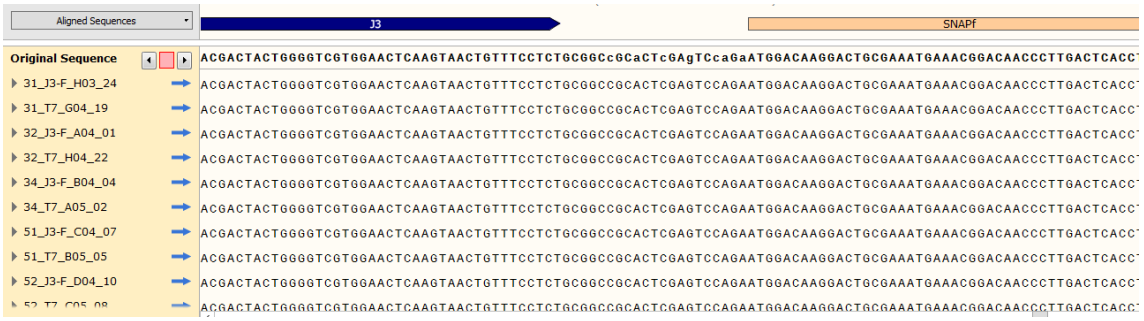

Figure 3.6: Nucleotide insertion by overlap extension PCR. J3 and SNAP were amplified individually by PCR using two external primers and two overlapping internal primers, then amplified using the external primers to make J3-SNAP. A) SnapGene® software (v.5.0.8, GSL Biotech LLC, USA) was used to simulate an agarose gel depicting PCR-amplified J3 (lane 2), SNAP (lane 3), J3-SNAP (lane 4), and *Sfi*I + *Blp*I digested pMT-J3-SNAP (lane 5). B) J3-specific and SNAP-specific primers were used to amplify J3 and SNAP from pMT-J3-SNAP. C) J3 and SNAP were fused using external primers. D) J3-SNAP was digested using *Sfi*I + *Blp*I at 50 °C for 3 hours and 37 °C overnight respectively. E) pMT-J3-SNAP was digested using *Sfi*I + *Blp*I at 50 °C for 3 hours and 37 °C overnight respectively. UD - undigested, *Sfi*I, and *Blp*I single enzyme digested controls were included. 50 µL of PCR and digest products were mixed with a 1:6 dilution Gel Loading Dye, Purple (6X) [NEB - #B7024S] and analysed using a 1.2 % agarose gel at 120 V for 1 hour before being viewed under blue light excitation (470 nm) (as detailed in Chapter 2.2.1). F) Alignment of J3-SNAP Sanger sequences to the consensus sequence (as detailed in Chapter 2.2.1.8).

T4 DNA ligase (1000 U/mL) was used to ligate the J3-SNAP insert into the pMT plasmid vector in a 3:1 (24 ng – 50 ng), and a 5:1 (42 ng – 50 ng) insert to vector molar ratio. A vector + ligase control comprised of the linearized vector without the insert was included. The ligation product was transformed into DH5α *E. coli* cells before being inoculated on LB-agar plates supplemented with 50 µg/mL kanamycin and incubated overnight at 37 °C. Colonies were selected from the 3:1 and the 5:1 LB-agar plates at random and inoculated into 5 mL LB-broth medium supplemented with 50 µg/mL of kanamycin and incubated at 37 °C overnight. The pMT-J3-SNAP plasmid was isolated from the cultures by miniprep plasmid isolation before being analysed by Sanger sequencing. Multiple sequence alignment of the Sanger sequences to the consensus sequence (Figure 3.6 F) showed thatJ3-SNAP had been successfully inserted

into the pMT plasmid vector without any nucleotides missing. For protein expression, pMT-J3-SNAP DNA confirmed by Sanger sequencing was transformed into *E. coli* BL21 DE3 cells, which were inoculated onto LB-agar plates supplemented with kanamycin (50 µg/mL). The CFU/mL values were 0.34 x 10^4 and 1.5 x 10^5 for the untransformed control plate and test plate respectively.

A **B**

Bacteria only control **pMT-J3-SNAP**

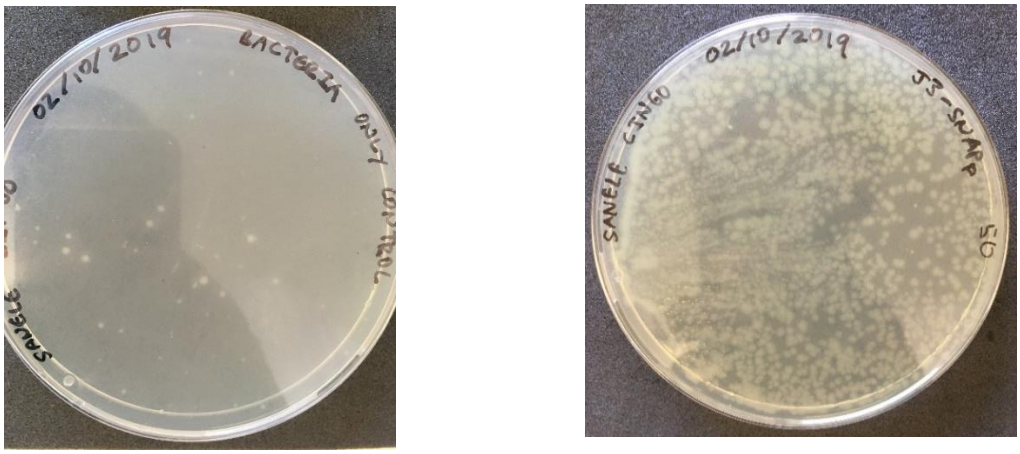

Figure 3.7: LB-agar plates with BL21 DE3 *E. coli* cells transformed with pMT-J3-SNAP. 1200 ng of recombinant plasmid pMT-J3-SNAP was transformed into *E. coli* Bl21 DE3 cells. Transformed cells were inoculated on LB-agar plates supplemented with 50 µg/mL of kanamycin. Plates were incubated at 37 °C for 16 hours (as detailed in Chapter 2.2.2.1).

3.1.3 Osmotic-stress expression in the presence of compatible solutes

As described in Chapter 2.2.2, a single colony was inoculated into a 50 mL culture of TB media supplemented with 50 µg/mL of kanamycin before being incubated at 28 °C overnight. 40 mL of this "starter culture" was inoculated into 2.8 L of TB "main culture" supplemented with 50 µg/mL of kanamycin before being incubated at 26 °C. Osmotic stress was induced by adding 4 % NaCl in the presence of compatible solutes (0.5M sorbitol, 40 mM glycine-betaine, 0.5 mM ZnCl) when the OD_{600} value reached 1.6. After 30 minutes, 1 M IPTG was added to induced periplasmic expression. The culture was allowed to grow for 16 hours at 26 °C. The bacterial cells were centrifuged at 4000 rcf for 10 minutes at 4 °C before being resuspended in cell lysis buffer (75 mM Tris HCl, 300 mM NaCl, 5 mM DTT, protease inhibitor cocktail, 10 % v/v glycerol). The protein was extracted from the periplasmic space by sonication for 2 minutes. The bacterial lysate was subsequently centrifuged at 24 000 rcf for 30 minutes at 4 °C. The supernatant was filtered using a 0.45 µM syringe filter before being applied onto a HisTrap™ High Performance column (GE Healthcare, 17-5247-01). Protein interaction with

the column was facilitated by the 10x histidine tags located on the N-terminus of J3-SNAP. Imidazole was used to elute the protein from the column through competitive binding (Buffers – Chapter 2.1.2). Eluted fractions were collected and analysed by SDS-PAGE, where 15 µL of each fraction of eluted protein was mixed with 5 µL 4x Laemmli Sample Buffer (Bio-rad, USA #1610747) and resolved on a 7.5 % acrylamide gel. SDS-PAGE allowed separation of protein, based on molecular weight and thus visualization of the protein of interest. SDS-PAGE was performed at 80 V for 30 minutes, then 120 V for 1 hour. The acrylamide gel was then stained with AcquaStain® protein gel stain for no less than 30 minutes before being visualised (Figure 3.8 A-B). In Figure 3.8 A, multiple protein bands were observed from lanes 1 - 9, corresponding to the order in which the fractions were eluted from the HisTrap™ High Performance column (GE Healthcare, 17-5247-01). Distinct and consistent protein bands were observed at approximately 72 kDa and 70 kDa, at 46 kDa, 34 kDa, 32 kDa, and at 26 kDa. Figure 3.8 B shows the remaining fractions eluted from the HisTrap™ High Performance column (GE Healthcare, 17-5247-01) and were represented in the order in which they were eluted. The bands at 72 kDa and 70 kDa persisted, together with the bands at 34 kDa, 32 kDa, and 26 kDa. The concentration of the protein appeared to intensify in Figure 3.8 B from lanes 4 - 8, with more distinct bands of the protein at approximately 32 kDa (suspected to be J3-SNAP). To verify the identity of the protein purified, the protein fractions depicted in Figure 3.8 B were pooled and concentrated using a 50 kDa column. To select for and concentrate the protein of interest, protein concentration was performed using a 50 kDa and a 10 kDa Amicon® Ultra-15 centrifugal filter unit. Fractions from Figure B 1 - 9 were pooled applied to a 50 kDa Amicon® Ultra-15 centrifugal filter unit and centrifuged at 4000 rcf for 25 minutes at 4 °C. The flow-through was thereafter concentrated using a 10 kDa Amicon® Ultra-15 centrifugal filter unit which further excluded all proteins below 10 kDa. The total concentrated protein was then quantified at 280nm using the Denovix DS-11 spectrophotometer (Alliance Global, USA) and determined to be 0.42 mg/mL in a total volume of 1 mL, from a 3-litre culture.

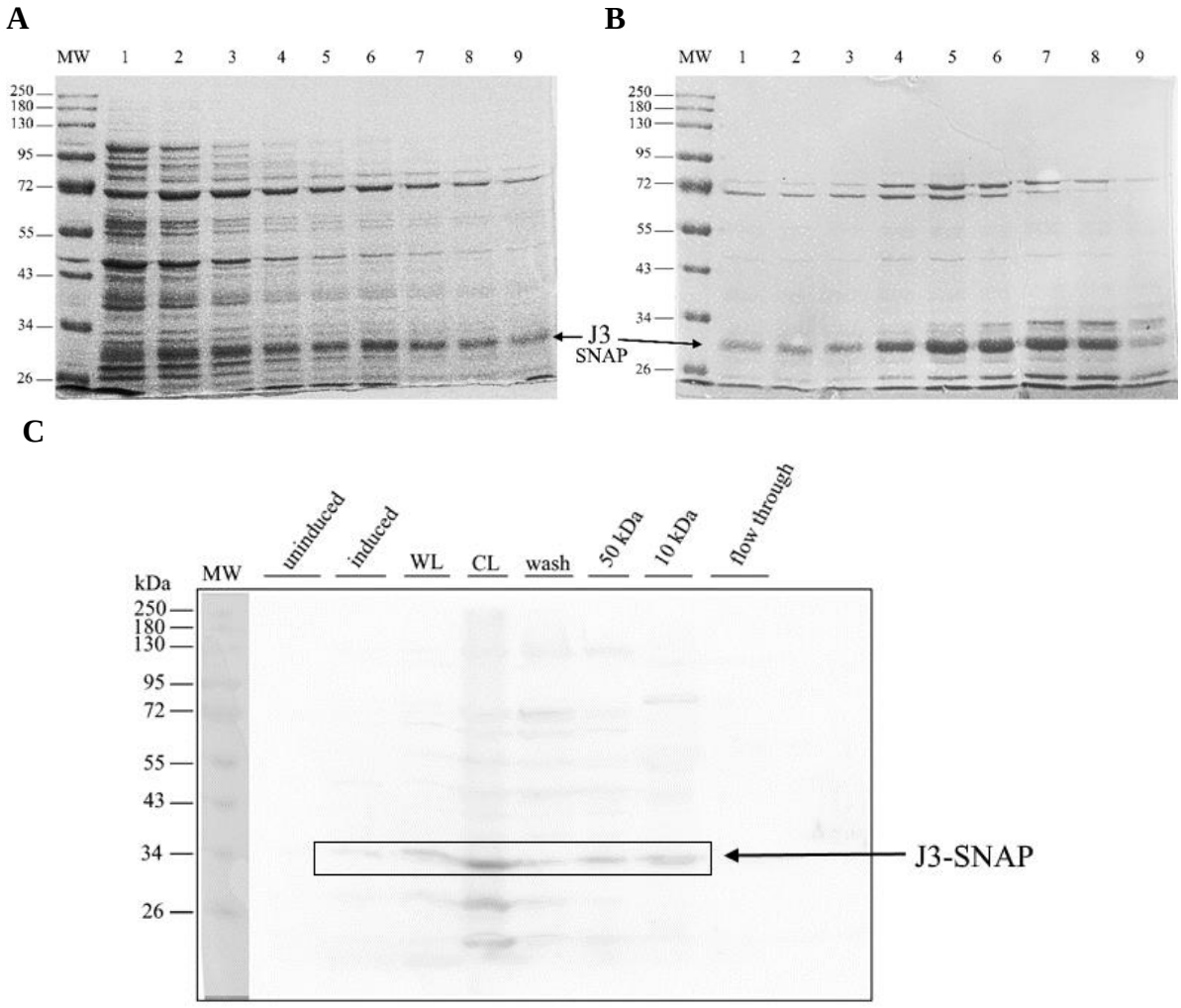

Figure 3.8: Purification of J3-SNAP by immobilised-metal affinity chromatography. Following the periplasmic expression of J3 in *E. coli*, fractions of his-tagged protein were analysed by SDS-PAGE using a 10 % (w/v) acrylamide gel (A & B). 15 µL of the fraction was mixed with 5 µL of 4x Laemmli Sample Buffer (Bio-rad, USA #1610747) before being boiled and analysed by SDS-PAGE. Fraction were eluted at 7 % imidazole (A) then 60 % (B). C) cell lysates and fractions [uninduced – 5 µL; induced 5 µL; who-cell lysate (WL) – 10 µL; cleared-cell lysate (CL) – 10 µL; wash – 20 µL; >50 kDa fractions – 15 µL, >10 kDa fractions – 15 µL; flow-through – 20 µL] were mixed with 5 µL of 4x Laemmli Sample Buffer (Bio-rad, USA #1610747) before being analysed by SDS-PAGE at 120 V for 1 hour. Protein was then transferred to nitrocellulose membrane at 90 V for 2 hours. Rabbit anti-His tag antibody (Cell Signalling Technologies, USA) and goat anti-rabbit horseradish peroxidase-conjugate antibody (Bio-rad Laboratories, USA) were used to detect His-tag protein. Pierce™ ECL Plus Western blotting Substrate (Thermo Scientific, USA #32134) was used to detect chemiluminescence (as described in chapter 2.2.3).

The concentrated protein was analysed by SDS-PAGE and Western blot, together with cell lysates including "induced", "uninduced", "whole-cell" and "cleared cell" lysate. Rabbit anti-histidine primary antibody (Cell Signalling Technologies, USA) and goat anti-rabbit horseradish peroxidase-conjugate antibody (Bio-rad Laboratories, USA) were used to detect

10x histidine in the cell lysates. In Figure 3.8 C, no bands were visible in the “uninduced cell lysate” sample. Two faint bands were visible at approximately 34 kDa and 26 kDa in the “induced” lysate “whole-cell” lysate, “cleared cell” lysate, “wash”, “50 kDa” fraction, and “10 kDa” samples. The third band below 26 kDa was observed for the “cleared cell” lysate and “wash” samples.

3.1.4 Generation of Env protein-expressing HEK293T-cells

To generate an Env protein-expressing cell line on which to evaluate the functionality of J3-SNAP, plasmid DNA (pcDNA-TOPO-gp120), kindly donated by Dr. Zenda Woodman (University of Cape Town, South Africa), encoding recombinant full-length Env protein subtype C was transfected using polyethyleneimine (PEI) into HEK293T-cells for cell-surface expression. For this experiment (as described in Chapter 2.2.4.1), 3 x 10^5 HEK293T-cells were seeded per well in a 6-well plate before and incubated at 37 °C overnight with 5 % CO_2. The following day, 3 µg of pcDNA-TOPO-gp120 plasmid was mixed with 9 µL PEI (1 mg/mL) in supplement RPMI medium and vortexed for 15 seconds and incubated at room temperature for 20 minutes. Before the addition of the DNA-PEI complex, 1.5 mL fresh medium was added to each well and the complex was added gently in a dropwise manner. The HEK293T-cells were incubated at 37 °C with 5 % CO2 for 6 hours. The medium was changed thereafter, and the cells were incubated for a further 48 hours. To assess if Env protein had been expressed, the cells were washed with 1x PBS, lysed with RIPA buffer (Table 2.1.2), and centrifuged at 13 000 rcf for 5 minutes. The cellular protein was separated by SDS-PAGE and transferred onto a nitrocellulose membrane where gp120 of the Env protein was detected using sheep anti-gp120 (ARP #288) and horseradish peroxidase goat-anti-sheep IgG (Santa Cruz 2473). Bands were observed at approximately 160 kDa and 42 kDa across all samples. The bands at 160 kDa were thought to be that of the Env protein (gp120 + gp41 complex), and β-actin was detected at 42 kDa (Figure 3.9).

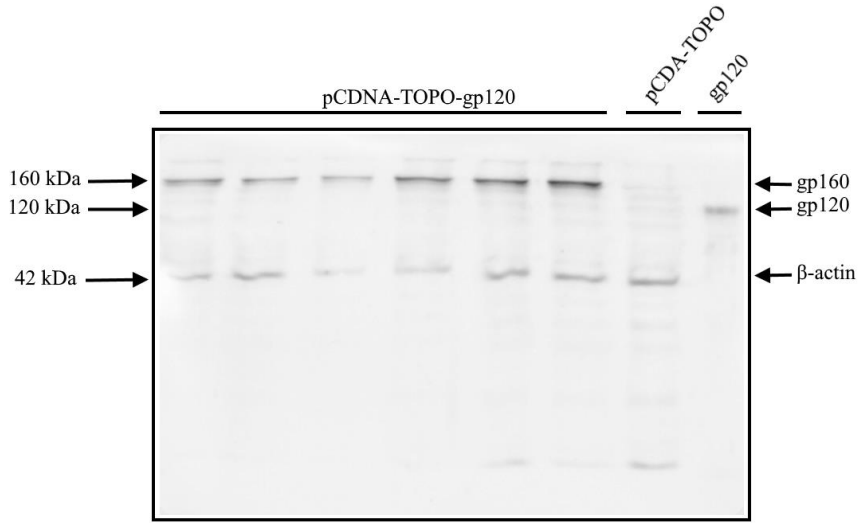

Figure 3.9: Cell-surface expression of HIV Env protein in HEK293T-cells. Recombinant pcDNA-TOPO-gp120 (3 µ) plasmid was transfected into HEK293T-cells using PEI (9 µL) (1 mg/mL). After 48 hours, cells were lysed using RIPA buffer (Table 2.1.2) and centrifuged at 15 000 rcf for 5 minutes. 20 µL of supernatant was mixed with 5 µL of 4x Laemmli Sample Buffer (Bio-rad, USA #1610747) and analysed by SDS-PAGE at 120 V for 1 hour. Protein was transferred onto a nitrocellulose membrane at 80 V for 2 hours. Sheep anti-gp120 (ARP # 288) and Horseradish Peroxidase-Goat anti-sheep IgG (Santa Cruz 2473) were used to detect HIV Env. Mouse anti-actin and goat anti-mouse IgG were used to detect β-actin. Pierce™ ECL Plus Western blotting Substrate (Thermo Scientific, USA #32134) was used to detect chemiluminescence. pcDNA without Env DNA was used as a negative control. Recombinant gp120 protein was used as a positive control (as described in Chapter 2.2.4.1).

3.1.5 Evaluation of the binding of J3-SNAP-Alexa Flour ® 488 to envelope protein localised on the surface of HEK293T-cells

After generating an Env protein-expressing cell line, the cell-surface binding of J3-SNAP conjugated to SNAP-Surface® Alexa Fluor® 488, to the surface of Env protein-expressing cells was evaluated by confocal microscopy. For this experiment, 3 x 10^5 Env protein-expressing HEK293T-cells were seeded per well in a 6-well plate before and incubated at 37 °C overnight with 5 % CO_2. The protein J3-SNAP was conjugated to 10 µM of SNAP-Surface® Alexa Fluor® 488 in the presence of DTT and incubated at 37 °C for 30 minutes (Figure 1.6). Env protein-expressing HEK-293T-cells were incubated with 2 µg of J3-SNAP-Alexa Flour® 488 for 30 minutes on ice before being visualised by confocal microscopy. A green signal was observed on the surface of the HEK293T-cells (Figure 3.10 A). The cell nucleus was visualised using Hoechst 33343 (Figure 3.10 B) [as described in Chapter 2.2.4.2].

A **B**

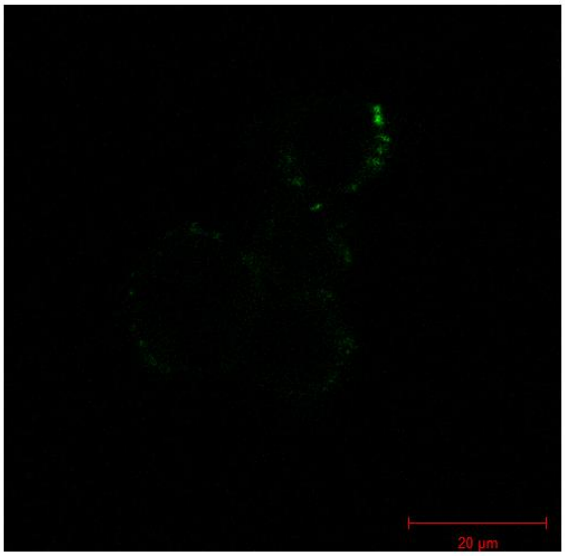

SNAP-Surface® Alexa Fluor® 488

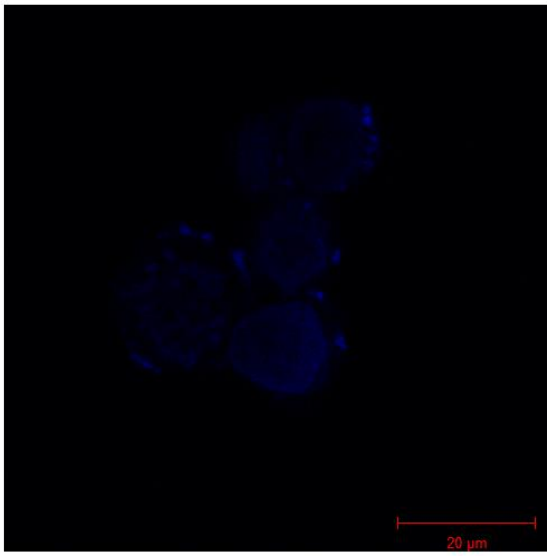

Hoechst 33342

C

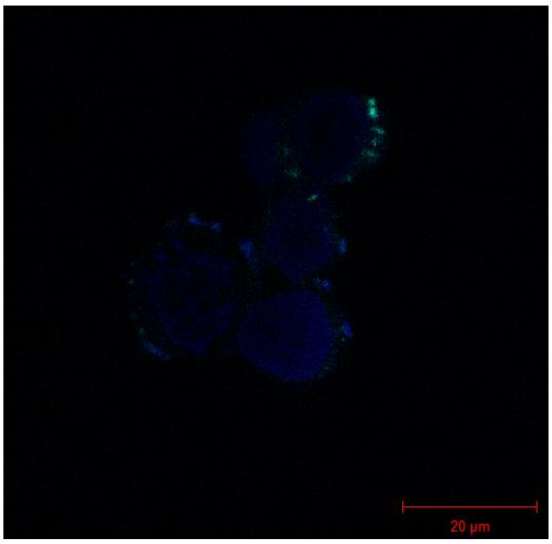

SNAP-Surface® Alexa Fluor® 488 + Hoechst 33342

D

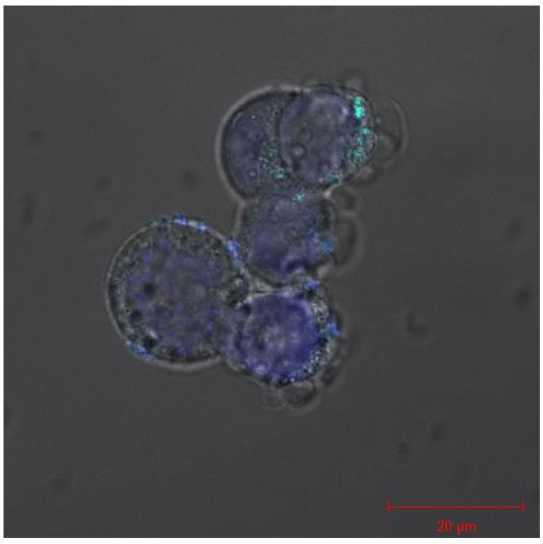

Bright light image

Figure 3.10 Confocal microscopy depicting SNAP-Surface® Alexa Fluor® 488-labelled J3-SNAP targeting gp120 on HEK293T-cells. To label the SNAP-fusion protein, 5 µM of J3-SNAP was conjugated to

SNAP-Surface® Alexa Fluor® 488 (10 µM) and incubated at 37 °C for 30 minutes. $3x10^5$ Env protein-expressing HEK293T-cells were seeded in supplemented RPMI-1640 medium in a 4-chambered 35 mm dish and allowed to settle overnight. The cells were washed with 1x PBS twice before being incubated with 2 µg of protein in 100 µL of 1x PBS for 30 minutes on ice. The cells were then stained with Hoechst 33342 (1 µg/mL) in supplemented-free media for 10 minutes. Subsequently, the cells were washed twice with 1x PBS before being viewed using the Zeiss LSM 880 confocal microscope together with ZEN software (Zeiss, South Africa). **A) SNAP-Surface® Alexa Fluor® 488 -conjugated J3-SNAP. B) Hoechst 33342 nuclear stain. C) merge of SNAP-Surface® Alexa Fluor® 488 and Hoechst 33342. D) bright light image.**

3.2. Development of J3-ETA

Toward the aim of generating the expression construct pMT-J3-ETA, plasmid DNA was isolated from DH5α *E. coli* cells. Glycerol stocks of DH5α *E. coli* cells containing pMT-H22-ETA were inoculated into kanamycin-supplemented (50 µg/mL) LB agar, incubated overnight and subsequently lysed for plasmid isolation by alkaline-lysis method (as described in Chapter 2.2.1.2). The isolated DNA was digested by *Sfi*I and *Not*I restriction endonucleases (as described in Chapter 2.2.1.4) to generate 5' and 3' overhangs compatible with those generated in J3 using the same restriction endonucleases. The digestion fragments were separated by agarose gel electrophoresis (Figure 3.11). Undigested pMT-H22-ETA (Figure 3.11 C - lane 1) resulted in bands above 10 kb. The *Sfi*I and *Not*I linearized controls (Figure 3.11 C lanes 2 and 3) produced single bands between 6.0 kb and 8.0 kb. Double bands of plasmid vector pMT-H22-ETA digested with both *Sfi*I and *Not*I were observed at approximately 7.0 kb and, more significantly, at approximately 700 bp. The band at 7.0 kb was thought to be the plasmid vector without H22 and the band at 700 bp was believed to be the H22 (*Sfi*I-*Not*I) fragment that was removed from the plasmid vector pMT-H33-ETA.

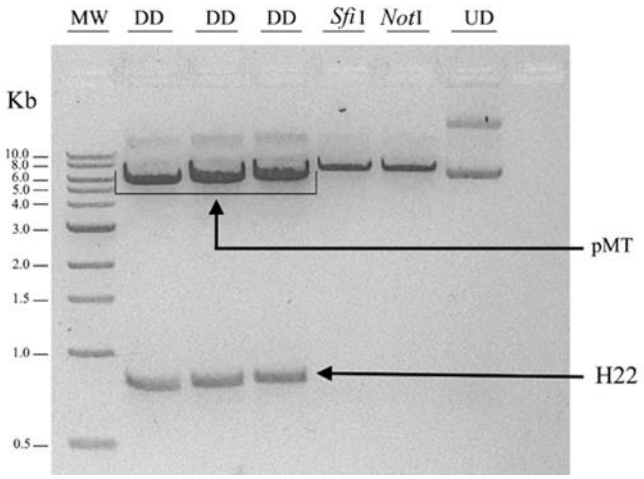

Figure 3.11: Construction of pMT-J3-ETA by PCR amplification of J3 and endonuclease digest of pMT-H22-ETA. 3 µg of pMT-H22-ETA was digested using 1000 U/mL *Sfi*I and *Not*I restriction endonucleases for 3 hours at 50 °C and overnight at 37 °C respectively. 50 µL of digest product was mixed with 1:6 dilution of Gel Loading Dye, Purple (6X) [NEB - #B7024S] immediately before being loaded onto 1.2 % agarose gels and run at 120 V for 1 hour before being viewed under blue light excitation (470 nm). UD – undigested control. NotI/SfiI - single-enzyme digest control. DD, double enzyme digest. MW – molecular weight marker.

The J3 (*Sfi*I-*Not*I) insert and the plasmid vector pMT-ETA were then ligated using their 5'-phosphorylated and 3'-hydroxylated compatible ends generated through *Sfi*I + *Not*I restriction endonuclease digestion. For this reaction, 9 ng and 14 ng of J3 were ligated to using T4 DNA ligase 50 ng of pMT-ETA in a 3:1 and 5:1 insert to vector molar ratio respectively (as described in Chapter 2.2.1.6). The ligation reaction product, pMT-J3-ETA was transformed into chemically competent DH5α *E. coli* cells before being grown on LB-agar plates supplemented with kanamycin (50 µg/mL) overnight at 37 °C (as described in Chapter 2.2.1.7). A vector + ligase control was included as a negative control that lacks the insert J3 and hence has linearized plasmid. Nevertheless, we observed a CFU of 3.8 x 10^3 in the negative control (Figure 3.12 A). The CFU for the 3:1 (Figure 3.12 B) and 5:1 (Figure 3.12 C) test samples were approximated 4.32 x 10^4 and 6.88 x 10^4 respectively.

A

pMT-J3-ETA

vector + ligase control

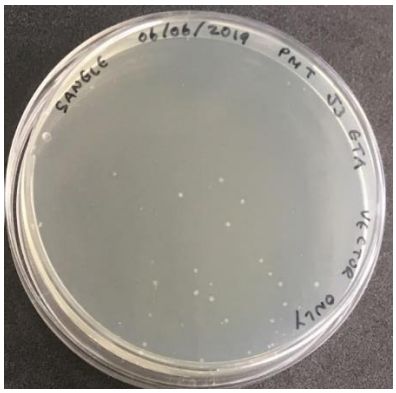

B

pMT-J3-ETA

3:1

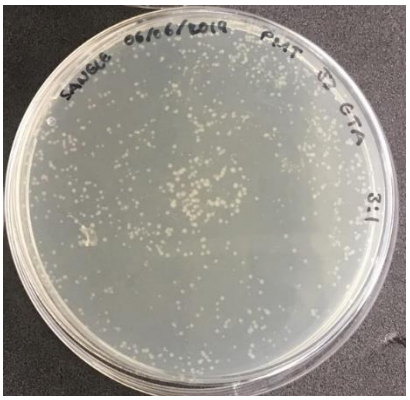

C

pMT-J3-ETA

5:1

Figure 3.12: LB-Agar plates of DH5-α *E. coli* cells transformed with pMT-J3-ETA.
The recombinant plasmid was generated through ligation of various insert-to-vector molar rations [8 ng (B, 1:3), 14 ng C, 1:5)] of J3 to 50ng of pMT-ETA plasmid vector to generate pMT-J3-ETA. 5 µL ligation product was then transformed into 50 µL competent DH5-α *E. coli* cells which subsequently grown on LB-agar plates supplemented with 50 ug/mL of kanamycin. A) kanamycin-containing LB-agar plate with DH5-α *E. coli* cells transformed with linearized plasmid vector. B-C), kanamycin-supplemented LB-agar plates with DH5-α *E. coli* cells transformed with pMT-J3-ETA.

To verify the identity of the plasmids in Figure 3.11 B and C, four colonies were selected at random from each plate and inoculated into 5 mL LB-broth media supplemented with 50 µg/mL kanamycin. The inoculated 5 mL cultures were incubated to grow overnight at 37 °C, after which 4 mL of the 5 mL culture was used for pMT-J3-ETA plasmid DNA isolation. Isolated plasmid (pMT-J3-ETA) was used for restriction endonuclease mapping using *Pvu*II, and pMT-H22-ETA was used as a control. For restriction mapping,100 µg of the plasmid (pMT-J3-ETA and pMT-H22-ETA) was digested using 1000 U/mL of *Pvu*II at 37 °C for 2 hours before being analysed by agarose gel electrophoresis. SnapGene® software (v.5.0.8, GSL Biotech LLC, USA) was used to simulate an agarose gel depicting the DNA fragments resulting from the *Pvu*II restriction endonuclease digest of either pMT-H22-ETA or pMT-J3-ETA (Figure 3.13 A). The simulation predicted that pMT-H22-ETA digested using *Pvu*II resulted in four fragments of sizes 4730 bp, 1599 bp, 999 bp and a band below 0.5 kb. The simulation predicted that pMT-J3-ETA digested using *Pvu*II resulted in two fragments of sizes 5998 bp and 999 bp. In accordance with the simulation, pMT-H22-ETA digested using *Pvu*II resulted in 4 bands at the approximate size of the simulated gel (Figure 3.13 B). However, although all four of the 3:1 and three of the 5:1 insert-to-vector ratio colonies corresponded to the SnapGene ® simulation, one of the 5:1 colony (Figure 3.13 B – lane 8) resembled pMT-H22-ETA control instead of pMT-J3-ETA. A second verification step was used to confirm that the cloning of pMT-J3-ETA had been successful. For this, the remaining 1 mL of cultures prepared from select colonies which most resembled the pMT-J3-ETA SnapGene® simulation

were each inoculated into a 50 mL LB-broth supplemented with 50 µg/mL of kanamycin and incubated at 37 °C overnight. Plasmid DNA was isolated by alkaline lysis method (as described in Chapter 2.2.1.2) and subjected to Sanger sequencing. (Figure 3.13 C) depicts the alignment of the Sanger sequences to the consensus sequence, confirming that the recombinant plasmid contained pMT-J3-ETA.

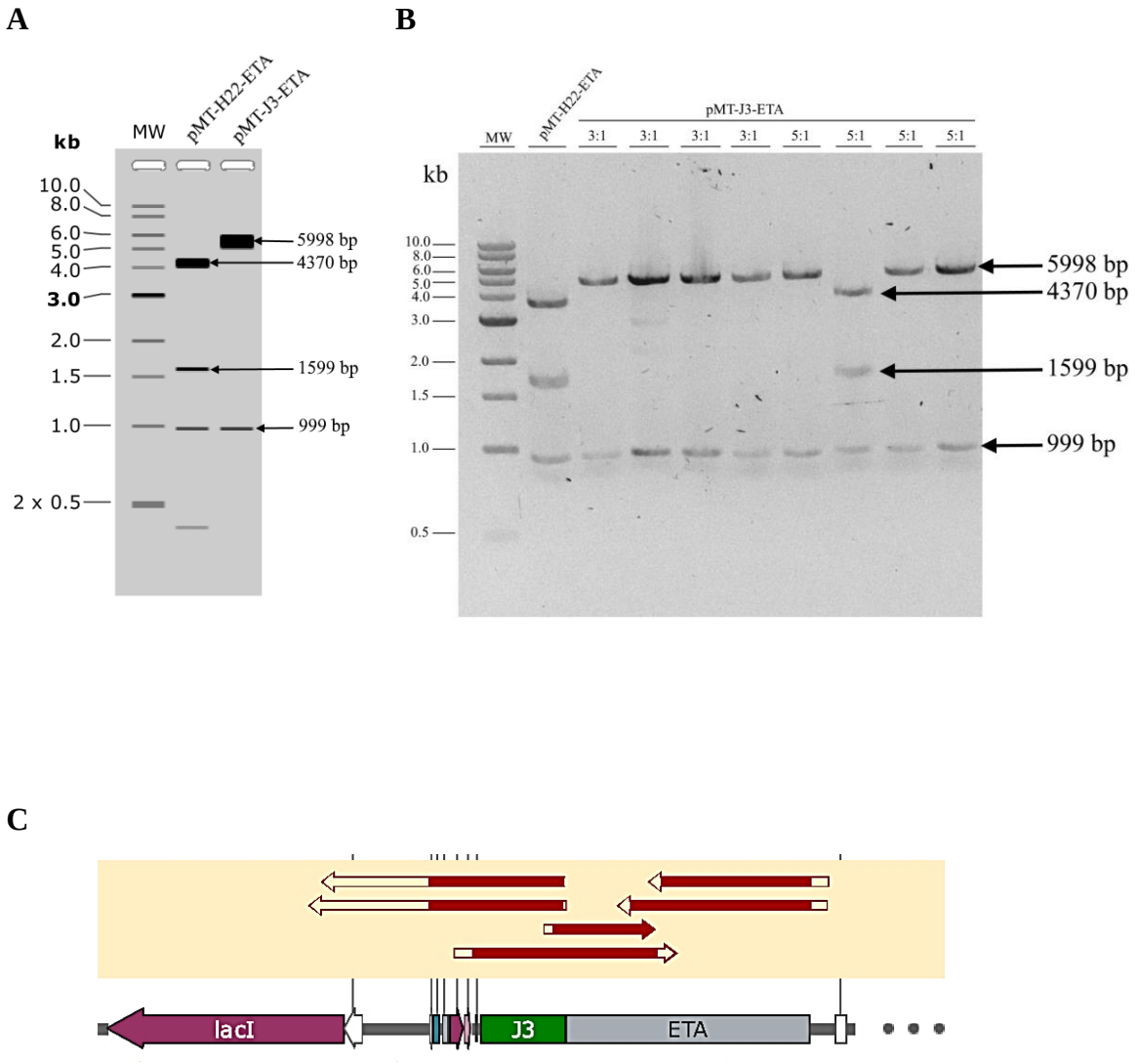

Figure 3.13: Sequence confirmation by restriction endonuclease mapping of the recombinant plasmid. A) SnapGene® software (v.5.0.8, GSL Biotech LLC, USA) was used to simulate an agarose gel of pMT-H22-ETA and pMT-J3-ETA digested using *Pvu*II. B) 3 µg pMT-H22-ETA, pMT-J3-ETA was digested using 1000 U/mL of restriction endonuclease *Pvu*II at 37 °C overnight. 50 µL of restriction endonuclease digest product was mixed with 1:6 dilution of Gel Loading Dye, Purple (6X) [NEB - #B7024S] and run on 1.2 % agarose gel at 120 V for 1 hour before being visualised under blue light excitation (470 nm). C) Alignment of J3-ETA Sanger sequences to the consensus sequence.

Chapter 4: Discussion and Conclusion

4.1 Purpose of this study

Since the discovery of HIV in 1984 and its identification as the causative agent of AIDS, great strides have been made to combat this pandemic. The use of cART to strategically target specific stages in the pathogenesis of HIV, including entry, reverse transcription, integration, and protease processing, has led to a reduction in the viremia of infected people to undetectable levels [2], [3] ,[102 -120]. cART has reduced the global infection and fatality rate, allowing infected people to lead relatively normal lives [4] [7] [8]. The use of cART allows the restoration of immune function and prevents progression to AIDS, thus negating the susceptibility of HIV infected people to opportunistic infections such as MTB, OPC, and PCP [79-101]. A cure for HIV, however, remains elusive owing to its establishment of viral reservoirs in long-lived memory CD4+T-cells in the early stages of infection. Following the cessation of cART, a rapid relapse of viremia occurs. Multiple studies have proposed that a cure for HIV may lie in a combinatory approach comprised mainly of latency-reversing agents, combination antiretroviral therapy, and the targeted elimination of HIV-infected immune cells [147], [177], [178]. The use of antibody-based therapies has taken a lead in cancer therapy with more than one hundred antibody-based therapeutics being approved for clinical application in recent decades [178]-[180]. ITs composed of antibody targeting moieties and protein toxins have demonstrated antitumor effects prompting approval for clinical use [181]-[184],[190]. For instance, Moxetumomab pasudotox is an IT composed of ETA and anti-CD22 monoclonal antibody and received approval for clinical application against hairy cell leukaemia [191]. Lessons can be learnt from such ITs to inform the design of potential therapeutics against HIV. Anti-HIV antibodies that can be used against HIV have previously been described [197], [198], [237], [238]. The use of an antibody targeting domain for an HIV gp120-specific antibody domain is a promising therapeutic strategy. These therapeutics have, however, shown poor efficacy in phase 1 clinical trials. This has been attributed to the affinity of the antibody to gp120 [193], [199], [239]–[241]. Interestingly, a highly potent antibody, J3, was described and demonstrated high specificity for HIV gp120, neutralising 96 % of the HIV-strains tested [208]. This study, therefore, aimed to understand whether a J3-ETA IT can be used for the selective elimination of HIV-infected CD4+ T-cells. To investigate, a reporter protein, **J3-SNAP, was developed in order to validate whether: (1) J3 can bind to cell-surface Env protein, and (2) functional J3 protein recombinantly fused to the reporter protein SNAP-tag can be expressed in the periplasmic space of *E. coli***. Once functional J3-SNAP protein produced in

E. coli would be produced and shown to bind to cell-surface Env protein, the development and expression of J3-ETA could begin.

4.2 *In silico* design of recombinant plasmid

Bioinformatic tools play a critical role in the design of antibody-based fusion proteins and ITs. These tools are used to analyse antibody sequences obtained from public databases such as Protein Data Bank, Uniprot, and patents [242], [243]. The analysis typically involves the use of web-based tools such as IMGT V-QUEST, and IgBLAST to identify the region of the antibody being analysed by sequence alignment to germline sequences [242]–[244]. For instance, McCoy *et al*. (2012) used IMGT V-QUEST for the alignment of J3 to the human germline sequence and was able to verify that J3 was a V gene and identified the FR and CDR regions [208]. Similarly, this study sourced the sequence for J3 from patent no. WO 2013/036130 AI and performed a sequence alignment to the germline sequence IgHV3, further validating that this was a V gene, and identified intact FR and CDR regions. These findings were verified by IgBLAST. The sequence for the plasmid vector of interest is then obtained and analysed for restriction endonuclease sites to facilitate the insertion of foreign genes into specific regions of the plasmid [245]. The pET plasmid vector is commonly used for the expression of recombinant proteins in *E. coli* [246]. pMT, a derivative of pET, has been used for the expression of the recombinant IT H22(scFv)-ETA [247]. In this study, SnapGene® software was used to virtually clone the bacteria-optimised DNA sequence for J3, following the insertion of appropriate restriction endonuclease sites, into the pMT plasmid vector. The H22(scFv) was replaced by J3 to generate J3-ETA and ETA was then replaced with SNAP-tag to generate J3-SNAP. Protein parameters such as the pI and the MW are assessed using web-based tools such as the "ExPASY Compute pI/MW" tool, as was done in this study [248]–[251].

4.3 Molecular cloning of pMT-J3-SNAP

Described procedures for the generation of recombinant plasmids include the amplification of the gene to be inserted into the plasmid by PCR. The gene is then visualized on an agarose gel, purified and digested with the appropriate restriction endonucleases to facilitate site-directed inclusion into the plasmid to be used for protein expression. DNA ligase is then used to insert the gene of interest into the desired vector thus creating a recombinant plasmid [252]–[254]. For instance, Kampmeier *et al.* (2009) described the development of scFv-SNAP recombinant plasmids where *Sfi*I + *Not*I were used to introduce the protein ligand, and *Xba*I + *Blp*I were used to introduce SNAP-tag. A similar protocol was described by Hussain *et al.* (2019) and

was thus adopted for the development of pMT-J3-SNAP. J3 (SfiI + NotI) was ligated into a pre-existing pMT-SNAP plasmid. Successful molecular cloning was confirmed by restriction endonuclease mapping and Sanger sequencing. Interestingly, a deletion was observed in the Sanger sequences and was, upon investigation, identified to be due to an error in the synthesis of SNAP-tag. Site-directed mutagenesis by overlap extension (OE) PCR has been used to create insertions and deletions in DNA sequences. This is a two-step procedure that involves the use of two overlapping primers specific for the site to be mutated, and two primers flanking both sides of the gene to be mutated (Figure 3.5). First, two amplicons are generated by the reverse site-specific primer and the forward gene-specific primer, and the second amplicon is generated by the forward site-specific primer and the reverse gene-specific primer in a separate reaction. The two amplicons are then sewed together using the gene-specific primers [255]–[258]. This protocol was used to insert the deleted nucleotide in the J3-SNAP gene. The OE-PCR-generated J3-SNAP was then digested by *Sfi*I + *Blp*I before being ligated into the pMT plasmid to generate pMT-J3-SNAP. The alignment of the OE-PCR-mutated Sanger sequences to the consensus sequence confirmed successful repair of the mutation and as such, **the successful development of pMT-J3-SNAP recombinant plasmid**.

4.4 Protein expression

As a host of expression, mammalian expression systems are preferred because they induce post-translational modification and correct protein folding of recombinant proteins. Furthermore, HEK293T cells are capable of secreting recombinant proteins into the medium, making the harvesting of protein easier, and removing the need for cell lysis for protein extraction [259]–[261]. As a result, the production of SNAP-tag fusion proteins has been carried out mainly in mammalian cells. The expression antibody-based SNAP-tag fusion proteins in HEK293T cells, secreted into the medium and purified by the interaction of an N-terminal poly (His)-tag with IMAC column, has been well reported [252], [253], [262], [263]. Functionality was demonstrated by BG-modified fluorophore conjugation to SNAP-tag, and antibody binding to the target antigen [252], [253]. The relatively high cost of production in HEK293T cells means that more cost-effective measures may prove beneficial. Fortunately, Djender *et al*. (2014) reported the expression of fully-functional SNAP fusion protein in bacteria. The study reported successful cytoplasmic expression of poly (His)-tagged anti-HER2(VHH)-SNAP-fusion protein which was subsequently purified by IMAC. Djender *et al*. (2014) also reported that the periplasmic expression of SNAP-tag fusion proteins resulted in poorly folded and aggregated protein [264]. However, Barth *et al*. (2000) demonstrated that

difficult-to-express proteins can be expressed in the periplasmic space under osmotic stress conditions, aided by compatible solutes. The rationale being that cell stress response mechanisms such as the induction of heat shock proteins, together with compatible solutes which were shown to protect the proteins of interest from degradation, aggregation and misfolding; and increase the production of otherwise difficult to express proteins by up to one thousand fold [224]. The VHH antibody format, due to its small size, offers some advantages. For instance, compared to larger antibody formats, it has a less complex tertiary structure, has fewer disulphide bridges and has thus been produced in *E. coli* [264]. With this taken into consideration, and preliminary data from colleagues within our research group demonstrating successful periplasmic expression of SNAP-tag fusion proteins, **this study set out to express J3-SNAP in the periplasmic space of *E. coli* BL21 DE3 under osmotic stress conditions in the presence of compatible solutes**.

Despite the rarity of literature reporting on the successful periplasmic expression of SNAP-tag fusion proteins, and lack of means to predict the quality of protein that can be produced under such conditions, **successful expression of J3-SNAP was achieved**. This was demonstrated by the presence of strong protein bands at approximately 32 kDa on the SDS-PAGE gel and verification by Western blot using a rabbit anti-His tag primary antibody and a goat anti-rabbit horseradish peroxidase-conjugate secondary antibody. Further optimisation of the protocol is required due to the protein yield and the purity obtained being comparably lower than that obtained by previous studies of periplasmic expression by osmotic stress by Barth *et al*. (2000), and cytoplasmic expression of SNAP-tag fusion protein by Djender *et al*. (2014) [224], [264]. The SDS-PAGE and Western blot showed a contaminant band at approximately 72 kDa, and what appears to be degradation products. The misfolding of protein is known to lead to protein degradation in the periplasmic space [265], [266]. To address protein misfolding, other studies reduced the IPTG concentration to prevent overexpression which may lead to aggregation and reduced the temperature at which the expression was carried out to as low as 20 °C [264], [267]–[269]. A second purification step such as size exclusion chromatography should be applied as it has been shown to increase the purity of recombinant proteins expressed in the periplasmic space [224], [270], [271]. Nevertheless, **this study reports the successful periplasmic expression of J3-SNAP protein under osmotic stress in the presence of compatible solutes**.

4.4 Protein functionality

To assess protein functionality, J3-SNAP was conjugated to SNAP-Surface® Alexa Fluor® 488 before being incubated with Env-expressing HEK293T-cells *in vitro*. HEK293T-cells transfected with recombinant HIV Env are typically developed and used as pseudoviruses in the development of vaccines. To achieve this, the HEK293T-cells are seeded and allowed to reach the desired confluency. Thereafter, plasmid DNA, typically pcDNA, is mixed with a transfection reagent such as PEI to form a complex. The complex is then added to cells and allowed to carry the DNA into the cells by endocytosis. Medium is then changed after six hours, and the cells are harvested for analysis after 48 hours [272], [273]. In this study, the same protocol was followed using the plasmid pcDNA-TOPO-gp120, and Env expression was confirmed by SDS-PAGE and Western blot. β-actin was used as a loading control and to show that where no HIV Env signal was observed, it was due to lack of expression rather than the absence of cells. **The presence of a signal at 160 kDa (gp120 + gp41) confirmed successful cloning and expression of HIV Env protein**. However, uncleaved gp160 suggested incomplete processing of the recombinant protein and this is known to significantly reduce its presence at the cell surface and its incorporation into budding virions [274]–[277]. Furthermore, the transient expression of the HIV Env proten in HEK294T cells has previously been shown to result in a poorly cleaved product with reduced membrane incorporation [278]. For the purposes of this study, however, less than optimal membrane expression was acceptable as the goal was to determine whether or not J3-SNAP could bind to the HIV Env protein. Therefore, these cells were then used to detect the antigen-binding of J3 to the Env protein.

Cell-surface labelling of antigen-positive cells using SNAP-tag-based antibody fusion proteins is preceded by the conjugation of the SNAP-tag to a substrate such as SNAP-Surface® Alexa Fluor® 488. Protocols described by Kampmeier *et al.* (2009) and Hussain *et al.* (2019) describe protein labelling as follows; SNAP-tag-based protein is incubated with at least two-fold molar excess BG-modified substrate at room temperature in the dark for two hours. Thereafter, a desalting column may be used to remove excess dye and SDS-PAGE can be used to validate successful conjugation through UV transillumination. Thereafter, 1 µg the fluorophore-conjugated protein is then incubated with the antigen-presenting cells on ice for 30 minutes. The cells are then washed to remove unbound stain protein and counterstained using Hoechst 33342 nuclear stain before being analysed by microscopy [252], [253]. In this study, the above-described protocol was used but with some modifications. Firstly, 2 µg of labelled protein was used instead of 1 µg to compensate for the poor purity which meant that less J3-SNAP was

present in the protein sample. Secondly, confirmation of protein conjugation by SDS-PAGE was omitted as cell-surface labelling can itself act as confirmation of SNAP-tag activity. A negative control was omitted from the results due to poor image quality. Nevertheless, the green fluorescence around the cell membrane suggested the following; (1) That SNAP-tag was functional as it was able to react with the SNAP-Surface® Alexa Fluor® 488, and (2) J3 was able to bind to recombinant Env protein on the surface of HEK293T-cells *in vitro*. There was, however, not much green fluorescence around the surface of the HEK293T-cells. This may have been due to the following; (1) a low number of recombinant Env protein proteins on the surface of the HEK293T-cells; (2) the previously mentioned proteolytic degradation or possible misfolding of protein which may have led to a reduction in the activity of the J3, SNAP-tag, or both; and (3) membrane blebbing evidenced by the presence of a blue DNA stain around the surface of the HEK293T-cells may indicative of an apoptotic cell [279]–[281]. Taken together with the rounded morphological appearance of the cell, as opposed to their native spindle-shaped morphology, this was indicative that the cells may have been undergoing apoptosis [279]–[281]. Hypothermia has been known to cause cell death in mammalian cells [282], [283]. In this experiment, the incubation of SNAP-Surface® Alexa Fluor® 488-conjugated J3-SNAP with the Env protein-expressing HEK293T-cells was carried out on ice. Thereafter, the cells were kept on ice before being viewed under confocal microscopy, possibly causing hypothermic stress. Though the cells are kept on ice to prevent protein internalization upon membrane binding, successful membrane binding has been demonstrated at room temperature [284]. With the limitations of this experiment considered, the results remain indicative of cell surface binding of Env-specific J3-SNAP protein conjugated to SNAP-Surface® Alexa Fluor® 488 thereby suggesting functionality of the antibody domain and reported domain of the developed fusion protein.

4.5 Development of J3-ETA

The elimination of latently infected HIV reservoir cells is an essential step in achieving a cure for HIV. The use of antibody ITs targeting virus antigens on diseased cells is a promising avenue currently being pursued [237], [285]. For instance, Spiess *et al.* (2015) published data on the use of an ETA-based fusion protein targeting chemokine receptors on human cytomegalovirus (HCMV) infected cells, which showed anti-HCMV potency both *in vitro* and *in vivo* [286]. ETA-based VHH ITs have been used to kill herpes simplex virus 2 (HSV-2) infected cells [287]. This study, therefore, aimed to design and develop an ETA-based IT using the highly potent broadly specific VHH antibody, J3. Following the confirmation of the

periplasmic expression and functionality of J3-SNAP, the next step involved the development of J3-ETA. This began with the generation of the pMT-J3-ETA recombinant plasmid. This involved removal of H22 from the pre-existing recombinant plasmid pMT-H22-ETA using restriction endonucleases, followed by replacement of H22 with J3 using T4 DNA ligase. pMT-J3-ETA was subsequently transformed into competent *E. coli* DH5α competent cells. Kanamycin was used to select for positive clones, which were subsequently confirmed by restriction endonuclease mapping and Sanger sequencing. This experiment, therefore, demonstrated the successful construction of the pMT-J3-ETA recombinant plasmid.

4.6 Conclusion and future perspectives

The data reported herein suggest that SNAP-tag based fusion proteins previously expressed in a poorly folded state in the periplasmic space can be expressed and exhibit functionality when expressed under compatible solute-guided osmotic stress conditions. Bacteria is the most widely used and cost-effective means of producing recombinant proteins and is scalable to meet high quantity demands [288]. The periplasmic space is often known to produce functional antibody formats due to the capacity to form disulphide bonds. The periplasm is also free from several bacterial proteases, and the harvesting of protein is easier in the periplasm [222], [289], [290]. The expression of J3-SNAP in the periplasm, therefore, presents an alternative to the previously described cytoplasmic expression of SNAP-tag-based fusion proteins [264]. Furthermore, preliminary binding data depicted this study suggests that J3 can be used to target Env-expressing cells *in vitro*. Upon learning the binding capacity of J3, the IT J3-ETA was developed, and forms part of an ongoing study aimed at developing anti-HIV ITs.

Future perspectives will be focused on the following; (1) The optimization of the periplasmic expression of J3-SNAP; (2) The periplasmic expression and characterisation of J3-ETA; and (3) Validation of the binding of J3-SNAP and J3-ETA against HEK293T-cells expressing recombinant Env protein from various strains of HIV. There is a growing resistance to current antiretroviral therapy suggesting that other therapeutic strategies need to be explored at accelerated rate. For instance, in 2018 it was reported that approximately 15 % of infected people in South Africa were resistant to one or more ARVs and this number is projected to exceed 30 % by 2030 [291]. This highlights the potential for broadly specific anti-HIV

antibodies such as J3. The collaboration with Dr Zenda Woodman (University of Cape Town, South Africa) is crucial to our study as it will allow us access to various Env protein isoforms from South African patients. Given the disproportionate burden of HIV in South Africa, we are very interested in developing an anti-HIV IT capable of eliminating cells infected with various strains and particularly strains that affect the South African population.

References

[1] M. S. Gottlieb, “Pneumocystis Pneumonia—Los Angeles,” *Am. J. Public Health*, vol. 96, no. 6, pp. 980–981, Jun. 2006.

[2] W. C. Greene, “A history of AIDS: Looking back to see ahead,” *Eur. J. Immunol.*, vol. 37, no. S1, pp. S94–S102, Nov. 2007.

[3] M. H. Merson, J. O’Malley, D. Serwadda, and C. Apisuk, “The history and challenge of HIV prevention,” *The Lancet*. 2008.

[4] UNAIDS, “FACT SHEET – GLOBAL AIDS UPDATE 2019,” *Unaids*, 2018.

[5] M. Mahy, K. Marsh, K. Sabin, I. Wanyeki, J. Daher, and P. D. Ghys, “HIV estimates through 2018: data for decision-making,” *AIDS*, vol. 33, 2019.

[6] G. B. D. 2017 H. I. V collaborators, “Global, regional, and national incidence, prevalence, and mortality of HIV, 1980-2017, and forecasts to 2030, for 195 countries and territories: a systematic analysis for the Global Burden of Diseases, Injuries, and Risk Factors Study 2017,” *lancet. HIV*, vol. 6, no. 12, pp. e831–e859, Dec. 2019.

[7] T. D. Frank *et al.*, “Global, regional, and national incidence, prevalence, and mortality of HIV, 1980–2017, and forecasts to 2030, for 195 countries and territories: a systematic analysis for the Global Burden of Diseases, Injuries, and Risk Factors Study 2017,” *Lancet HIV*, vol. 6, no. 12, pp. e831–e859, 2019.

[8] J. Fettig, M. Swaminathan, C. S. Murrill, and J. E. Kaplan, “Global epidemiology of HIV,” *Infect. Dis. Clin. North Am.*, vol. 28, no. 3, pp. 323–337, 2014.

[9] A. A. Awofala and O. E. Ogundele, “HIV epidemiology in Nigeria,” *Saudi Journal of Biological Sciences*. 2018.

[10] N. Harawa and A. Adimora, “Incarceration, African Americans and HIV: Advancing a research agenda,” *J. Natl. Med. Assoc.*, 2008.

[11] CDC Centers for Disease Control and Prevention, “HIV Among Incarcerated Populations,” *CDC Fact Sheet*, 2015.

[12] B. A. Tarver, J. Sewell, and N. Oussayef, “State laws governing HIV testing in correctional settings,” *J. Correct. Heal. Care*, 2016.

[13] F. L. Altice *et al.*, “The perfect storm: incarceration and the high-risk environment perpetuating transmission of HIV, hepatitis C virus, and tuberculosis in Eastern Europe and Central Asia,” *The Lancet*. 2016.

[14] T. Lyons, E. Osunkoya, I. Anguh, A. Adefuye, and J. Balogun, “HIV Prevention and Education in State Prison Systems: An Update,” *J. Correct. Heal. Care*, 2014.

[15] D. Gökengin, F. Doroudi, J. Tohme, B. Collins, and N. Madani, “HIV/AIDS: Trends in the Middle East and North Africa region,” *International Journal of Infectious Diseases*. 2016.

[16] S. L. James *et al.*, “Global, regional, and national incidence, prevalence, and years lived with disability for 354 diseases and injuries for 195 countries and territories, 1990–2017: a systematic analysis for the Global Burden of Disease Study 2017,” *Lancet*, vol. 392, no. 10159, pp. 1789–1858, Nov. 2018.

[17] A. D. Castel, M. Magnus, and A. E. Greenberg, “Update on the Epidemiology and Prevention of HIV/AIDS in the United States,” *Curr. Epidemiol. reports*, vol. 2, no. 2, pp. 110–119, Jun. 2015.

[18] L. Dwyer-Lindgren *et al.*, “Mapping HIV prevalence in sub-Saharan Africa between 2000 and 2017,” *Nature*, vol. 570, no. 7760, pp. 189–193, 2019.

[19] M. N. I. Mondal and M. Shitan, “Factors affecting the HIV/AIDS epidemic: an ecological analysis of global data,” *Afr. Health Sci.*, vol. 13, no. 2, pp. 301–310, Jun. 2013.

[20] M. Mahathir, “Women at greater risk of HIV infection.,” *Arrows Change*, vol. 3, no. 1, pp. 1–2, Apr. 1997.

[21] D. F. Cuadros *et al.*, “Mapping the spatial variability of HIV infection in Sub-Saharan Africa: Effective information

for localized HIV prevention and control," *Sci. Rep.*, vol. 7, no. 1, pp. 1–11, 2017.

[22] L. F. Johnson, R. E. Dorrington, and H. Moolla, "HIV epidemic drivers in South Africa: A model-based evaluation of factors accounting for inter-provincial differences in HIV prevalence and incidence trends," *South. Afr. J. HIV Med.*, vol. 18, no. 1, pp. 1–9, 2017.

[23] A. M. L. Lever and B. Berkhout, "2008 Nobel prize in Medicine for discoverers of HIV," *Retrovirology*, vol. 5, no. 1966, pp. 1–2, 2008.

[24] A. Brus-Chojnicka, M. Bura, M. Chojnicki, and Ś. Walentyna, "The history of the Human Immunode fi ciency Virus research," vol. 1, no. Cdc, pp. 62–64, 2014.

[25] O. Ergonul *et al.*, "Who can get the next Nobel Prize in infectious diseases?," *Int. J. Infect. Dis.*, vol. 45, pp. 88–91, 2016.

[26] F. Clavel *et al.*, "Isolation of a New Human Retrovirus from West African Patients with AIDS Katlama , Christine Rouzioux , David Klatzmann , J . L . Champalimaud and Luc Montagnier Published by : American Association for the Advancement of Science Stable URL : http://www.js," vol. 233, no. 4761, pp. 343–346, 1986.

[27] J. D. Reeves and R. W. Doms, "Human immunodeficiency virus type 2," *J. Gen. Virol.*, vol. 83, no. 6, pp. 1253–1265, 2002.

[28] P. Swanson, V. Soriano, … S. D.-J. of clinical, and undefined 2001, "Comparative performance of three viral load assays on human immunodeficiency virus type 1 (HIV-1) isolates representing group M (subtypes A to G) and group O," *Am Soc Microbiol*, vol. 4, no. 9, 1998.

[29] M. M. Thomson, L. Pérez-Álvarez, and R. Nájera, "Molecular epidemiology of HIV-1 genetic forms and its significance for vaccine development and therapy," *Lancet Infect. Dis.*, vol. 2, no. 8, pp. 461–471, 2002.

[30] D. L. Robertson *et al.*, "HIV-1 Nomenclature Proposal," *Science (80-.).*, vol. 288, no. 5463, pp. 55 LP – 55, Apr. 2000.

[31] C. Williamson and D. P. Martin, "HIV-1 genetic diversity," *HIV/AIDS South Africa Second Ed.*, vol. 3, no. January, pp. 117–126, 2010.

[32] P. A. Ngoupo *et al.*, "First evidence of transmission of an HIV-1 M/O intergroup recombinant virus," *Aids*, vol. 30, no. 1, pp. 1–8, 2016.

[33] R. A. Subbramanian and E. A. Cohen, "Molecular biology of the human immunodeficiency virus accessory proteins.," *J. Virol.*, vol. 68, no. 11, pp. 6831–6835, 1994.

[34] A. D. Frankel and J. A. T. Young, "HIV-1: Fifteen Proteins and an RNA," *Annu. Rev. Biochem.*, 1998.

[35] M. H. Malim and M. Emerman, "HIV-1 Accessory Proteins-Ensuring Viral Survival in a Hostile Environment," *Cell Host and Microbe*. 2008.

[36] S. Richter, I. Frasson, and G. Palu, "Strategies for Inhibiting Function of HIV-1 Accessory Proteins: A Necessary Route to AIDS Therapy?," *Curr. Med. Chem.*, 2008.

[37] S. 'Assessment of P. T. by B. German Advisory Committee Blood (Arbeitskreis Blut), "Human Immunodeficiency Virus (HIV)," *Transfus. Med. Hemother.*, vol. 43, no. 3, pp. 203–222, May 2016.

[38] A. C. S. Saphire, "Host cyclophilin A mediates HIV-1 attachment to target cells via heparans," *EMBO J.*, vol. 18, no. 23, pp. 6771–6785, 1999.

[39] P. J. Klasse, "The molecular basis of HIV entry," *Cell. Microbiol.*, vol. 14, no. 8, pp. 1183–1192, 2012.

[40] J. P. Moore, A. Trkola, and T. Dragic, "Co-receptors for HIV-1 entry," *Curr. Opin. Immunol.*, vol. 9, no. 4, pp. 551–562, Aug. 1997.

[41] D. C. Chan and P. S. Kim, "HIV Entry and Its Inhibition," *Cell*, vol. 93, no. 5, pp. 681–684, May 1998.

[42] C. LABRANCHE, G. GALASSO, J. MOORE, D. BOLOGNESI, M. HIRSCH, and S. HAMMER, "HIV fusion and its inhibition," *Antiviral Res.*, vol. 50, no. 2, pp. 95–115, May 2001.

[43] L. J. Earp, S. E. Delos, H. E. Park, and J. M. White, “The Many Mechanisms of Viral Membrane Fusion Proteins,” in *Membrane Trafficking in Viral Replication*, Berlin/Heidelberg: Springer-Verlag, 2004, pp. 25–66.

[44] C. B. Wilen, J. C. Tilton, and R. W. Doms, “HIV: Cell Binding and Entry,” *Cold Spring Harb. Perspect. Med.*, vol. 2, no. 8, pp. a006866–a006866, Aug. 2012.

[45] L. Bracq, M. Xie, S. Benichou, and J. Bouchet, “Mechanisms for Cell-to-Cell Transmission of HIV-1,” *Front. Immunol.*, vol. 9, Feb. 2018.

[46] D. Yu *et al.*, “Molecular mechanism of HIV-1 resistance to sifuvirtide, a clinical trial–approved membrane fusion inhibitor,” *J. Biol. Chem.*, vol. 293, no. 33, pp. 12703–12718, Aug. 2018.

[47] V. Simon, D. D. Ho, and Q. A. Karim, “Seminar HIV / AIDS epidemiology , pathogenesis , prevention , and treatment,” *Science (80-.).*, vol. 368, no. 9534, pp. 489–504, 2006.

[48] A. Telesnitsky and S. Goff, *Reverse Transcriptase and the Generation of Retroviral DNA*. 1997.

[49] A. Herschhorn and A. Hizi, “Retroviral reverse transcriptases,” *Cellular and Molecular Life Sciences*. 2010.

[50] W. S. Hu and S. H. Hughes, “HIV-1 reverse transcription,” *Cold Spring Harb. Perspect. Med.*, 2012.

[51] U. Scherdin, K. Rhodes, and M. Breindl, “Transcriptionally active genome regions are preferred targets for retrovirus integration.,” *J. Virol.*, vol. 64, no. 2, pp. 907–912, 1990.

[52] A. R. W. Schröder, P. Shinn, H. Chen, C. Berry, J. R. Ecker, and F. Bushman, “HIV-1 Integration in the Human Genome Favors Active Genes and Local Hotspots,” *Cell*, vol. 110, no. 4, pp. 521–529, Aug. 2002.

[53] F. Bushman *et al.*, “Genome-wide analysis of retroviral DNA integration,” *Nat. Rev. Microbiol.*, vol. 3, no. 11, pp. 848–858, Nov. 2005.

[54] E. M. Anderson and F. Maldarelli, “The role of integration and clonal expansion in HIV infection: live long and prosper,” *Retrovirology*, vol. 15, no. 1, p. 71, Dec. 2018.

[55] Y. Wu, “HIV-1 gene expression: Lessons from provirus and non-integrated DNA,” *Retrovirology*. 2004.

[56] K. A. Nilson and D. H. Price, “The Role of RNA Polymerase II Elongation Control in HIV-1 Gene Expression, Replication, and Latency,” *Genet. Res. Int.*, vol. 2011, pp. 1–9, 2011.

[57] C. Van Lint, S. Bouchat, and A. Marcello, “HIV-1 transcription and latency: an update,” *Retrovirology*, vol. 10, no. 1, p. 67, Dec. 2013.

[58] R. Liu, J. Wu, R. Shao, and Y. Xue, “Mechanism and factors that control HIV-1 transcription and latency activation,” *J. Zhejiang Univ. Sci. B*, vol. 15, no. 5, pp. 455–465, May 2014.

[59] A. Panday, M. E. Inda, P. Bagam, M. K. Sahoo, D. Osorio, and S. Batra, “Transcription Factor NF-κB: An Update on Intervention Strategies,” *Arch. Immunol. Ther. Exp. (Warsz).*, vol. 64, no. 6, pp. 463–483, Dec. 2016.

[60] E. Ne, R.-J. Palstra, and T. Mahmoudi, “Transcription: Insights From the HIV-1 Promoter,” in *International Review of Cell and Molecular Biology*, 2018, pp. 191–243.

[61] H. Garoff, R. Hewson, and D.-J. E. Opstelten, “Virus Maturation by Budding,” *Microbiol. Mol. Biol. Rev.*, vol. 62, no. 4, pp. 1171–1190, 1998.

[62] E. Morita and W. I. Sundquist, “RETROVIRUS BUDDING,” *Annu. Rev. Cell Dev. Biol.*, vol. 20, no. 1, pp. 395–425, Nov. 2004.

[63] D. G. Demirov and E. O. Freed, “Retrovirus budding,” *Virus Res.*, vol. 106, no. 2, pp. 87–102, Dec. 2004.

[64] N. M. Sherer *et al.*, “Visualization of retroviral replication in living cells reveals budding into multivesicular bodies,” *Traffic*, 2003.

[65] D. R. Larson, M. C. Johnson, W. W. Webb, and V. M. Vogt, “Visualization of retrovirus budding with correlated light and electron microscopy,” *Proc. Natl. Acad. Sci.*, vol. 102, no. 43, pp. 15453–15458, Oct. 2005.

[66] A. M. Booth *et al.*, “Exosomes and HIV Gag bud from endosome-like domains of the T cell plasma membrane,” *J. Cell Biol.*, 2006.

[67] D. Perez-Caballero *et al.*, “Tetherin Inhibits HIV-1 Release by Directly Tethering Virions to Cells,” *Cell*, 2009.

[68] B. Yavuz *et al.*, “Pharmaceutical Approaches to HIV Treatment and Prevention,” *Adv. Ther.*, p. 1800054, Jul. 2018.

[69] D. Guha and V. Ayyavoo, “Innate Immune Evasion Strategies by Human Immunodeficiency Virus Type 1,” *Isrn Aids*, vol. 2013, pp. 1–10, 2013.

[70] K. Kedzierska and S. M. Crowe, “Cytokines and HIV-1: Interactions and clinical implications,” *Antiviral Chemistry and Chemotherapy*. 2001.

[71] L. Flórez-Álvarez, J. C. Hernandez, and W. Zapata, “NK cells in HIV-1 infection: From basic science to vaccine strategies,” *Front. Immunol.*, vol. 9, no. OCT, pp. 1–13, 2018.

[72] C. F. Thobakgale *et al.*, “Frequent and Strong Antibody-Mediated Natural Killer Cell Activation in Response to HIV-1 Env in Individuals with Chronic HIV-1 Infection,” *J. Virol.*, vol. 86, no. 12, pp. 6986–6993, Jun. 2012.

[73] A. A. Okoye and L. J. Picker, “CD4+ T-Cell Depletion In Hiv Infection: Mechanisms Of Immunological Failure,” *Immunol. Rev.*, vol. 254, no. 1, pp. 54–64, 2013.

[74] N. R. Klatt and J. M. Brenchley, “Th17 cell dynamics in HIV infection,” *Current Opinion in HIV and AIDS*. 2010.

[75] B. Kanwar, D. Favre, and J. M. McCune, “Th17 and regulatory T cells: Implications for AIDS pathogenesis,” *Current Opinion in HIV and AIDS*. 2010.

[76] S. Dandekar, M. D. George, and A. J. Bäumler, “Th17 cells, HIV and the gut mucosal barrier,” *Current Opinion in HIV and AIDS*. 2010.

[77] L. Guglani and S. A. Khader, “Th17 cytokines in mucosal immunity and inflammation,” *Current Opinion in HIV and AIDS*. 2010.

[78] A. ElHed and D. Unutmaz, “Th17 cells and HIV infection,” *Curr. Opin. HIV AIDS*, vol. 5, no. 2, pp. 146–150, Mar. 2010.

[79] J. M. Brenchley *et al.*, “Microbial translocation is a cause of systemic immune activation in chronic HIV infection,” *Nat. Med.*, 2006.

[80] R. M. Donovan, C. E. Bush, N. P. Markowitz, D. M. Baxa, and L. D. Saravolatz, “Changes in virus load markers during AIDS-associated opportunistic diseases in human immunodeficiency virus-infected persons,” *J. Infect. Dis.*, vol. 174, no. 2, pp. 401–403, 1996.

[81] E. H. Moylett and W. T. Shearer, “HIV: Clinical manifestations,” *J. Allergy Clin. Immunol.*, vol. 110, no. 1, pp. 3–16, Jul. 2002.

[82] C. Chu and P. A. Selwyn, “Complications of HIV infection: A systems-based approach,” *Am. Fam. Physician*, vol. 83, no. 4, pp. 395–406, 2011.

[83] A. Sandhu, & Amanpreet, and K. Samra, “Opportunistic infections and disease implications in HIV/AIDS,” *Int. J. Pharm. Sci. Invent. ISSN (Online*, vol. 2, no. 5, pp. 2319–6718, 2013.

[84] G. R. Thompson *et al.*, “Oropharyngeal candidiasis in the era of antiretroviral therapy,” *Oral Surgery, Oral Med. Oral Pathol. Oral Radiol. Endodontology*, vol. 109, no. 4, pp. 488–495, Apr. 2010.

[85] P. K. Patel *et al.*, “The Changing Epidemiology of Oropharyngeal Candidiasis in Patients with HIV/AIDS in the Era of Antiretroviral Therapy,” *AIDS Res. Treat.*, vol. 2012, p. 262471, 2012.

[86] A. Berberi, Z. Noujeim, and G. Aoun, “Epidemiology of Oropharyngeal Candidiasis in Human Immunodeficiency Virus/Acquired Immune Deficiency Syndrome Patients and CD4+ Counts,” *J. Int. oral Heal. JIOH*, vol. 7, no. 3, pp. 20–23, Mar. 2015.

[87] J. N. Jarvis and T. S. Harrison, “HIV-associated cryptococcal meningitis,” *AIDS*, vol. 21, no. 16, 2007.

[88] T. Warkentien and N. F. Crum-Cianflone, “An update on Cryptococcus among HIV-infected patients,” *Int. J. STD AIDS*, vol. 21, no. 10, pp. 679–684, Oct. 2010.

[89] S. Antinori, “New Insights into HIV/AIDS-Associated Cryptococcosis,” *ISRN AIDS*, vol. 2013, p. 471363, 2013.

[90] S. Srichatrapimuk and S. Sungkanuparph, “Integrated therapy for HIV and cryptococcosis,” *AIDS Res. Ther.*, vol. 13, no. 1, p. 42, 2016.

[91] L. Gounder, P. Moodley, P. K. Drain, A. J. Hickey, and M.-Y. S. Moosa, “Hepatic tuberculosis in human immunodeficiency virus co-infected adults: a case series of South African adults,” *BMC Infect. Dis.*, vol. 17, no. 1, p. 115, 2017.

[92] S. D. Lawn and G. Churchyard, “Epidemiology of HIV-associated tuberculosis,” *Curr. Opin. HIV AIDS*, vol. 4, no. 4, pp. 325–333, Jul. 2009.

[93] P. Glaziou, K. Floyd, and M. C. Raviglione, “Global Epidemiology of Tuberculosis,” 2018.

[94] D. Westreich *et al.*, “Effect of pulmonary tuberculosis on mortality in patients receiving HAART,” *AIDS*, vol. 23, no. 6, pp. 707–715, Mar. 2009.

[95] L. Huang *et al.*, “HIV-associated Pneumocystis pneumonia,” *Proc. Am. Thorac. Soc.*, vol. 8, no. 3, pp. 294–300, Jun. 2011.

[96] A. Morris, K. Wei, K. Afshar, and L. Huang, “Epidemiology and Clinical Significance of Pneumocystis Colonization,” *J. Infect. Dis.*, vol. 197, no. 1, pp. 10–17, Jan. 2008.

[97] R. Kaur, A. Wadhwa, P. Bhalla, and M. S. Dhakad, “Pneumocystis pneumonia in HIV patients: a diagnostic challenge till date,” *Med. Mycol.*, vol. 53, no. 6, pp. 587–592, Jul. 2015.

[98] F. J. Vilar, S. H. Khoo, and T. Walley, “The management of Pneumocystis carinii pneumonia,” *Br. J. Clin. Pharmacol.*, vol. 47, no. 6, pp. 605–609, Jun. 1999.

[99] V. L. Pereira-Chioccola, J. E. Vidal, and C. Su, “Toxoplasma gondii infection and cerebral toxoplasmosis in HIV-infected patients,” *Future Microbiol.*, vol. 4, no. 10, pp. 1363–1379, 2009.

[100] C. S. Meira, J. E. Vidal, T. A. Costa-Silva, N. Frazatti-Gallina, and V. L. Pereira-Chioccola, “Immunodiagnosis in cerebrospinal fluid of cerebral toxoplasmosis and HIV-infected patients using Toxoplasma gondii excreted/secreted antigens,” *Diagn. Microbiol. Infect. Dis.*, vol. 71, no. 3, pp. 279–285, 2011.

[101] J. E. Vidal, A. V. Hernandez, A. C. Penalva De Oliveira, R. F. Dauar, S. P. Barbosa, and R. Focaccia, “Cerebral toxoplasmosis in HIV-positive patients in Brazil: Clinical features and predictors of treatment response in the HAART era,” *AIDS Patient Care STDS*, vol. 19, no. 10, pp. 626–634, 2005.

[102] A. Basavaraju, “Toxoplasmosis in HIV infection: An overview,” *Trop. Parasitol.*, vol. 6, no. 2, pp. 129–135, 2016.

[103] E. J. Arts, D. J. Hazuda, E. F. D. Bushman, G. J. Nabel, and R. Swanstrom, “HIV-1 Antiretroviral Drug Therapy BASIC PRINCIPLES OF ANTIRETROVIRAL ir,” *Cold Spring Harb. Perspect. Med.*, vol. 2, no. a007161, pp. 1–23, 2012.

[104] S. Broder, “The development of antiretroviral therapy and its impact on the HIV-1/AIDS pandemic,” *Antiviral Res.*, vol. 85, no. 1, pp. 1–18, Jan. 2010.

[105] R. Danesi, A. Falcone, P. F. Conte, and M. Del Tacca, “Pharmacokinetic Optimisation of the Treatment of Cancer with High Dose Zidovudine,” *Clin. Pharmacokinet.*, vol. 34, no. 2, pp. 173–180, 1998.

[106] E. Scholar, “HIV Protease Inhibitors,” in *xPharm: The Comprehensive Pharmacology Reference*, Elsevier, 2007, pp. 1–4.

[107] E. De Clercq, “The role of non-nucleoside reverse transcriptase inhibitors (NNRTIs) in the therapy of HIV-1 infection1Presented at the Eleventh International Conference on Antiviral Research, San Diego, CA, 5–10 April 1998.1,” *Antiviral Res.*, vol. 38, no. 3, pp. 153–179, 1998.

[108] O. S. Pedersen and E. B. Pedersen, “Non-Nucleoside Reverse Transcriptase Inhibitors: The NNRTI Boom,” *Antivir. Chem. Chemother.*, vol. 10, no. 6, pp. 285–314, Dec. 1999.

[109] M.-P. de Béthune, “Non-nucleoside reverse transcriptase inhibitors (NNRTIs), their discovery, development, and use in the treatment of HIV-1 infection: A review of the last 20 years (1989–2009),” *Antiviral Res.*, vol. 85, no. 1, pp. 75–90, 2010.

[110] I. Usach, V. Melis, and J.-E. Peris, “Non-nucleoside reverse transcriptase inhibitors: a review on pharmacokinetics, pharmacodynamics, safety and tolerability,” *J. Int. AIDS Soc.*, vol. 16, no. 1, pp. 1–14, Sep. 2013.

[111] M. Westby and E. Van Der Ryst, “CCR5 antagonists: Host-targeted antivirals for the treatment of HIV infection,” *Antivir. Chem. Chemother.*, vol. 16, no. 6, pp. 339–354, 2005.

[112] R. Kondru *et al.*, “Molecular interactions of CCR5 with major classes of small-molecule anti-HIV CCR5 antagonists,” *Mol. Pharmacol.*, vol. 73, no. 3, pp. 789–800, 2008.

[113] P. L. Anderson, T. N. Kakuda, and K. A. Lichtenstein, “The Cellular Pharmacology of Nucleoside- and Nucleotide-Analogue Reverse-Transcriptase Inhibitors and Its Relationship to Clinical Toxicities,” *Clin. Infect. Dis.*, vol. 38, no. 5, pp. 743–753, Mar. 2004.

[114] M. G. Atta, S. De Seigneux, and G. M. Lucas, “Clinical Pharmacology in HIV Therapy,” *Clin. J. Am. Soc. Nephrol.*, vol. 14, pp. 435–444, 2019.

[115] Y. Wang, E. De Clercq, and G. Li, “Current and emerging non-nucleoside reverse transcriptase inhibitors (NNRTIs) for HIV-1 treatment Current and emerging non-nucleoside reverse transcriptase inhibitors (NNRTIs) for HIV-1 treatment,” *Expert Opin. Drug Metab. Toxicol.*, vol. 00, no. 00, pp. 1–17, 2019.

[116] J. L. Adams, B. N. Greener, and A. D. M. Kashuba, “Pharmacology of HIV integrase inhibitors,” *Curr. Opin. HIV AIDS*, vol. 7, no. 5, pp. 390–400, Sep. 2012.

[117] W. G. Powderly, “Integrase inhibitors in the treatment of HIV-1 infection,” *J. Antimicrob. Chemother.*, vol. 65, no. 12, pp. 2485–2488, Dec. 2010.

[118] P. Monini, C. Sgadari, G. Barillari, and B. Ensoli, “HIV protease inhibitors: antiretroviral agents with anti-inflammatory, anti-angiogenic and anti-tumour activity,” *J. Antimicrob. Chemother.*, vol. 51, no. 2, pp. 207–211, Feb. 2003.

[119] Z. Lv, Y. Chu, and Y. Wang, “HIV protease inhibitors: a review of molecular selectivity and toxicity,” *HIV. AIDS. (Auckl).*, vol. 7, pp. 95–104, Apr. 2015.

[120] S. A. Bozzette, C. F. Ake, H. K. Tam, S. W. Chang, and T. A. Louis, “Cardiovascular and Cerebrovascular Events in Patients Treated for Human Immunodeficiency Virus Infection,” *N. Engl. J. Med.*, vol. 348, no. 8, pp. 702–710, Feb. 2003.

[121] V. Soontornniyomkij *et al.*, “HIV protease inhibitor exposure predicts cerebral small vessel disease,” *AIDS*, vol. 28, no. 9, pp. 1297–1306, Jun. 2014.

[122] M. C. Pitman, J. S. Y. Lau, J. H. McMahon, and S. R. Lewin, “Barriers and strategies to achieve a cure for HIV,” *lancet. HIV*, vol. 5, no. 6, pp. e317–e328, Jun. 2018.

[123] R. Lorenzo-Redondo *et al.*, “Persistent HIV-1 replication maintains the tissue reservoir during therapy,” *Nature*, vol. 530, no. 7588, pp. 51–56, 2016.

[124] J. D. Siliciano *et al.*, “Long-term follow-up studies confirm the stability of the latent reservoir for HIV-1 in resting CD4+ T cells,” *Nat. Med.*, vol. 9, no. 6, pp. 727–728, 2003.

[125] A. J. Kandathil, S. Sugawara, and A. Balagopal, “Are T cells the only HIV-1 reservoir,” *Retrovirology*, vol. 13, no. 1, pp. 1–10, 2016.

[126] A. Aikaterini, L. Yujie, and W. Brian, “Cellular reservoirs of HIV-1 and their role in viral persistence,” *Curr. HIV Res.*, vol. 6, no. September, pp. 388–400, 2008.

[127] J. Blazkova *et al.*, “CpG methylation controls reactivation of HIV from latency,” *Retrovirology*, vol. 7, no. Suppl 1, pp. O8–O8, May 2010.

[128] J. Blazkova *et al.*, “Paucity of HIV DNA Methylation in Latently Infected, Resting CD4⁺ T Cells from Infected Individuals Receiving Antiretroviral Therapy,” *J. Virol.*, vol. 86, no. 9, pp. 5390 LP – 5392, May

2012.

[129] X. Zhang *et al.*, “Epigenome-wide differential DNA methylation between HIV-infected and uninfected individuals,” *Epigenetics*, vol. 11, no. 10, pp. 750–760, Oct. 2016.

[130] Y. Matsuda, M. Kobayashi-Ishihara, D. Fujikawa, T. Ishida, T. Watanabe, and M. Yamagishi, “Epigenetic Heterogeneity in HIV-1 Latency Establishment,” *Sci. Rep.*, vol. 5, no. 1, p. 7701, 2015.

[131] S. D. Narasipura, S. Kim, and L. Al-Harthi, “Epigenetic Regulation of HIV-1 Latency in Astrocytes,” *J. Virol.*, vol. 88, no. 5, pp. 3031 LP – 3038, Mar. 2014.

[132] C. Marban *et al.*, “Recruitment of chromatin-modifying enzymes by CTIP2 promotes HIV-1 transcriptional silencing,” *EMBO J.*, vol. 26, no. 2, pp. 412–423, Jan. 2007.

[133] G. E. Martin *et al.*, “CD32-expressing CD4 T cells are phenotypically diverse and can contain proviral HIV DNA,” *Front. Immunol.*, vol. 9, no. MAY, pp. 1–13, 2018.

[134] R. R. Sharaf and J. Z. Li, “The Alphabet Soup of HIV Reservoir Markers,” *Curr. HIV/AIDS Rep.*, vol. 14, no. 2, pp. 72–81, 2017.

[135] T. F. Leite *et al.*, “Reduction of HIV-1 reservoir size and diversity after 1 year of cART among Brazilian individuals starting treatment during early stages of acute infection,” *Front. Microbiol.*, vol. 10, no. FEB, 2019.

[136] A. J. Murray, K. J. Kwon, D. L. Farber, and R. F. Siliciano, “The Latent Reservoir for HIV-1: How Immunologic Memory and Clonal Expansion Contribute to HIV-1 Persistence,” *J. Immunol.*, vol. 197, no. 2, pp. 407–417, Jul. 2016.

[137] N. Goonetilleke, G. Clutton, R. Swanstrom, and S. B. Joseph, “Blocking formation of the stable HIV reservoir: A new perspective for HIV-1 cure,” *Front. Immunol.*, vol. 10, no. AUG, pp. 1–12, 2019.

[138] N. N. Hosmane *et al.*, “Proliferation of latently infected CD4(+) T cells carrying replication-competent HIV-1: Potential role in latent reservoir dynamics,” *J. Exp. Med.*, vol. 214, no. 4, pp. 959–972, Apr. 2017.

[139] R. Liu, F. R. Simonetti, and Y.-C. Ho, “The forces driving clonal expansion of the HIV-1 latent reservoir,” *Virol. J.*, vol. 17, no. 1, p. 4, Jan. 2020.

[140] J. K. Bui *et al.*, “Proviruses with identical sequences comprise a large fraction of the replication-competent HIV reservoir,” *PLoS Pathog.*, vol. 13, no. 3, pp. e1006283–e1006283, Mar. 2017.

[141] S. H. Hughes and J. M. Coffin, “What Integration Sites Tell Us about HIV Persistence,” *Cell Host Microbe*, vol. 19, no. 5, pp. 588–598, May 2016.

[142] S. D. Rezaei and P. U. Cameron, “Human immunodeficiency virus (HIV)-1 integration sites in viral latency,” *Curr. HIV/AIDS Rep.*, vol. 12, no. 1, pp. 88–96, Mar. 2015.

[143] F. Maldarelli *et al.*, “HIV latency. Specific HIV integration sites are linked to clonal expansion and persistence of infected cells,” *Science*, vol. 345, no. 6193, pp. 179–183, Jul. 2014.

[144] S. M. Kariuki, P. Selhorst, K. K. Ariën, and J. R. Dorfman, “The HIV-1 transmission bottleneck,” *Retrovirology*, vol. 14, no. 1, p. 22, 2017.

[145] S. B. Joseph, R. Swanstrom, A. D. M. Kashuba, and M. S. Cohen, “Bottlenecks in HIV-1 transmission: insights from the study of founder viruses,” *Nat. Rev. Microbiol.*, vol. 13, no. 7, pp. 414–425, Jul. 2015.

[146] R. Craigie and F. D. Bushman, “HIV DNA integration,” *Cold Spring Harb. Perspect. Med.*, vol. 2, no. 7, pp. a006890–a006890, Jul. 2012.

[147] G. Darcis, B. Van Driessche, and C. Van Lint, “HIV Latency: Should We Shock or Lock?,” *Trends Immunol.*, vol. 38, no. 3, pp. 217–228, 2017.

[148] C. Schwartz *et al.*, “On the way to find a cure: Purging latent HIV-1 reservoirs,” *Biochemical Pharmacology*, vol. 146. pp. 10–22, 2017.

[149] T. A. Rasmussen, M. Tolstrup, and O. S. Søgaard, “Reversal of Latency as Part of a Cure for HIV-1,” *Trends in*

Microbiology, vol. 24, no. 2. pp. 90–97, 2016.

[150] C. Katlama *et al.*, "Barriers to a cure for HIV: new ways to target and eradicate HIV-1 reservoirs," *Lancet (London, England)*, vol. 381, no. 9883, p. 2109—2117, Jun. 2013.

[151] L. Luo *et al.*, "The effects of antiretroviral therapy initiation time on HIV reservoir size in Chinese chronically HIV infected patients: a prospective, multi-site cohort study," *BMC Infect. Dis.*, vol. 19, no. 1, p. 257, 2019.

[152] A. A. Okoye *et al.*, "Early antiretroviral therapy limits SIV reservoir establishment to delay or prevent post-treatment viral rebound," *Nat. Med.*, vol. 24, no. 9, pp. 1430–1440, Sep. 2018.

[153] S. S. Jensen *et al.*, "Initiation of Antiretroviral Therapy (ART) at Different Stages of HIV-1 Disease Is Not Associated with the Proportion of Exhausted CD8+ T Cells," *PLoS One*, vol. 10, no. 10, p. e0139573, Oct. 2015.

[154] D. H. Barouch and S. G. Deeks, "Remission and Eradication," *Science (80-.).*, vol. 345, no. 6193, 2014.

[155] A. L. Ferre *et al.*, "Mucosal immune responses to HIV-1 in elite controllers: a potential correlate of immune control," *Blood*, vol. 113, no. 17, pp. 3978–3989, Apr. 2009.

[156] J. A. Warren, G. Clutton, and N. Goonetilleke, "Harnessing CD8+ T cells under HIV antiretroviral therapy," *Front. Immunol.*, vol. 10, no. FEB, pp. 1–14, 2019.

[157] R. B. Belshe *et al.*, "Induction of immune responses to HIV-1 by canarypox virus (ALVAC) HIV-1 and gp120 SF-2 recombinant vaccines in uninfected volunteers," *AIDS*, vol. 12, no. 18, 1998.

[158] T. G. Evans *et al.*, "A Canarypox Vaccine Expressing Multiple Human Immunodeficiency Virus Type 1 Genes Given Alone or with Rgp120 Elicits Broad and Durable CD8+ Cytotoxic T Lymphocyte Responses in Seronegative Volunteers," *J. Infect. Dis.*, vol. 180, no. 2, pp. 290–298, Aug. 1999.

[159] R. B. Belshe *et al.*, "Safety and Immunogenicity of a Canarypox-Vectored Human Immunodeficiency Virus Type 1 Vaccine with or without gp120: A Phase 2 Study in Higher- and Lower-Risk Volunteers," *J. Infect. Dis.*, vol. 183, no. 9, pp. 1343–1352, May 2001.

[160] Y. Gao, F. P. McKay, and F. S. J. Mann, "Advances in HIV-1 Vaccine Development," *Viruses* , vol. 10, no. 4. 2018.

[161] B. Sahay, C. Q. Nguyen, and J. K. Yamamoto, "Conserved HIV Epitopes for an Effective HIV Vaccine," *J. Clin. Cell. Immunol.*, vol. 8, no. 4, p. 518, Aug. 2017.

[162] J. Carrillo, B. Clotet, and J. Blanco, "Antibodies and antibody derivatives: New partners in HIV eradication strategies," *Front. Immunol.*, vol. 9, no. OCT, pp. 1–11, 2018.

[163] D. Sok and D. R. Burton, "Recent progress in broadly neutralizing antibodies to HIV," *Nat. Immunol.*, vol. 19, no. 11, pp. 1179–1188, Nov. 2018.

[164] A. Pegu, A. J. Hessell, J. R. Mascola, and N. L. Haigwood, "Use of broadly neutralizing antibodies for HIV- - 1 prevention," vol. 275, pp. 296–312, 2017.

[165] H. Gruell and F. Klein, "Antibody-mediated prevention and treatment of HIV-1 infection," *Retrovirology*, vol. 15, no. 1, p. 73, Nov. 2018.

[166] J. F. Scheid *et al.*, "HIV-1 antibody 3BNC117 suppresses viral rebound in humans during treatment interruption," *Nature*, vol. 535, no. 7613, pp. 556–560, Jul. 2016.

[167] H.-I. I. Vivo *et al.*, "Non-neutralizing Antibodies Alter the Course of Article Non-neutralizing Antibodies Alter the Course of HIV-1 Infection In Vivo," *Cell*, vol. 170, no. 4, pp. 637-643.e10, 2017.

[168] T. Bruel *et al.*, "Lack of ADCC Breadth of Human Nonneutralizing Anti-HIV-1 Antibodies," *J. Virol.*, vol. 91, no. 8, pp. e02440-16, Apr. 2017.

[169] C. Petritsch and S. R. Vandenberg, *in the central nervous system*, Third Edit. Elsevier Ltd, 2011.

[170] G. Hütter *et al.*, "Long-Term Control of HIV by CCR5 Delta32/Delta32 Stem-Cell Transplantation," *N. Engl. J. Med.*, vol. 360, no. 7, pp. 692–698, Feb. 2009.

[171] T. J. Henrich *et al.*, “Antiretroviral-free HIV-1 remission and viral rebound after allogeneic stem cell transplantation: report of 2 cases,” *Ann. Intern. Med.*, vol. 161, no. 5, pp. 319–327, Sep. 2014.

[172] R. K. Gupta *et al.*, “Evidence for HIV-1 cure after CCR5Δ32/Δ32 allogeneic haemopoietic stem-cell transplantation 30 months post analytical treatment interruption: a case report,” *Lancet HIV*, Mar. 2020.

[173] L. Li *et al.*, “Genomic Editing of the HIV-1 Coreceptor CCR5 in Adult Hematopoietic Stem and Progenitor Cells Using Zinc Finger Nucleases,” *Mol. Ther.*, vol. 21, no. 6, pp. 1259–1269, 2013.

[174] Q. Xiao, D. Guo, and S. Chen, “Application of CRISPR/Cas9-Based Gene Editing in HIV-1/AIDS Therapy,” *Front. Cell. Infect. Microbiol.*, vol. 9, p. 69, Mar. 2019.

[175] A. Kwarteng, S. T. Ahuno, and G. K. Nuako, “The therapeutic landscape of HIV - 1 via genome editing,” *AIDS Res. Ther.*, pp. 1–16, 2017.

[176] G. Darcis, B. Van Driessche, and C. Van Lint, “HIV Latency: Should We Shock or Lock?,” *Trends in Immunology*, vol. 38, no. 3. pp. 217–228, 2017.

[177] C. Schwartz *et al.*, “On the way to find a cure: Purging latent HIV-1 reservoirs,” *Biochem. Pharmacol.*, vol. 146, pp. 10–22, 2017.

[178] C. Katlama *et al.*, “Barriers to a cure: New concepts in targeting and eradicating HIV-1 reservoirs,” *Lancet*, vol. 381, no. 9883, 2013.

[179] S. Singh *et al.*, “Monoclonal Antibodies: A Review.,” *Curr. Clin. Pharmacol.*, vol. 13, no. 2, pp. 85–99, 2018.

[180] M. J. Adler and D. S. Dimitrov, “Therapeutic antibodies against cancer,” *Hematol. Oncol. Clin. North Am.*, vol. 26, no. 3, pp. 447–vii, Jun. 2012.

[181] R.-M. Lu *et al.*, “Development of therapeutic antibodies for the treatment of diseases,” *J. Biomed. Sci.*, vol. 27, no. 1, p. 1, 2020.

[182] K. Naran, T. Nundalall, S. Chetty, and S. Barth, “Principles of Immunotherapy: Implications for Treatment Strategies in Cancer and Infectious Diseases,” *Front. Microbiol.*, vol. 9, p. 3158, Dec. 2018.

[183] M. Li *et al.*, “Clinical targeting recombinant immunotoxins for cancer therapy,” *Onco. Targets. Ther.*, vol. 10, pp. 3645–3665, Jul. 2017.

[184] A. Antignani and D. Fitzgerald, “Immunotoxins: the role of the toxin,” *Toxins (Basel).*, vol. 5, no. 8, pp. 1486–1502, Aug. 2013.

[185] H. Allahyari, S. Heidari, M. Ghamgosha, P. Saffarian, and J. Amani, “Immunotoxin: A new tool for cancer therapy,” *Tumor Biol.*, vol. 39, no. 2, p. 1010428317692226, Feb. 2017.

[186] D. J. FitzGerald, R. Kreitman, W. Wilson, D. Squires, and I. Pastan, “Recombinant immunotoxins, for treating cancer,” *Int. J. Med. Microbiol.*, vol. 293, no. 7–8, pp. 577–582, 2004.

[187] V. Joosten, C. Lokman, C. A. van den Hondel, and P. J. Punt, “The production of antibody fragments and antibody fusion proteins by yeasts and filamentous fungi,” *Microb. Cell Fact.*, vol. 2, no. 1, p. 1, 2003.

[188] H. W. Schroeder Jr and L. Cavacini, “Structure and function of immunoglobulins,” *J. Allergy Clin. Immunol.*, vol. 125, no. 2 Suppl 2, pp. S41–S52, Feb. 2010.

[189] G. Vidarsson, G. Dekkers, and T. Rispens, “IgG Subclasses and Allotypes: From Structure to Effector Functions ,” *Frontiers in Immunology* , vol. 5. p. 520, 2014.

[190] J.-S. Kim, S.-Y. Jun, and Y.-S. Kim, “Critical Issues in the Development of Immunotoxins for Anticancer Therapy,” *J. Pharm. Sci.*, vol. 109, no. 1, pp. 104–115, 2020.

[191] Y. Leshem and I. Pastan, “Pseudomonas exotoxin immunotoxins and anti-tumor immunity: From observations at the patient’s bedside to evaluation in preclinical models,” *Toxins (Basel).*, vol. 11, no. 1, 2019.

[192] R. J. Kreitman and I. Pastan, “Importance of the glutamate residue of KDEL in increasing the cytotoxicity of Pseudomonas exotoxin derivatives and for increased binding to the KDEL receptor.,” *Biochem. J.*, vol. 307 (Pt 1, pp.

29–37, 1995.

[193] V. K. Chaudhary *et al.*, “Selective killing of HIV-infected cells by recombinant human CD4-Pseudomonas exotoxin hybrid protein,” *Nature*, vol. 335, no. 6188, pp. 369–372, 1988.

[194] E. A. Berger and I. Pastan, “Immunotoxin complementation of HAART to deplete persisting HIV-infected cell reservoirs,” *PLoS Pathog.*, vol. 6, no. 6, pp. e1000803–e1000803, Jun. 2010.

[195] P. Aullo, J. Alcami, M. R. Popoff, D. R. Klatzmann, J. R. Murphy, and P. Boquet, “A recombinant diphtheria toxin related human CD4 fusion protein specifically kills HIV infected cells which express gp120 but selects fusion toxin resistant cells which carry HIV,” *EMBO J.*, vol. 11, no. 2, pp. 575–583, Feb. 1992.

[196] R. Ramachandran V, D. A. Katzenstein, R. Wood, D. H. Batts, and T. C. Merigan, “Failure Of Short-Term Cd4-Pe40 Infusions To Reduce Virus Load In Human Immunodeficiency Virus-Infected Persons,” *J. Infect. Dis.*, vol. 170, no. 4, pp. 1009–1013, Oct. 1994.

[197] R. T. Davey Jr. *et al.*, “Use Of Recombinant Soluble Cd4 Pseudomonas Exotoxin, A Novel Immunotoxin, For Treatment Of Persons Infected With Human Immunodeficiency Virus,” *J. Infect. Dis.*, vol. 170, no. 5, pp. 1180–1188, Nov. 1994.

[198] S. MATSUSHITA, A. KOITO, Y. MAEDA, T. HATTORI, and K. TAKATSUKI, “Selective Killing of HIV-Infected Cells by Anti-gp120 Immunotoxins,” *AIDS Res. Hum. Retroviruses*, vol. 6, no. 2, pp. 193–203, Feb. 1990.

[199] T. K. Bera, P. E. Kennedy, E. A. Berger, C. F. Barbas 3rd, and I. Pastan, “Specific killing of HIV-infected lymphocytes by a recombinant immunotoxin directed against the HIV-1 envelope glycoprotein,” *Mol. Med.*, vol. 4, no. 6, pp. 384–391, Jun. 1998.

[200] M. A. Checkley, B. G. Luttge, and E. O. Freed, “HIV-1 envelope glycoprotein biosynthesis, trafficking, and incorporation,” *J. Mol. Biol.*, vol. 410, no. 4, pp. 582–608, Jul. 2011.

[201] T. Murakami, “Retroviral Env Glycoprotein Trafficking and Incorporation into Virions,” *Mol. Biol. Int.*, vol. 2012, p. 682850, 2012.

[202] Q. Sattentau, “Envelope Glycoprotein Trimers as HIV-1 Vaccine Immunogens,” *Vaccines*, vol. 1, no. 4, pp. 497–512, 2013.

[203] S. Ugolini, I. Mondor, and Q. J. Sattentau, “HIV-1 attachment: another look,” *Trends Microbiol.*, vol. 7, no. 4, pp. 144–149, 1999.

[204] L. Yu and Y. Guan, “Immunologic Basis for Long HCDR3s in Broadly Neutralizing Antibodies Against HIV-1,” *Front. Immunol.*, vol. 5, p. 250, Jun. 2014.

[205] P. Bannas, J. Hambach, and F. Koch-Nolte, “Nanobodies and Nanobody-Based Human Heavy Chain Antibodies As Antitumor Therapeutics ,” *Frontiers in Immunology* , vol. 8. p. 1603, 2017.

[206] Y. Yu *et al.*, “Humanized CD7 nanobody-based immunotoxins exhibit promising anti-T-cell acute lymphoblastic leukemia potential,” *Int. J. Nanomedicine*, vol. 12, pp. 1969–1983, Mar. 2017.

[207] J. Tang *et al.*, “Novel CD7-specific nanobody-based immunotoxins potently enhanced apoptosis of CD7-positive malignant cells,” *Oncotarget*, vol. 7, no. 23, pp. 34070–34083, Jun. 2016.

[208] L. E. McCoy *et al.*, “Potent and broad neutralization of HIV-1 by a llama antibody elicited by immunization,” *J. Exp. Med.*, vol. 209, no. 6, pp. 1091–1103, Jun. 2012.

[209] A. Keppler, S. Gendreizig, T. Gronemeyer, H. Pick, H. Vogel, and K. Johnsson, “A general method for the covalent labeling of fusion proteins with small molecules in vivo,” *Nat. Biotechnol.*, vol. 21, no. 1, pp. 86–89, 2003.

[210] A. Gautier *et al.*, “An Engineered Protein Tag for Multiprotein Labeling in Living Cells,” *Chem. Biol.*, vol. 15, no. 2, pp. 128–136, 2008.

[211] K. H. Jung *et al.*, “A SNAP-tag fluorogenic probe mimicking the chromophore of the red fluorescent protein Kaede,” *Org. Biomol. Chem.*, vol. 17, no. 7, pp. 1906–1915, 2019.

[212] E. R. Padayachee *et al.*, “Applications of SNAP-tag technology in skin cancer therapy,” *Heal. Sci. reports*, vol. 2, no.

2, pp. e103–e103, Jan. 2019.

[213] M.-R. Nejadmoghaddam, A. Minai-Tehrani, R. Ghahremanzadeh, M. Mahmoudi, R. Dinarvand, and A.-H. Zarnani, "Antibody-Drug Conjugates: Possibilities and Challenges," *Avicenna J. Med. Biotechnol.*, vol. 11, no. 1, pp. 3–23, 2019.

[214] N. Dan *et al.*, "Antibody-Drug Conjugates for Cancer Therapy: Chemistry to Clinical Implications," *Pharmaceuticals (Basel).*, vol. 11, no. 2, p. 32, Apr. 2018.

[215] S. Choudhary, S. Barth, and R. S. Verma, "SNAP-Tag Technology: A Promising Tool for Ex Vivo Immunophenotyping," *Mol. Diagn. Ther.*, vol. 21, no. 3, pp. 315–326, 2017.

[216] G. J. Gopal and A. Kumar, "Strategies for the Production of Recombinant Protein in Escherichia coli," *Protein J.*, vol. 32, no. 6, pp. 419–425, 2013.

[217] G. Sezonov, D. Joseleau-Petit, and R. D'Ari, "Escherichia coli physiology in Luria-Bertani broth," *J. Bacteriol.*, vol. 189, no. 23, pp. 8746–8749, Dec. 2007.

[218] N. K. Tripathi and A. Shrivastava, "Recent Developments in Bioprocessing of Recombinant Proteins: Expression Hosts and Process Development ," *Frontiers in Bioengineering and Biotechnology* , vol. 7. p. 420, 2019.

[219] B. Owczarek, A. Gerszberg, and K. Hnatuszko-Konka, "A Brief Reminder of Systems of Production and Chromatography-Based Recovery of Recombinant Protein Biopharmaceuticals," *Biomed Res. Int.*, vol. 2019, p. 4216060, 2019.

[220] S. K. Gupta and P. Shukla, "Microbial platform technology for recombinant antibody fragment production: A review," *Crit. Rev. Microbiol.*, vol. 43, no. 1, pp. 31–42, Jan. 2017.

[221] G. L. Rosano and E. A. Ceccarelli, "Recombinant protein expression in Escherichia coli: advances and challenges," *Front. Microbiol.*, vol. 5, p. 172, Apr. 2014.

[222] H. P. Sørensen and K. K. Mortensen, "Advanced genetic strategies for recombinant protein expression in Escherichia coli," *J. Biotechnol.*, vol. 115, no. 2, pp. 113–128, 2005.

[223] B. Jia and C. O. Jeon, "High-throughput recombinant protein expression in Escherichia coli: current status and future perspectives," *Open Biol.*, vol. 6, no. 8, p. 160196, Apr. 2020.

[224] S. Barth, M. Huhn, B. Matthey, A. Klimka, E. A. Galinski, and A. Engert, "Compatible-solute-supported periplasmic expression of functional recombinant proteins under stress conditions," *Appl. Environ. Microbiol.*, vol. 66, no. 4, pp. 1572–1579, Apr. 2000.

[225] Q. Zhang, R. Li, J. Li, and H. Shi, "Optimal Allocation of Bacterial Protein Resources under Nonlethal Protein Maturation Stress," *Biophys. J.*, vol. 115, no. 5, pp. 896–910, 2018.

[226] S. Barth *et al.*, "Ki-4(scFv)-ETA', a new recombinant anti-CD30 immunotoxin with highly specific cytotoxic activity against disseminated hodgkin tumors in SCID mice," *Blood*, vol. 95, no. 12, pp. 3909–3914, 2000.

[227] W. Lu *et al.*, "The Polar Region of the HIV-1 Envelope Protein Determines Viral Fusion and Infectivity by Stabilizing the gp120-gp41 Association," *J. Virol.*, vol. 93, no. 7, Apr. 2019.

[228] E. Margolin *et al.*, "Production and Immunogenicity of Soluble Plant-Produced HIV-1 Subtype C Envelope gp140 Immunogens ," *Frontiers in Plant Science* , vol. 10. p. 1378, 2019.

[229] A. Ooi, A. Wong, L. Esau, F. Lemtiri-Chlieh, and C. Gehring, "A Guide to Transient Expression of Membrane Proteins in HEK-293 Cells for Functional Characterization," *Front. Physiol.*, vol. 7, p. 300, Jul. 2016.

[230] J. Andréll and C. G. Tate, "Overexpression of membrane proteins in mammalian cells for structural studies," *Mol. Membr. Biol.*, vol. 30, no. 1, pp. 52–63, Feb. 2013.

[231] I. Feliciello and G. Chinali, "A Modified Alkaline Lysis Method for the Preparation of Highly Purified Plasmid DNA from Escherichia Coli," *Anal. Biochem.*, vol. 212, no. 2, pp. 394–401, 1993.

[232] B. Autran *et al.*, "Positive effects of combined antiretroviral therapy on CD4 + T cell homeostasis and function in advanced HIV disease," *Science (80-.).*, 1997.

[233] W. E.M.P. and S. I., “Immune Restoration After Antiretroviral Therapy: The Pitfalls Of Hasty Or Incomplete Repairs,” *Immunol. Rev.*, 2013.

[234] A. Chawla *et al.*, “A Review of Long-Term Toxicity of Antiretroviral Treatment Regimens and Implications for an Aging Population,” *Infect. Dis. Ther.*, vol. 7, no. 2, pp. 183–195, 2018.

[235] B. Castelnuovo *et al.*, “Antiretroviral treatment Long-Term (ALT) cohort: A prospective cohort of 10 years of ART-experienced patients in Uganda,” *BMJ Open*, vol. 8, no. 2, pp. 1–8, 2018.

[236] J. Vanhamel, A. Bruggemans, and Z. Debyser, “Establishment of latent HIV-1 reservoirs: what do we really know?,” *J. virus Erad.*, vol. 5, no. 1, pp. 3–9, 2019.

[237] K. Spiess, M. H. Jakobsen, T. N. Kledal, and M. M. Rosenkilde, “The future of antiviral immunotoxins,” vol. 99, no. June, pp. 911–925, 2016.

[238] T. K. Bera, P. E. Kennedy, E. A. Berger, C. F. Barbas, and I. Pastan, “Specific killing of HIV-infected lymphocytes by a recombinant immunotoxin directed against the HIV-1 envelope glycoprotein,” *Mol. Med.*, 1998.

[239] P. W. Denton *et al.*, “Targeted cytotoxic therapy kills persisting HIV infected cells during ART,” *PLoS Pathog.*, vol. 10, no. 1, pp. e1003872–e1003872, Jan. 2014.

[240] M. Perreau, R. Banga, and G. Pantaleo, “Targeted Immune Interventions for an HIV-1 Cure,” *Trends in Molecular Medicine*. 2017.

[241] M. P. Davenport, D. S. Khoury, D. Cromer, S. R. Lewin, A. D. Kelleher, and S. J. Kent, “Functional cure of HIV: the scale of the challenge,” *Nat. Rev. Immunol.*, 2019.

[242] A. Vafadar *et al.*, “In silico design and evaluation of scFv-CdtB as a novel immunotoxin for breast cancer treatment,” *Int. J. Cancer Manag.*, 2020.

[243] B. Briney and D. Burton, “Massively scalable genetic analysis of antibody repertoires,” *bioRxiv*, 2018.

[244] R. A. Norman *et al.*, “Computational approaches to therapeutic antibody design: established methods and emerging trends,” *Brief. Bioinform.*, 2019.

[245] K. M. Elkins, “An in silico DNA cloning experiment for the biochemistry laboratory,” *Biochem. Mol. Biol. Educ.*, 2011.

[246] U. Reischl, R. C. Mierendorf, B. B. Morris, B. Hammer, and R. E. Novy, “Expression and Purification of Recombinant Proteins Using the pET System,” in *Molecular Diagnosis of Infectious Diseases*, 2003.

[247] T. Ribbert, T. Thepen, M. K. Tur, R. Fischer, M. Huhn, and S. Barth, “Recombinant, ETA′-based CD64 immunotoxins: Improved efficacy by increased valency, both in vitro and in vivo in a chronic cutaneous inflammation model in human CD64 transgenic mice,” *Br. J. Dermatol.*, vol. 163, no. 2, pp. 279–286, 2010.

[248] U. K. Nandal *et al.*, “Candidate prioritization for low-abundant differentially expressed proteins in 2D-DIGE datasets,” *BMC Bioinformatics*, 2015.

[249] E. Gasteiger *et al.*, “Protein Identification and Analysis Tools on the ExPASy Server,” in *The Proteomics Protocols Handbook*, Totowa, NJ: Humana Press, 2005, pp. 571–607.

[250] Z. Goleij, H. M. Hosseini, M. Amin, J. Amani, E. Behzadi, and A. A. I. Fooladi, “In silico evaluation of two targeted chimeric proteins based on bacterial toxins for breast cancer therapy,” *Int. J. Cancer Manag.*, vol. 12, no. 2, pp. 1–10, 2019.

[251] Z. M. Moghadam, R. Halabian, H. Sedighian, E. Behzadi, J. Amani, and A. A. I. Fooladi, “Designing and analyzing the structure of DT-STXB fusion protein as an anti-tumor agent: An in silico approach,” *Iran. J. Pathol.*, 2019.

[252] F. Kampmeier *et al.*, “Site-specific, covalent labeling of recombinant antibody fragments via fusion to an engineered version of 6-O-alkylguanine DNA alkyltransferase,” *Bioconjug. Chem.*, 2009.

[253] A. F. Hussain, P. A. Heppenstall, F. Kampmeier, I. Meinhold-Heerlein, and S. Barth, “One-step site-specific antibody fragment auto-conjugation using SNAP-tag technology,” *Nat. Protoc.*, 2019.

[254] D. Kong *et al.*, “Design, expression and characterization of single chain Fv, Mms13 and the single chain Fv-mms13 fusion protein,” *Mol. Med. Rep.*, 2015.

[255] H. Hussain and N. F. M. Chong, “Combined Overlap Extension PCR Method for Improved Site Directed Mutagenesis,” *Biomed Res. Int.*, 2016.

[256] K. L. Heckman and L. R. Pease, “Gene splicing and mutagenesis by PCR-driven overlap extension,” *Nat. Protoc.*, vol. 2, no. 4, pp. 924–932, Apr. 2007.

[257] S. N. Ho, H. D. Hunt, R. M. Horton, J. K. Pullen, and L. R. Pease, “Site-directed mutagenesis by overlap extension using the polymerase chain reaction,” *Gene*, vol. 77, no. 1, pp. 51–59, Apr. 1989.

[258] M. Forloni, A. Y. Liu, and N. Wajapeyee, “Creating insertions or deletions using overlap extension polymerase chain reaction (PCR) mutagenesis,” *Cold Spring Harb. Protoc.*, 2018.

[259] P. Thomas and T. G. Smart, “HEK293 cell line: A vehicle for the expression of recombinant proteins,” *J. Pharmacol. Toxicol. Methods*, vol. 51, no. 3, pp. 187–200, May 2005.

[260] A. C. Dalton and W. A. Barton, “Over-expression of secreted proteins from mammalian cell lines,” *Protein Sci.*, vol. 23, no. 5, pp. 517–525, May 2014.

[261] H. Aydin, F. C. Azimi, J. D. Cook, and J. E. Lee, “A convenient and general expression platform for the production of secreted proteins from human cells.,” *J. Vis. Exp.*, 2012.

[262] X. Sun *et al.*, “Development of SNAP-tag fluorogenic probes for wash-free fluorescence imaging,” *Chembiochem*, vol. 12, no. 14, pp. 2217–2226, Sep. 2011.

[263] G. Lukinavičius, L. Reymond, and K. Johnsson, “Fluorescent Labeling of SNAP-Tagged Proteins in Cells,” in *Methods in Molecular Biology , vol 1266. Humana Press*, A. Gautier and M. J. Hinner, Eds. New York, NY: Springer New York, 2015, pp. 107–118.

[264] S. Djender *et al.*, “Bacterial cytoplasm as an effective cell compartment for producing functional VHH-based affinity reagents and Camelidae IgG-like recombinant antibodies,” *Microb. Cell Fact.*, 2014.

[265] M. Miot and J.-M. Betton, “Protein quality control in the bacterial periplasm,” *Microb. Cell Fact.*, vol. 3, no. 1, p. 4, May 2004.

[266] B. Gasser *et al.*, “Protein folding and conformational stress in microbial cells producing recombinant proteins: a host comparative overview,” *Microb. Cell Fact.*, vol. 7, p. 11, Apr. 2008.

[267] K. Koch *et al.*, “Selection of nanobodies with broad neutralizing potential against primary HIV-1 strains using soluble subtype C gp140 envelope trimers,” *Sci. Rep.*, 2017.

[268] N. M. Strokappe *et al.*, “Super Potent Bispecific Llama VHH Antibodies Neutralize HIV via a Combination of gp41 and gp120 Epitopes,” *Antibodies*, 2019.

[269] L. E. McCoy *et al.*, “Molecular Evolution of Broadly Neutralizing Llama Antibodies to the CD4-Binding Site of HIV-1,” *PLoS Pathog.*, 2014.

[270] A. Karyolaimos *et al.*, “Enhancing Recombinant Protein Yields in the E. coli Periplasm by Combining Signal Peptide and Production Rate Screening ,” *Frontiers in Microbiology* , vol. 10. p. 1511, 2019.

[271] S. A. Mireku, M. M. Sauer, R. Glockshuber, and K. P. Locher, “Structural basis of nanobody-mediated blocking of BtuF, the cognate substrate-binding protein of the Escherichia coli vitamin B12 transporter BtuCD,” *Sci. Rep.*, vol. 7, no. 1, p. 14296, 2017.

[272] T.-H. Bruun, K. Mühlbauer, T. Benen, A. Kliche, and R. Wagner, “A Mammalian Cell Based FACS-Panning Platform for the Selection of HIV-1 Envelopes for Vaccine Development,” *PLoS One*, vol. 9, no. 10, p. e109196, Oct. 2014.

[273] T. H. Bruun *et al.*, “Mammalian cell surface display for monoclonal antibody-based FACS selection of viral envelope proteins,” *MAbs*, 2017.

[274] J. M. Binley *et al.*, “Enhancing the Proteolytic Maturation of Human Immunodeficiency Virus Type 1 Envelope Glycoproteins,” *J. Virol.*, vol. 76, no. 6, pp. 2606 LP – 2616, Mar. 2002.

[275] V. Bosch and M. Pawlita, “Mutational analysis of the human immunodeficiency virus type 1 env gene product proteolytic cleavage site.,” *J. Virol.*, vol. 64, no. 5, pp. 2337 LP – 2344, May 1990.

[276] H.-G. Guo *et al.*, “Characterization of an HIV-1 point mutant blocked in envelope glycoprotein cleavage,” *Virology*, vol. 174, no. 1, pp. 217–224, 1990.

[277] J. M. McCune *et al.*, “Endoproteolytic cleavage of gp160 is required for the activation of human immunodeficiency virus,” *Cell*, vol. 53, no. 1, pp. 55–67, 1988.

[278] C. Herrera *et al.*, “The impact of envelope glycoprotein cleavage on the antigenicity, infectivity, and neutralization sensitivity of Env-pseudotyped human immunodeficiency virus type 1 particles,” *Virology*, vol. 338, no. 1, pp. 154–172, 2005.

[279] M. L. Coleman, E. A. Sahai, M. Yeo, M. Bosch, A. Dewar, and M. F. Olson, “Membrane blebbing during apoptosis results from caspase-mediated activation of ROCK I,” *Nat. Cell Biol.*, 2001.

[280] J. D. Lane, V. J. Allan, and P. G. Woodman, “Active relocation of chromatin and endoplasmic reticulum into blebs in late apoptotic cells,” *J. Cell Sci.*, 2005.

[281] R. Andrade, L. Crisol, R. Prado, M. D. Boyano, J. Arluzea, and J. Aréchaga, “Plasma membrane and nuclear envelope integrity during the blebbing stage of apoptosis: a time-lapse study,” *Biol. Cell*, 2010.

[282] S. J. Chen *et al.*, “UV irradiation/cold shock-mediated apoptosis is switched to bubbling cell death at low temperatures,” *Oncotarget*, 2015.

[283] Z. P. Liu *et al.*, “Effects of both cold and heat stress on the liver of the giant spiny frog (Quasipaa spinosa): Stress response and histological changes,” *J. Exp. Biol.*, 2018.

[284] R. K. Koppisetti *et al.*, “Ambidextrous binding of cell and membrane bilayers by soluble matrix metalloproteinase-12,” *Nat. Commun.*, 2014.

[285] B. A. Krishna *et al.*, “Targeting the latent cytomegalovirus reservoir with an antiviral fusion toxin protein,” *Nat. Commun.*, 2017.

[286] K. Spiess *et al.*, “Rationally designed chemokine-based toxin targeting the viral G protein-coupled receptor US28 potently inhibits cytomegalovirus infection in vivo,” *Proc. Natl. Acad. Sci. U. S. A.*, 2015.

[287] E. M. Geoghegan, H. Zhang, P. J. Desai, A. Biragyn, and R. B. Markham, “Antiviral activity of a single-domain antibody immunotoxin binding to glycoprotein D of herpes simplex virus 2,” *Antimicrob. Agents Chemother.*, 2015.

[288] T. S. Castiñeiras, S. G. Williams, A. G. Hitchcock, and D. C. Smith, “E. coli strain engineering for the production of advanced biopharmaceutical products,” *FEMS Microbiology Letters*. 2018.

[289] T. Baumgarten, A. J. Ytterberg, R. A. Zubarev, and J. W. de Gier, “Optimizing recombinant protein production in the Escherichia coli periplasm alleviates stress,” *Appl. Environ. Microbiol.*, 2018.

[290] S. C. Makrides, “Strategies for achieving high-level expression of genes in Escherichia coli,” *Microbiological Reviews*. 1996.

[291] U. L. Abbas, R. L. Glaubius, Y. Ding, and G. Hood, “Drug resistance from preferred antiretroviral regimens for HIV infection in South Africa: A modeling study,” *PLoS One*, 2019.